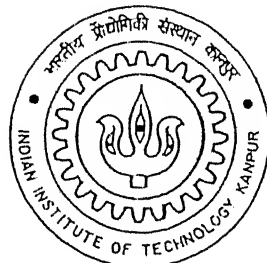


Effect of Joint Panel Design on Seismic Energy Dissipation in Steel Frames

A Thesis Submitted
in Partial Fulfillment of the Requirements
for the Degree of
Master of Technology (Civil Engineering)

by

Kintali Sankara Narayana Gupta



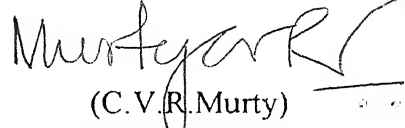
to the

**DEPARTMENT OF CIVIL ENGINEERING
INDIAN INSTITUTE OF TECHNOLOGY KANPUR**

April 1996

Certificate

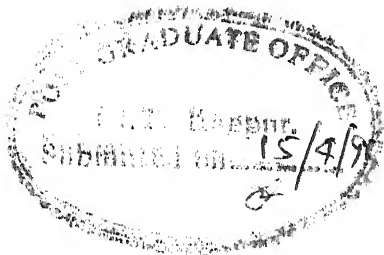
It is certified that the work contained in this thesis entitled "*Effect of Joint Panel Design on Seismic Energy Dissipation in Steel Frames*" by mr. **Kintali Sankara Narayana Gupta**, has been carried out under my supervision and that this work has not been submitted elsewhere for the award of a degree.



(C.V.R. Murty)

Department of Civil Engineering
Indian Institute of Technology Kanpur

15 April 1996



23 JUL 1976
CENTRAL LIBRARY
I.I.T., KANPUR
~~Inv. No. A. 121812~~

CE-188B-M-GUP-EFF



A121912

ABSTRACT

Experiences from the post-earthquake investigations clearly demonstrate the vulnerability of beam-column joints in steel moment-resisting frames (MRFs) under strong seismic shaking. These joints have finite size, stiffness and strength. Experimental and analytical investigations showed strong dependence of the seismic performance of steel structures on joint panel design. The current design specifications for steel joints are based on strength considerations. Since the performance of a frame is evaluated based on how well it dissipates the seismic energy input to it during ground shaking, it is of interest to study the performance of different joint panel designs *vis-à-vis* energy dissipation characteristics.

In this thesis, the parameters that affect the energy dissipation characteristics of steel planar MRFs *vis-à-vis* joint panel designs are emphasized through example single-storey single-bay portal frames. The various analytical models proposed in the literature for simulating the behaviour of joint panel zones are reviewed. The seismic design codes provide specifications for design of joint panels. These specifications are derived based on studies on typical interior joints, and are also employed for design of exterior joint panel zones. However, the requirements of strength and stiffness of exterior and interior joint panels may not be same under seismic conditions. So, the impacts of exterior and interior joint panel zone designs are studied separately under pseudo-static cyclic loading through the energy dissipation characteristics of storey sub-assemblages. Based on the above analytical study, a new approach for design of exterior as well as interior joint panel zones is proposed.

The performances of these proposed designs are also studied through dynamic time history analyses of a 20-storey steel planar MRF under various ground motions.

To my family members . . .

ACKNOWLEDGEMENTS

I wish to record with utmost pride and deep sense of gratitude, the valuable guidance, critical discussions, timely help, continuous encouragement and kind hearted affection given by my thesis supervisor, C.V.R. Murty, throughout my association with him.

I am sincerely grateful to all the faculty members who have taught me during the course work : Professors Aswini Kumar, N.S.V. Kameswara Rao, N.N. Kishore and Sudhir K. Jain; Drs. S.K. Chakraborty, V.K. Gupta and Sudhir Misra. I am thankful to Professor Sudir K. Jain for his timely suggestions on both academic and non-academic matters.

I am deeply indebted to all my family members for their love and affection. No words can aptly describe my feelings towards the rest of the *GANG* : Varsha (Varshu), Aparna (Appu) and Rajesh (Giraffe). Their kind help, valuable words of consolation from them during my lean times, and their deep sense of attachment made them an inseparable part of my family. I dedicate my thesis to all of my family members

I owe special thanks to Mr. K.S. Reddy and family, and Dr. B.S. Murty and family, for their moral support throughout my stay in this Institute. My sincere thanks are due to Dr. S.C. Dutta, Mr. M. Shrikande and Mr. B. Basu for their cooperation. I would also like to extend my gratitude to Mr. Grover, Vidyanath, Aachari, Umasankar, Debjit, Sujit, and the rest of my junior M.Tech (Structures) students for their encouragement and help.

Last, but not the least, I am gratefully indebted to Mr. G. Subramanyam without whom this thesis would not have taken its present form.

TABLE OF CONTENTS

Abstract	iii
Acknowledgements	v
Table of Contents	vi
List of Tables	ix
List of Figures	x
List of Symbols	xiii
Chapter 1 :: INTRODUCTION	
1.0 General	1
1.1 Object and Scope of Present Study	3
1.2 Organization of the Thesis	4
1.3 Sign Convention, Notation and Units	4
Chapter 2 :: LITERATURE REVIEW	
2.0 General	5
2.1 Performance in Past Earthquakes	5
2.2 Behaviour of Joint Panel Zone under Cyclic Loading	6
2.3 Past Research on Joint Panel Zones	8
2.3.1 Effect of Axial Load on Shear Strength of Joint Panel Zone	9
2.3.2 Effect of Joint Panel Design On Energy Dissipation in MRFs	10
2.3.3 Analytical Modeling of Joint Panel Zones	11
2.3.3.1 <i>Ellipsoidal Joint Hysteresis Model</i>	12
2.3.4 Design Recommendations	13
2.3.4.1 <i>Fielding and Huang, 1971</i>	14
2.3.4.2 <i>Krawinkler, 1978</i>	14
2.3.4.3 <i>Fukumoto and Lee, 1992</i>	15
2.3.4.4 <i>Tabuchi, et al, 1992</i>	16
2.4 Codal Specifications for Design of Joint Panel Zones	17
2.4.1 Shear Strength of Joint Panel Zone	17
2.4.2 Thickness of Joint Panel Zone Plate	18
2.4.3 Relative Strengths of Columns, Beams and Joint Panel Zones	19
2.4.3.1 <i>UBC 94 and SEAOC 88</i>	19
2.4.3.2 <i>AISC 91</i>	19
2.4.4 Indian Codes	20
2.5 Conclusions	21

Chapter 3 :: PARAMETERS INFLUENCING SEISMIC RESPONSE OF MRFs	
3.0 General	22
3.1 Hysteretic Behaviour Under Pseudo-Static Cyclic Loading	23
3.2 Analysis of Steel Planar MRFs with Joint Elements	23
3.3 Parameters and their Variation	24
3.3.1 Axial Force in Columns	24
3.3.2 Ratio R_{bc} of Beams and Columns Plastic Moment Capacities	25
3.3.3 Ratio R_{jb} of Joint Distorsional Yield Moment Capacity and Beams Plastic Moment Capacities	26
3.4 Response Quantities of Interest	26
3.4.1 Energy Dissipation E_d	27
3.4.2 Lateral Force H	27
3.5 Numerical Study	28
3.6 Results and Discussions	28
3.6.1 Energy Dissipation E_d	28
3.6.2 Lateral Force H	30
3.6.3 Normalized Energy Dissipation E_{dn}	31
3.7 Conclusions	31

Chapter 4 :: ENERGY CONSIDERATIONS IN DESIGN OF MRFs	
4.0 General	33
4.1 Storey Sub-Assemblages	34
4.2 Parameters Considered in Numerical Study	35
4.3 Numerical Study through Example Storey Sub-assemblages	35
4.3.1 Specified Drift	36
4.3.2 Loads in Columns and Beams	36
4.3.3 Exterior and Interior Joint Panel Designs	37
4.4 Analysis	37
4.5 Responses of Interest	38
4.6 Results and Discussions	38
4.6.1 Energy Dissipation E_d	38
4.6.2 Lateral Force H	39
4.6.3 Normalized Energy Dissipation E_{dn}	39
4.6.4 Normalized Lateral Force H_n	40
4.7 Design Implications	40
4.8 Seismic Behaviour of 20-Storey Steel Planar MRF	41
4.8.1 Results and Discussions	42
4.8.1.1 <i>El Centro</i>	42
4.8.1.2 <i>1.5 El Centro</i>	43
4.8.1.3 <i>San Fernando (Pacoima Dam)</i>	43
4.8.1.4 <i>Synthetic Pulse</i>	44
4.9 Conclusions	44

Chapter 5 :: SUMMARY AND CONCLUSIONS

5.1 Summary	46
5.2 Conclusions	47
5.3 Recommendations for Future Work	48

References	49
-------------------	----

Tables	52
---------------	----

Figures	55
----------------	----

• • •

LIST OF TABLES

Table	Caption	Page
3.1	Details of cross section properties of beams and columns in structure cases C1 and C2.	52
3.2	Details of cross section properties of beams and columns in structure cases B1 and B2.	52
3.3	Details of joint panel zone plate considered in the study.	52
3.4	Details of vertical nodal load P in each structure case studied.	53
4.1	Details of loading and strength parameters of the sub-assemblages studied.	53
4.2	Details of members cross sectional properties of the sub-assemblage studied.	53
4.3	Details of earthquake ground motions and the interior and exterior joint panel designs used in the frame.	54

LIST OF FIGURES

Figure	Caption	Page
1.1	A schematic view of a typical interior joint panel zone region of a steel MRF.	55
2.1	Loads transferred through a planar joint panel zone.	56
2.2	Typical joint sub-assemblages experimentally tested by past researchers.	56
2.3	Typical interior sub-assemblage of a frame structure considered in experimental and analytical studies by various researchers.	57
2.4	Shear distribution in a planar joint in the (a) elastic range, and (b) inelastic range.	57
2.5	Shear behaviour caused by unbalanced moments.	57
2.6	Shear resistance due to (a) panel zone plate, (b) joint panel boundary elements and (c) restraint to flexural deformation by the adjacent beams and columns.	58
2.7	Degrees of freedom considered at each global node in the discretisation of planar steel MRF (a) frame without joint elements, and (b) frame with joint elements.	59
2.8	Bilinear Model for monotonic joint panel zone behaviour [Fielding and Chen, 1973].	59
2.9	Trilinear Model for monotonic joint panel zone behaviour [Krawinkler, <i>et al</i> , 1978].	60
2.10	Summary of the experimental data (Kato, and Nakao, 1973) of the monotonic stress-strain curves of the joint shear response from steel beam-column sub-assemblages test.	60
2.11	Trilinear Model for monotonic joint panel zone behaviour [Kato, 1982].	61
2.12	Joint moment <i>versus</i> joint shear strain curve for Ellipsoidal Hysteresis Joint Model [Hall and Murty, 1994].	61
2.13	Quadratic ellipses for virgin curves and backbone curves, and cubic ellipses for positive and negative hysteresis loops in the ellipsoidal joint hysteresis model [Hall and Murty, 1994].	62
2.14	Comparison of the experimental hysteresis loops [Krawinkler, <i>et al</i> , 1975] of the shear response of a steel joint from sub-assemblage test with the theoretical prediction using ellipsoidal joint hysteresis model [Hall and Murty, 1994].	62
2.15	Geometry of the quadratic ellipses modeling the nonlinear virgin curve in the ellipsoidal joint hysteresis model [Hall and Murty, 1994].	63
2.16	Forces and deformations at the degrees of freedom of the planar joint element.	63
2.17	Interior joint panel referred to in the design specification [Tabuchi, <i>et al</i> , 1992].	64
3.1	A typical hysteresis loop formation under one complete cycle of application of lateral load.	64

3.2	Geometry and the loading on Portal Frame used in the study.	65
3.3	Geometric description of the static energy associated with the initial loading path OA in the lateral load H versus lateral displacement Δ curve.	65
3.4	Effect of joint panel zone design on the energy dissipation E_d in the example portal frames with different R_{hc} values (a) C1, (b) B1, (c) C2 and (d) B2.	66
3.5	Effect of joint panel design on the energy dissipation E_d in the example portal frames with two separated values of R_{hc} , showing the sequence of formation of hinges.	67
3.6	Effect of joint panel zone design on the lateral force H in the example portal frames with different R_{hc} values (a) C1, (b) B1, (c) C2 and (d) B2.	68
3.7	Effect of joint panel zone design on the normalized energy dissipation E_{dn} in the example portal frames with different R_{hc} values (a) C1, (b) B1, (c) C2 and (d) B2.	69
4.1	A storey sub-assembly of a three-bay three-storey MRF.	70
4.2	Boundary condition employed in the analysis of the storey sub-assembly extracted from a three-bay three-storey MRF.	70
4.3	Member cross-section sizes of the planar MRF studied.	71
4.4	Storey sub-assemblies used in the analytical study (a) SSA-T, (b) SSA-M and (c) SSA-B.	72
4.5	Gravity and fluctuating loads applied in the analysis of the sub-assembly of a three-bay MRF.	73
4.6	Effect of joint panel zone designs on the energy dissipation in the storey sub-assembly SSA-T (a) energy surface, and (b) energy contours.	74
4.7	Effect of joint panel zone designs on the energy dissipation in the storey sub-assembly SSA-M (a) energy surface, and (b) energy contours.	75
4.8	Effect of joint panel zone designs on the energy dissipation in the storey sub-assembly SSA-B (a) energy surface, and (b) energy contours.	76
4.9	Typical hysteresis loops of the lateral force H versus lateral displacement Δ curves for the extreme cases of joint panel zone designs in storey sub-assembly SSA-T.	77
4.10	Effect of joint panel zone designs on the lateral force H carrying capacity in sub-assembly SSA-T (a) lateral force surface, and (b) lateral force contours.	78
4.11	Effect of joint panel zone designs on the lateral force H carrying capacity in sub-assembly SSA-M (a) lateral force surface, and (b) lateral force contours.	79
4.12	Effect of joint panel zone designs on the lateral force H carrying capacity in sub-assembly SSA-B (a) lateral force surface, and (b) lateral force contours.	80
4.13	Effect of joint panel zone designs on normalized energy dissipation in storey sub-assembly SSA-T (a) normalized energy surface, and (b) normalized energy contours.	81

4.14	Effect of joint panel zone designs on normalized energy dissipation in storey sub-assembly SSA-M (a) normalized energy surface, and (b) normalized energy contours.	82
4.15	Effect of joint panel zone designs on normalized energy dissipation in storey sub-assembly SSA-B (a) normalized energy surface, and (b) normalized energy contours.	83
4.16	Effect of joint panel zone designs on normalized lateral force in storey sub-assemblies SSA-T (a) normalized lateral force surface, and (b) normalized lateral force contours.	84
4.17	Effect of joint panel zone designs on normalized lateral force in storey sub-assemblies SSA-M (a) normalized lateral force surface, and (b) normalized lateral force contours.	85
4.18	Effect of joint panel zone designs on normalized lateral force in storey sub-assemblies SSA-B (a) normalized lateral force surface, and (b) normalized lateral force contours.	86
4.19	Synthetic ground motion with large velocity pulse.	87
4.20	Response spectra of the ground motion used in the study.	88
4.21	Floor responses of the 20-storey MRF with (a) Design 1, (b) Design 2, and (c) Design 4	89
4.22	Ductility factors of internal and external joint panels of 20-storey MRF with (a) Design 1, (b) Design 2, and (c) Design 4	90
4.23	Floor responses of the 20-storey MRF with (a) Design 1 (b) Design 2, (c) Design 3, and (d) Design 4	91-92
4.24	Ductility factors of internal and external joint panels of 20-storey MRF with (a) Design 1, (b) Design 2, (c) Design 3, and (d) Design 4	93
4.25	Floor responses of the 20-storey MRF with (a) Design 1, (b) Design 2, (c) Design 3, and (d) Design 4	94-95
4.26	Ductility factors of internal and external joint panels of 20-storey MRF with (a) Design 1, (b) Design 2, (c) Design 3, and (d) Design 4	96
4.27	Response of Exterior and Interior panel zones of typical storey in a 20-storey MRF	97
4.28	Floor responses of the 20-storey MRF with (a) Design 1, (b) Design 2, (c) Design 3, and (d) Design 4	98-99
4.29	Ductility factors of internal and external joint panels of 20-storey MRF with (a) Design 1, (b) Design 2, (c) Design 3, and (d) Design 4	100

LIST OF SYMBOLS

Symbol	Description
A_g	Gross cross sectional area of a column
b_{cf}	Breadth of column flange
d_b	Depth of beam web; Distance between centerlines of beam flanges; Average overall depth of beams framing into the joint
d_c	Depth of column web; Distance between centerlines of column flanges
d_z	$d_b - t_{bf}$
E_d	Energy dissipated in one complete cycle of loading
E_{dn}	Normalized energy dissipation
F_{yb}	Specified minimum yield strength of a beam
F_{yc}	Specified minimum yield strength of a column
f_a	Axial stress in column
f_y	Yield stress of steel
G	Shear modulus of steel
H	Average of the storey heights above and below the joint; Lateral force required for a specified drift in a storey sub-assembly
H_n	Normalized lateral force for a specified drift in a storey sub-assembly
K_{ej}	Elastic shear stiffness of joint panel
M	Moment developed in the component (column, beam or joint) due to applied external loads
M_{pb}	Beam plastic moment capacity
M_e	Moment developed in beam at the end due to earthquake forces
M_g	Moment developed in beam at the end due to gravity load
M_l	Moment developed in a beam which is on left side of the joint
M_r	Moment developed in a beam which is on right side of the joint
M_{py}	Yield distorsional moment of joint panel zone; Yield strength of joint panel
M_{pb}^R, M_{pb}^L	Full plastic moments capacities of beams to the left and right of the joint, respectively
M_{pc}^U, M_{pc}^L	Full plastic moments capacities of columns above and below the joint, respectively
M_p^r	<div style="display: flex; align-items: center;"> <div style="font-size: 4em; margin-right: 10px;">{</div> <div> Plastic moment capacity reduced due to applied external axial loads <i>in case of beams and / columns</i> Yield distorsional moment capacity <i>in case of joints</i> </div> </div>
$\sum M_{pb}$	Sum of plastic moment capacities of beams meeting at a joint
$\sum M_{pc}$	sum of plastic moment capacities of the columns meeting at a joint
M_{yj}	Yield distorsional moment capacity of joint panel zone

M_{μ}	Sum of beam moments at a joint
M_v	Sum of column moments at a joint
N_i	Number of interior joint panels present in a storey
P	Axial load applied on a column
P_u	Required axial strength of a column
P_y	Axial yield capacity of the a column
P_{uc}	Required compressive axial strength in a column (taken to be positive)
P_{top}	Cumulative axial load of each floors above the floor under consideration
P_{floor}	Axial load on column due to the gravity loads on a floor
Q_{py}	Yield distortional shear of joint panel zone
R_{bc}	Ratio of sum of plastic moment capacities of beams to that of columns
R_{jb}	Ratio of yield joint distortional moment capacity of joint panel to that of sum of plastic Moment Capacities of beams
$(R_{jb})_E$	R_{jb} at an exterior joint panel
$(R_{jb})_I$	R_{jb} at an interior joint panel
R_{py}	Panel yield ratio
R_w	Response Modification Factor
t	Total thickness of a joint panel zone (including that of doubler plates)
t_{bf}	Thickness of beam flange
t_{cf}	Thickness of column flange
V	Shear force present in a column at a joint
n	Nominal shear strength of panel zone
n_{req}	Required shear strength of a joint panel zone
s	Design storey shear
$\sum V_{yj}$	Sum of yield strengths of joint panels present in the storey
w_z	$d_c - t_{cf}$
Z_b	Plastic section modulus of a beam
Z_c	Plastic section modulus of a column
Δ	Lateral displacement
γ	Distorsional shear strain in a joint panel zone
γ_p	Plastic distortional shear strain in a joint panel zone
γ_{yj}	Yield distortional shear strain in a joint panel zone
μ	Beam rotation
ν	Column rotation
ρ	$\frac{M}{M_p^r}$
σ_y	Yield stress of steel

Chapter 1

INTRODUCTION

1.0 General

The most common form of construction of buildings is that of *Moment Resisting Frame* (MRF) type, wherein a building is composed of lineal members (called beam-columns), slabs, walls, and the most important component of a frame, the finite-sized junction of the beams and columns, called *joint*. The joint primarily consists of the joint panel zone plate, the flanges of the surrounding beams and columns, and the connections *i.e.*, riveted, bolted, welded, or any combination of these (Figure 1.1). In this thesis, it is assumed that connections are ideal; the entire study is focused on the joint panel zones only.

Steel MRFs are more commonly used in the construction of tall buildings subjected to seismic loading, because of their versatility in connections and ease of erection. The nonlinear responses of these tall steel MRF building frames to earthquake ground motions have been studied analytically for many years. These investigations include the behaviour of the joint panel zones. The extensive experimental studies in the past three decades provide information to design the joint panel zone such that it can resist the complex combination of forces transferred through it despite its pronounced nonlinear behaviour. The stability and resistance to lateral loads of the MRF require the safe transfer of axial load, bending moments, torsional moments and shear forces, between beams and columns through the joint. Analytical studies enable

to ascertain whether the tall steel buildings can indeed withstand without collapse the earthquake shaking at the levels anticipated by the codes.

Most of the seismic codes allow joint panel zone to yield in shear prior to the development of the full beam moment capacities. This is based on the experimental evidence that a well-detailed panel zone can sustain large inelastic deformations with substantial inelastic shear strength. In the seismic design of MRFs, inelastic deformations are permitted to take place in the frame elements as well as in the joint panel zones. Allowing the frame to deform inelastically beyond its elastic limit helps in dissipating the seismic energy input by the earthquake. The *strong-column and weak-beam* design philosophy restricts the formation of plastic hinges to within the beams. In continuation to this philosophy, design codes allow not only plastic hinges in the beams but also partial yielding in the joint panel zones. By allowing the joint panel zone to yield in shear, the ductility demands on the beams and columns are reduced. However, allowing inelastic deformations in the panel zone may lead to increase in overall frame deformations, meaning increased inter-storey drifts, which in turn magnify the $P-\Delta$ forces. So, it is necessary to decide the extent of inelastic deformations that can be permitted in joint panel zones and decide the strength of joints accordingly. Hence, the relative strengths of joint panels and the beams become very important.

The design of joint panel zones recommended by seismic codes is based on the strength criterion. The recommendations are based on experimental and analytical studies of typical interior beam-column joint sub-assemblages subjected to cyclic lateral load. However, there is a need to study these joint panel design recommendations from two different points of view, namely:

- (a) The design recommendations which are based on strength criterion, should be evaluated in light of the energy dissipation in the structure under cyclic loading.
- (b) The current design recommendations, which are developed based on typical interior joint sub-assemblages, need to be examined for exterior joints in light of the hysteresis energy dissipation characteristics.

The performances of steel MRFs in the Los Angeles area during the 1994 Northridge earthquake in the United States indicate damage to joint panel zones in at least 15 buildings [NIST, 1995]. This re-iterates the need to relook at associated codal provisions.

1.1 Object and Scope of Present Study

An attempt is made in this thesis to evaluate the strength criterion for design of joint panel zones of steel planar MRF from energy dissipation point of view under cyclic loading. The present of the study focuses attention on :

- (1) The effect of various parameters influencing the joint panel design from energy dissipation point of view.
 - (2) The behaviour of internal and external joint panels, from energy dissipation point of view through storey sub-assemblages of an example 20-storey steel MRF building under *pseudo-static* cyclic loading.
 - (3) A criterion for the design of exterior as well as interior joint panel zones.
 - (4) The performance of an example 20-storey steel MRF with different joint panel designs as per above observations under some recorded and synthetic earthquake ground motion time histories, in light of the current strength based seismic design codal recommendations for joint panel zones.
-

1.2 Organization of the Thesis

This thesis is organized into five relatively independent chapters. Chapter 1 introduces the subject matter of this thesis. The purpose and scope of this study are outlined. A review of the literature on the overall behaviour of joint panel zones, effect of various parameters on joint design, energy dissipation characteristics of joint panel zones, and analytical modeling of joint panel zone, is presented in Chapter 2. The various codal provisions on design of joint panel zones are also discussed therein.

The effect of various parameters on energy dissipation characteristics of steel planar MRFs under pseudo-static cyclic loading are demonstrated in Chapter 3 through example portal frames. The issue of interior *versus* exterior joint panel zones in energy dissipation is discussed in Chapter 4 through storey sub-assemblages of an example 20-storey steel planar MRF. Based on this study, proposals for design of joint panel zones are discussed. Performance of these design proposals are also reviewed analytically through the response of the example 20-storey steel planar MRF subjected to recorded and synthetic earthquake ground motions time histories.

Finally, the summary and conclusions of this study are listed in Chapter 5. Specific recommendations are made for future work in this area.

1.3 Sign Convention, Notation and Units

Tensile displacements and axial loads are considered positive. Rotational deformations follow structural analysis convention; anti-clockwise rotations and bending moments are positive. A *meter (m)*, *Newton (N)* and *second (sec)* are taken as the units of linear dimension, force and time.

Chapter 2

LITERATURE REVIEW

2.0 General

The term *panel zone* and *connection* appear often in the literature describing studies associated with junctions of beams and columns in a steel MRF. The panel zone or the *joint*, refers to the finite-sized area of the junction into which the beams and columns frame-in (Figure 1.1). On the other hand, the connection refers to the means by which the beams are connected to the columns at these panel zones. The common methods for connection are welding, bolting and combinations of the two. Understandably, nonlinearities may arise in a frame from either the joint panel zones or the connections. This study assumes that the connections between the beam-columns and the joint panel zones are ideal, and that nonlinearities arise only from the joint panel zones.

2.1 Performance in Past Earthquakes

Many steel frame buildings have collapsed or partially damaged during the past earthquakes. The September 1985 Mexico earthquake caused collapse of 12 steel frame buildings [Marsh, 1993] in central Mexico City. The January 1994 Northridge earthquake damaged a variety of building types throughout the greater Los Angeles area. A survey on the various types of damage and the amount of damage due to the earthquake indicates that the damage to steel joint panel zones occurred in at least 15

buildings [NIST, 1994]. The damages to joint panel zones were in the form of (1) fracture, buckling, or yielding of continuity plate, (2) cracking of continuity plate welds, (3) buckling, yielding, or ductile deformation of doubler plate or column web, and (4) cracking of doubler plate welds. The report emphasizes the need to relook at the associated code provisions for the design of joint panel zones.

2.2 Behaviour of Joint Panel Zone under Cyclic Loading

The lateral resistance of a steel MRF depends on how well the bending moments are transferred between the beams and columns. This is, in fact, decided by the joints. The summary of loads transferred through the joints is presented through the free body diagram shown in Figure 2.1. Under the action of these forces, experiments have shown that the in-plane axial and flexural deformations are small. The predominant stress in the joint is due to shear caused by the unbalance of the beam moments. Usually, this unbalance exists at exterior and corner joints even under gravity loads. At the interior joints, the unbalance appears under wind or seismic load conditions. The high shear forces generated in the joint panel zone by the unbalanced moments result in large joint shear strains. Thus, the primary deformation is shear distortion. The shear strain in the joint panel increases the inter-storey drift and hence structural response.

The mechanics of joint panel zones involves a complex interaction of normal and shear stresses arising from axial load and bending moments in the columns and from bending moments in the beams. The joint panel zone itself is observed to be axially and flexurally stiff, and flexible in in-plane shear. Further, the construction of the joint is also very intricate. Thus, simple analytical expressions predicting the cyclic

response of joints are not easily derivable. Consequently, experiments are conducted on prototype joints to ascertain their response characteristics.

Experiments were conducted on planar beam-column-joint sub-assemblages of the types shown in Figure 2.2. The sub-assemblage represents a typical interior joint of a frame structure as shown in Figure 2.3. It includes column stubs of half storey height and beam stubs of half bay width. A symmetric cyclic load history is applied in a *pseudo-static* manner. The lateral load H is applied at the top end of the upper column stub and the relative lateral displacement Δ is measured at the same location. The joint distortional shear stress *versus* joint shear strain curves have been used by researchers to study the joint panel zones [Bertero, *et al*, 1972; Kato and Nakao, 1973; Krawinkler, *et al*, 1975; Krawinkler and Popov, 1982; Tsai, *et al*, 1995]. These experiments showed that the joint behaviour depends not only on the shear resistance of the panel zone plate, but also on the surrounding elements. When the joint is stressed beyond the elastic range, yielding propagates slowly from the center of the panel towards its boundaries, namely the beam and column flanges (Figure 2.4). Generally, the shear resistance of joint panel zones to the unbalanced beam moments (Figure 2.5) depends on

- (a) Shear resistance of the panel zone plate (Figure 2.6a);
 - (b) Resistance of the panel boundary elements, *i.e.*, the beam and column flanges (Figure 2.6b);
 - (c) Restraint to the panel zone flexural deformation by the neighboring beam and column webs (Figure 2.6c);
- and (d) Strain hardening of the panel zone plate under continued shear beyond yield.
-

However, a clear distinction of quantitative contribution of each of the surrounding elements in the inelastic range is not known, because of the strong inter-dependence.

2.3 Past Research on Joint Panel Zones

The seismic design of multistoreyed steel-framed buildings requires the understanding of their inelastic behaviour under cyclic loading. In the late 1960's, experimental investigations [Naka, *et al.*, 1969; Popov, *et al.*, 1969; Bertero, 1969] were conducted to understand the participation of joint-panel zones in the nonlinear seismic response of steel frames. It was pointed out [Bertero, 1969; Fielding and Huang, 1971; Bertero, *et al.*, 1972; Becker, 1975; Tsai, *et al.*, 1995] that joints possess both finite stiffness and finite strength. Under strong seismic shaking, the joints demonstrate highly nonlinear characteristics in the form of large ductilities and good hysteretic properties.

The early classical analytical methods idealized the joint panel zones as mere points with zero dimensions. Later, these finite-sized components were modeled as rigid elements in the frame analysis. However, once the necessity to consider the joint panel zone deformations in the analysis and design of frames subjected to lateral loading was pointed out by the experimental investigations [Popov and Pinkey, 1969; Popov, *et al.*, 1973; Vasuvez, *et al.*, 1973; Krawinkler, *et al.*, 1975; Krawinkler, 1978], analytical methods were developed [Naka, *et al.*, 1969; Fielding and Chen, 1973; Lui and Chen, 1986; Murty and Hall, 1994] to include joint panel as separate elements in the discretisation of the structure. The joint panel zone deformations were included by separating the beam and the column rotational degrees of freedom at a joint (Figure 2.7).

Ideally, a frame should be so designed that the inelastic actions in it during strong earthquake shaking be concentrated in those elements which can provide high ductility. Experiments showed the joint panel zones can withstand very high inelastic deformations [Kato and Nakao, 1973]. Significant research has been carried out on the various aspects related to joint panel zones. The issues are discussed in the sub-section below.

2.3.1 Effect of Axial Load on Shear Strength of Joint Panel Zone

As mentioned earlier, the distortional behaviour of the joint panel zone is primarily owing to the shear stresses in the joint panel zone. So, the strength of the joint panel zone is its shear strength. In the elastic range, the distribution of shear stress is parabolic. But, in the highly inelastic region, the shear stress is more or less uniform throughout the joint panel zone plate (Figure 2.4). So, the assumption of uniform shear stress in the panel zone is very reasonable. Since, the shear force acts along with in-plane (axial) force, failure theories suggest that the shear strength of the joint panel plate decreases owing to the presence of axial force. Earlier, it was proposed [Fielding and Huang, 1973; Fielding and Chen, 1973; Krawinkler, 1978] that the shear strength of the joint panel should be decreased as per Von Mises Criterion (Distortional Strain Energy Criterion). But later, experiments showed [Krawinkler and Popov, 1982; Kato, 1982; Tsai and Popov, 1990] that the ultimate shear strength of the joint panel zone is independent of the applied axial load on the column. Even in the elastic range, with the in-plane (axial) load upto 50% of the axial yield capacity of the column, the decrease in the shear strength of panel zone due to presence of axial load on the column is very small. This little effect of axial load on strength is attributed to the additional resistance

offered by the panel framing systems consisting of flanges and continuity plates [Kato, 1982; Tsai, *et al*, 1990].

2.3.2 Effect of Joint Panel Design On Energy Dissipation in MRFs

The seismic performance of a structure under strong ground motion also depends critically on its capacity to absorb and dissipate the seismic energy, and not merely on its strength. The overall energy dissipation capability of a structure arises out of the ability to absorb the input energy at the ground. It is generally accepted that beams, rather than columns, are the elements better suited to tolerate large inelastic deformations without failure, and absorb and dissipate a large share of the seismic energy imparted to the structure through the plastic hinges formed at their ends. This leads to the widely accepted *strong-column weak-beam* philosophy, in which beams and columns are sized such that flexure plastic hinges will occur only in beams and not in columns.

Experimental investigations [Becker, 1975; Fielding and Chen, 1973; Kato and Nakao, 1973; Krawinkler, *et al*, 1975] revealed that joint panel zones participate considerably in energy absorption and dissipation in the frame. In a well-designed frame, the participation of joint panel zones in absorbing and dissipating energy reduces the demand on the plastic hinge rotations in the beams [Nader and Astaneh, 1992; 1994]. However, improper joint design can lead to a significant drop in the strength as well as the energy absorption of the structural system.

Most experimental investigations were conducted on test specimen consisting of typical interior joint sub-assemblages. A few experiments were also conducted using the entire structure [Vann, 1973; Wakabayashi, *et al*, 1973]. Since testing of an entire

structural system involves numerous difficulties, analytical studies are normally resorted to in evaluating overall seismic performance characteristics of a structure. Qualitative analytical studies were reported on the behaviour of joint panel zones as energy absorbing and dissipating elements by taking multi-storeyed steel moment resisting frames and subjecting them to different earthquake time histories recorded during past earthquakes [Popov and Englehardt, 1989]. A quantitative study [Tabuchi, *et al*, 1992] of the effect of joint panel zone in energy absorption, using the joint panel zone model based on a bilinear virgin curve [Fielding and Chen, 1973], showed that the contribution of joint panel to energy absorption of a frame varies with number of stories in a MRF and with the relative proportions of stiffness and strength of the structural elements. Recommendations were made regarding certain parameters to be used in the design of joint panel zone to make it an effective energy absorbing element. However, these recommendations were based on monotonic loading characteristics of the structure. It is necessary to arrive at more meaningful design recommendations based on hysteretic characteristics under cyclic loading rather than on monotonic loading. An analytical procedure to quantify the influence of joint panel zones on the hysteretic energy dissipation characteristics of the frame using smooth cyclic hysteresis joint panel zone model has been proposed in the literature [Nagar and Murty, 1995].

2.3.3 Analytical Modeling of Joint Panel Zones

In spite of the difficulties in closely capturing the joint behaviour, a number of analytical models were developed [Fielding and Chen, 1973; Krawinkler, *et al*, 1975; Kato, 1983] as reasonable approximations. The bilinear model shown in Figure 2.8 [Fielding and Chen, 1973] is valid for monotonic loading and over-estimates the

ultimate strength of the joint. The trilinear model shown in Figure 2.9 [Krawinkler *et al*, 1975] considers monotonic loading behaviour only in a small range of inelasticity, *i.e.*, upto four times the yield strain of a joint panel. On the other hand, experiments [Kato and Nakao, 1973] recognized that joints can take upto maximum of 100 times the distortional yield strain without loosing their strength and stiffness (Figure 2.10). The trilinear model shown in Figure 2.11 [Kato, 1983] overcame the limited inelastic range of applicability by defining the stiffness over a very large range of joint panel strain values. Again, even this model is valid only for monotonic loading.

Eventhough flexibility of joint panel is accounted for in the models valid under monotonic loading, the real problem is in accurately modeling *cyclic* behaviour of the joint in the elastic as well as in the inelastic ranges. Thus, a simple semi-empirical model, called *Ellipsoidal Joint Hysteresis Model*, was proposed [Murty and Hall, 1994]. This model includes a realistic monotonic loading curve (Figure 2.12) and smooth loading, unloading and reloading curves (Figure 2.13). This model is very convenient for numerical implementation and compares very well with experimental results (Figure 2.14). In the current study, this model has been used for modeling cyclic inelastic behaviour of joint panel zones.

2.3.3.1 *Ellipsoidal Joint Hysteresis Model*

The *Ellipsoidal Joint Hysteresis Model* for steel joint panel zones in planar MRFs significantly superior to the other models currently in use. This model based on the macroscopic view of the overall joint behaviour and is supported by test data from steel beam-column sub-assemblages. It provides explicit expressions for the joint distortional moment in terms of its distortional shear strain. A few non-cumbersome

hysteretic rules make the model simple and computationally efficient. The smooth curvilinear virgin curve, applicability under cyclic loading, a realistic estimate of the ultimate capacity and the wide inelastic range of applicability are the strengths of this model. With hysteretic behaviour defined upto 100 times the yield strain of the joint (Figure 2.12, 2.15), this model is an excellent choice for the analytical modeling of joint panel zones in steel MRFs under strong seismic shaking.

The numerical implementation of the joint panel zone element is very simple. In the analysis of MRFs, the elastic stiffness matrix of the joint in terms of the two joint global degrees of freedom, *i.e.*, the beam rotation μ and the column rotation ν (Figure 2.16), is required. It is given by

$$\begin{Bmatrix} M_{\mu} \\ M_{\nu} \end{Bmatrix} = \begin{bmatrix} K_{ej} & -K_{ej} \\ -K_{ej} & K_{ej} \end{bmatrix} \begin{Bmatrix} \mu \\ \nu \end{Bmatrix}, \quad (2.1)$$

where M_{μ} , M_{ν} are the sum of beam moments at the joint, and sum of column moments at the joint, respectively. The elastic shear stiffness K_{ej} of the joint panel zone is given by

$$K_{ej} = \frac{M_{yj}}{\gamma_{yj}} = Gd_b d_c t, \quad (2.2)$$

where M_{yj} and γ_{yj} are the yield distorsional moment and yield distorsional shear strain in the joint panel zone, respectively.

2.3.4 Design Recommendations

Based on experimental and analytical studies, researchers proposed design criteria for proportioning strength and stiffness of joint panel zones. The

recommendations are in the form of shear capacity of the joint panel zones or the thickness of the joint panel plate. A summary of these design criteria are discussed in the subsections below.

2.3.4.1 Fielding and Huang, 1971

The thickness t of the joint panel to prevent yielding under the action of anti-symmetrical beam moments and column axial load shall satisfy the condition

$$t \geq \frac{\sqrt{3} \left(\frac{M_r + M_l}{d_b} - V \right)}{\sigma_y d_c \sqrt{1 - \left(\frac{P}{P_y} \right)^2}}, \quad (2.3)$$

where M_l, M_r, V, P, d_b, d_c and t are explained in Figure 2.1; σ_y is the yield stress of steel; and P_y is the axial yield capacity of the column.

2.3.4.2 Krawinkler, 1978

The shear resistance V_u of the joint panel zone is given by

$$u = \begin{cases} 0.6 \sigma_y d_c t \left(1 + \frac{3.45 b_{cf} t_{cf}^2}{d_b d_c t} \right) & \text{for } P_u \leq 0.75 P_y \\ 0.6 \sigma_y d_c t \left(1 + \frac{3.45 b_{cf} t_{cf}^2}{d_b d_c t} \right) \left(1.9 - 1.2 \frac{P_u}{P_y} \right) & \text{for } P_u > 0.75 P_y \end{cases} \quad (2.4)$$

where

t = Total thickness of the joint panel zone (including that of doubler plates);

b_{cf} = Breadth of column flange;

t_{cf} = Thickness of column flange;

d_b = Depth of beam web;

d_c = Depth of column web;

P_u = Required axial strength of column;

P_y = Yield axial load capacity of column;

and σ_y = Yield stress of steel.

The above expression is adopted by design codes [UBC 94, AISC 91, SEAOC 88] with minor modifications.

2.3.4.3 Fukumoto and Lee, 1992

The shear resistance V_u of the joint panel zone is given by

$$V_u = \phi R_v \quad (2.5)$$

where

$$\phi = 0.9$$

$$R_v = \begin{cases} 0.6 \sigma_y d_c t & \text{for } P_u \leq 0.4 P_y \\ 0.6 \sigma_y d_c t \left(1.4 - \frac{P_u}{P_y} \right) & \text{for } P_u > 0.4 P_y \end{cases}$$

in which

t = Total thickness of the joint panel zone (including that of doubler plates);

d_c = Depth of column web;

P_u = Required axial strength of column;

P_y = Yield axial load capacity;

and σ_y = Yield stress of steel.

2.3.4.4 Tabuchi, et al, 1992

The panel yield ratio R_{py} shall satisfy the condition

$$0.6 < R_{py} < 1.0 \quad (2.6)$$

where

$$R_{py} = \frac{M_{py}}{\min \left\{ \left| M_{bp}^L + M_{bp}^R \right|, \left| M_{cp}^U + M_{cp}^L \right| \right\}},$$

in which

M_{py} = Yield distortional moment of joint panel zone

$$= Q_{py} d_b \frac{\left(1 - \frac{d_c}{L_b} \right)}{\left(1 - \frac{d_c}{L_b} - \frac{d_b}{L_c} \right)};$$

Q_{py} = Yield distortional shear of joint panel zone

$$= \frac{\sigma_y}{\sqrt{3}} d_c t \sqrt{1 - \left(\frac{P_u}{P_y} \right)^2};$$

d_c = Distance between centerlines of column flanges;

d_b = Distance between centerlines of beam flanges;

t = Thickness of joint panel zone;

P_u = Required axial strength of column;

P_y = Yield axial load capacity;

σ_y = Yield stress of steel;

M_{pb}^R, M_{pb}^L = Full plastic moments capacities of beams to the left and right of the joint, respectively; and

M_{pc}^U, M_{pc}^L = Full plastic moments capacities of columns above and below the joint, respectively.

L_b and L_c are defined in Figure 2.17.

2.4 Codal Specifications for Design of Joint Panel Zones

The various specifications in seismic codes pertaining to the design of steel joint panel zones can be grouped into three sets. Each of these three sets is discussed in the sections below.

2.4.1 Shear Strength of Joint Panel Zone

Firstly, the shear strength V_u of the joint panel zone shall be given by

$$V_u = 0.55 \sigma_y d_c t \left(1 + \frac{3.45 b_{cf} t_{cf}^2}{d_b d_c t} \right). \quad (2.7)$$

And the required shear strength V_{req} shall be estimated by

$$V_{req} = \frac{\Delta M}{d_b}. \quad (2.8)$$

Different codes give different definitions for ΔM in Eq.(2.8). These definitions fall into three broad categories. These are:

(a) *Strong Panel Zones* [SEAOC 80]

$$\Delta M = M^l + M^r = \sum M_{pb}. \quad (2.9)$$

(b) *Intermediate Strength Panel Zones* [NZ 88; SEAOC 88; AISC 91; UBC 94]

$$\Delta M = \sum M_{pb} - 2 M_g \approx 0.8 \sum M_{pb} \quad (2.10)$$

(c) *Minimum Strength Panel Zone* [SEAOC 88, AISC 91, UBC 94]

$$\Delta M = \sum_{beam} (M_g + 1.85 M_e), \quad (2.11)$$

where $\sum M_{pb}$ is the sum of plastic moment capacities of beams meeting at that joint, M_g is the moment developed in beam at the end due to gravity load, and M_e is the moment developed in beam due to earthquake forces.

However, Eq.(2.7) was proposed [Krawinkler, 1978] as an empirical estimate for the ultimate strength of the joint at a shear strain of 4γ . However, the experimental investigations [Kato and Nakao, 1973] show an extended range of stable inelastic behaviour. Hence, the use of this expression for either the yield strength or the ultimate strength of the joint panel seems inconsistent [Murty, 1992].

2.4.2 Thickness of Joint Panel Zone Plate

The second specification ensures that the thickness of the panel zone plate is such that buckling of the panel plate under shear is avoided. The panel zone plate thickness t shall conform to the following inequality [AISC 91; UBC 94]

$$t \geq \frac{d_z + w_z}{90}, \quad (2.12)$$

where

$$d_z = d_b - t_{bf},$$

and $w_z = d_c - t_{cf}.$

In Eq.(2.12), t_{bf} and t_{cf} thickness of beam flange and of column flange, respectively.

2.4.3 Relative Strengths of Columns, Beams and Joint Panel Zones

The third specification controls the relative proportions of the strengths of the beams, columns and joints at any joint in a MRF.

2.4.3.1 UBC 94 and SEAOC 88

In the case of semi-rigid frames, in which joint panel zones are allowed to yield before the beams reach their plastic moment capacities, the commonly used *strong-column weak-beam* design philosophy of rigid jointed frames is amended to the *strong-column weak-beam and weaker-joint* design philosophy. The codes require that the following relations be satisfied at each joint :

$$\frac{\sum Z_c(f_y - f_a)}{\sum M_{pb}} \geq 1.0 \quad (2.13)$$

and
$$\frac{\sum Z_c(f_y - f_a)}{M_{py}} \geq 1.25 \quad (2.14)$$

where

Z_c = Plastic section modulus of column,

f_y = Yield stress of steel,

f_a = Axial stress in column,

M_{py} = Yield distortional moment capacity of the joint panel zone,

and M_{bp} = Plastic moment capacity of beam.

2.4.3.2 AISC 91

At any joint, at least one of the following inequalities shall be satisfied:

$$\frac{\sum Z_c \left(F_{yc} - \frac{P_{uc}}{A_g} \right)}{V_u d_b \frac{H}{H - d_b}} \geq 1.0, \quad (2.15)$$

and

$$\frac{\sum Z_c \left(F_{yc} - \frac{P_{uc}}{A_g} \right)}{\sum Z_b F_{yb}} \geq 1.0 \quad (2.16)$$

where

A_g = Gross cross sectional area of a column;

F_{yb} = Specified minimum yield strength of a beam;

F_{yc} = Specified minimum yield strength of a column;

H = Average of the storey heights above and below the joint;

P_{uc} = Required compressive axial strength in the column (taken to be positive);

V_n = Nominal shear strength of panel zone;

Z_b = Plastic section modulus of beam;

Z_c = Plastic section modulus of column;

and d_b = Average overall depth of beams framing into the joint.

These inequalities do not apply in case of columns with $P_{uc} < 0.3 F_{yc} A_g$, and in case of columns in any storey that have a ratio of design shear strength to the design shear force 50% greater than that in the storey above.

2.4.4 Indian Codes

The Indian codes pertaining to seismic design of steel structures [IS:1893-1984; IS:4326-1993; IS:800-1984] do not address the issue of joint flexibility. There

are no design provisions associated with either the strength or the stiffness of joint panel zones.

2.5 Conclusions

The behaviour, analysis and design of joint panel zones as recorded in the literature emphasizes the following salient points:

- (1) Experimental and analytical investigations show strong dependence of the seismic performance of steel MRF on the joint panel zone design.
- (2) The importance of energy dissipation along with the strength-based design of joint panel zone is recognized. However, this observation is based only on analytical studies limited to monotonic loading conditions. It is necessary to study this aspect also from the point of view of cyclic loading.
- (3) The effect of axial load on the strength of the joint panel zones is negligible when the axial load on column is less than 50% of its axial yield strength.
- (4) The expressions given in literature for the design of joint panel zone are based on the behaviour of a typical exterior joint panel zone in a MRF. It is assumed that the behaviour of exterior joint panel zones is similar to that of interior panel zone. However, the loading on exterior joints is not similar to that on interior joints. More studies are required to study the effect of exterior joint panel zone design on the overall performance of MRFs, especially from energy dissipation point of view.
- (5) The current strength-based design approach for joint panel zones needs to be reviewed in light of the hysteretic energy dissipation characteristics of MRFs.

Chapter 3

PARAMETERS INFLUENCING SEISMIC RESPONSE OF MRFs

3.0 General

How well an MRF responds during an earthquake depends on how much of the energy input at its base can be dissipated (or absorbed) by it. Clearly, the factors that influence this energy dissipation will be many. The components that participate in the energy dissipation are beams, columns, walls, slabs, joint panel zones at the beam-column junctions, and non-structural elements. While the structural components participating in the seismic performance of MRFs are few, the infinite possibilities of proportioning these components, from both strength and stiffness points of view, require a careful consideration of the practical values. Further, the structural components are subjected to loads whose magnitude vary over a wide range, along with their sense. With numerous possibilities for loading and of component strength and stiffness, it is of interest to see how some of the major factors influence the seismic behaviour of MRFs. Since the current study focuses on the design of joint panel zones, in particular, the variations may be evaluated in light of the joint panel zone designs.

Experiments showed [Hanson, 1966] that in most cases the dynamic hysteresis curves are more or less similar to the static hysteresis curves. So, the energy dissipation characteristics of MRFs under dynamic loading can be well understood by studying the hysteresis curves under *pseudo-static* but cyclic loading. Further, a general multi-storey frame can be considered to be a collection of storey sub-

assemblages. Each of these storey sub-assemblages contributes to the seismic energy dissipation of the overall frame. In this chapter, the energy dissipated E_d in one complete hysteresis loop under pseudo-static loading of the simplest storey-subassemblage structure namely single-storey portal frames with fixed base is studied, with a view to demonstrate the influence of the various parameters.

3.1 Hysteretic Behaviour Under Pseudo-Static Cyclic Loading

The energy dissipated in the first complete hysteresis loop of the lateral load H versus lateral displacement Δ curves (Figure 3.1) is studied. This loop basically consists of five segments namely positive loading path OA, positive unloading path AB, negative loading path BC, negative unloading path CD, and positive re-loading path DE. The energy that is absorbed in one complete cycle of loading, neglecting the initial loading path OA, is given by the area enclosed by loop segments ABC and CDE of the H - Δ curve.

In order to benchmark the parametric study, a specified maximum storey drift is maintained in all cases, irrespective of the beam, column or joint panel designs. This maximum drift is achieved in the initial loading path OA. In the negative direction of loading, this maximum storey drift may or may not be achieved, since the hysteretic loop is formed by considering equal maximum lateral force excursion.

3.2 Analysis of Steel Planar MRFs with Joint Elements

In the present study, the analytical models of beams, columns and joint panel zones are taken from the literature [Murty and Hall, 1994; Hall and Murty, 1995]. In

the parametric study, the *Plastic Hinge Model* is used for columns and beams, and the *Ellipsoidal Joint Hysteresis Model* is used for joint panel zones.

The available computer programme DNA2 for the small-strain and large-displacement analysis of planar steel MRFs with joint elements [Murty, 1992] is used in this thesis to conduct various analytical studies. This programme considers the joint panel zones as separate structural elements. The computer programme DNA2 is custom made for force control method of analysis. However, in order to achieve a specified maximum storey drift in the initial loading path OA (Figure 3.1), displacement control is required. This difficulty is overcome by iteratively ascertaining the maximum lateral force that would produce the required lateral storey drift in the initial loading path OA. Once this is known, the computer programme with force control is used. However, the load is applied gradually. For each of the segments OA, AB, BC, CD and DE, 100 load steps are used.

3.3 Parameters and their Variation

Amongst the factors that may influence seismic response of MRFs, some important ones are discussed in this section.

3.3.1 Axial Force in Columns

The axial force appears in the column due to both gravity loads and lateral loads. The axial force in a column due to gravity loads on the MRF remains constant throughout the loading, and the axial load due to overturning caused by the lateral load fluctuates in proportion to the lateral load. Since the magnitude of the lateral load due

to earthquake shaking is not known exactly, the influence of axial force has to be studied over the possible range of values.

In case of portal frames, the column axial load due to the lateral load is implicitly obtained through large deformation analysis. However, in case of storey sub-assemblages discussed in Chapter 4, the gravity axial load obtained as the sum of the gravity load acting on that storey and of the gravity loads transferred from the storeys above the storey sub-assemblage under consideration. And, the axial load due to the lateral load is estimated from the lateral loads acting at floors above the storey sub-assemblage under consideration.

3.3.2 Ratio R_{bc} of Beam and Column Plastic Moment Capacities

The *strong-column weak-beam* philosophy requires that, at any joint, the sum $\sum M_{pc}$ of full plastic moment capacities of columns be more than the sum $\sum M_{pb}$ of full plastic moment capacities of beams. Hence, their ratio R_{bc} , given by

$$R_{bc} = \frac{\sum M_{pb}}{\sum M_{pc}}, \quad (3.1)$$

shall always take values less than unity.

The effect of R_{bc} is studied by analyzing MRFs with different beams and columns moment capacities. In the case of multi-bay MRFs or the storey sub-assemblages, the above ratio needs to be controlled at exterior joints as well as at interior joints. And, in case of single-bay, single-storey portal frames that are symmetric, this issue does not arise.

3.3.3 Ratio R_{jb} of Joint Distorsional Yield Moment Capacity and Beam Plastic Moment Capacities

In order to decide the relative strengths of joint panel zones with respect to that of beams, a ratio R_{jb} of the yield joint distorsional moment M_{yj} and the sum $\sum M_{pb}$ of full beam plastic moment capacities,

$$R_{jb} = \frac{M_{yj}}{\sum M_{pb}} \quad (3.2)$$

draws prominence. This effect can be studied easily by analyzing MRF of different joint panel zone designs. In the case of multi-bay MRFs or the storey sub-assemblages, this ratio to be controlled at both the exterior joints as well as the interior joints. Again, in case of single-bay single-storey portal frames that are symmetric, there is only one ratio. Here, by different joint panel zones designs, it is meant that the thickness of the joint panel zone plate is varied; the depth of beam d_b and depth of column d_c are not varied. Thus, the yield distorsional joint moment M_{yj} considering the plate alone, which is given by

$$M_{yj} = \frac{\sigma_y}{\sqrt{3}} d_b d_c t, \quad (3.3)$$

varies linearly with t .

3.4 Response Quantities of Interest

The response quantities of interest are energy dissipation E_d , lateral force H , and normalized energy dissipation E_{dn} . The effect of the above quantities are studied as a function of joint panel zone design.

3.4.1 Energy Dissipation E_d

The lateral load H *versus* lateral displacement Δ curves shown in Figure 3.1 reflect the overall characteristics of the MRF and not just those of the joint panel zone. Thus, inelasticities developed in the beams and columns also get duly reflected in these curves. It is the relative stiffness and strength proportion of these components and joints that decides their share of inelastic effects. In general, very stiff joints lead to much smaller hysteresis loops. On the contrary, very flexible joints lead to large lateral drifts. Thus, a need arises to balance the joint design to balance the energy dissipation E_d (Figure 3.1) and maximum lateral drift Δ_{max} .

The energy dissipation is normalized as per

$$E_{dn} = \frac{E_d}{E_s}, \quad (3.4)$$

in which E_s is the linear static energy associated with the initial loading path OA in the lateral load H *versus* lateral displacement Δ curves. The geometrical definition of E_s is shown in Figure 3.3.

3.4.2 Lateral Force H

In the present analytical study, in order to benchmark all studies to a common platform, the cyclic response is considered under a specified maximum lateral drift of $35mm$. The amount of lateral load required to achieve this specified lateral drift depends not only on the relative strengths and stiffnesses of beams and columns but also on the joint panel zone designs.

3.5 Numerical Study

The influence of each parameter and its effect on the behaviour of MRFs is demonstrated through the simplest MRF, namely a single-bay single-storey portal frame with columns fixed at the base (Figure 3.2). Here, R_{bc} can be controlled as there is only one type of joints, namely exterior joints. Four cases of portal frames are considered. They are C1, C2, B1 and B2. In cases C1 and C2, the column section properties are kept constant. To get different values of R_{bc} , the beam section properties are changed (Table 3.1). However, in cases B1 and B2, the beam section properties are kept constant and for different values of R_{bc} , the column section properties are changed (Table 3.2). The study is carried out for different joint panel zones (Table 3.3). The loads applied are as shown in Figure 3.2. The values of the maximum lateral load H and the vertical nodal load P on each column are shown in Table 3.4.

3.6 Results and Discussions

The results of the parametric study are presented in the form of graphs of E_d , H and E_{dn} plotted as a function of the ratio R_{jb} for different values of R_{bc} and P . Here R_{jb} reflects the joint panel zone design.

3.6.1 Energy Dissipation E_d

The energy dissipation E_d increases with increase in R_{jb} and R_{bc} , in case C1 (Figure 3.4a). But, in case B1, E_d decreases with increase in R_{bc} (Figure 3.4b). This is

attributed to yielding of the columns at their base due to the decrease in their plastic moment capacity with increase in R_{bc} , and to the fact that the lateral load carrying capacity of MRF depends mainly on column section properties. However, the variation of E_d in B1 is irregular unlike in C1. This is attributed to the varying percentage of axial force in columns with respect to axial yield capacity with changing R_{bc} . By maintaining a constant (more or less) percentage of axial force in columns, the variation of E_d improved in case B2 (Figure 3.4d). But, the variation of E_d with increase in R_{bc} is not similar to that in case C1. E_d decreases once R_{bc} crosses certain value. So, there seems to be an optimum value of R_{bc} at which E_d is maximum. A more detailed investigation with varying amounts of column axial load is required to arrive at the best suited value of R_{bc} from energy dissipation point of view. By repeating the exercise of C1 with increased axial loads, the similar trend of variation in E_d with R_{jb} and R_{bc} is observed in case C2 (Figure 3.4c).

In all of the above cases, the energy dissipation is controlled by the sequence of the formation of hinges (Figure 3.5). In an MRF, the formation of hinges in column can be avoided by adopting *strong-column weak-beam* philosophy, but this philosophy does not fix the relative position of the strength of the joint panel zones. In fact, the sequence of formation of hinges in an MRF is controlled by the relative stiffness and strength of all its components. Consider the factor ρ for each component given by

$$\rho = \frac{M}{M_p^r}, \quad (3.6)$$

where

$$M = \begin{cases} \text{Bending moment developed due to applied external loads} \\ \text{in case of beams and columns} \\ \text{Distorsional moment developed due to applied external loads} \\ \text{in case of joint panel zones} \end{cases}$$

and

$$M_p^r = \begin{cases} \text{Reduced moment capacity due to applied external loads} \\ \text{in case of beams and columns} \\ \text{Yield distorsional moment capacity (Eq. (3.3))} \\ \text{in case of joint panel zones} \end{cases}$$

This factor may be calculated at the ends of all beams and columns, and at all joints in the MRF. The sequence of formation of hinges starts with the location with the largest value of ρ and follows to the locations with decreasing values of ρ .

3.6.2 Lateral Force H

The lateral force H increases with increase in R_{jb} and R_{bc} in both cases C1 and C2 (Figures 3.6a and 3.6c). However, in cases B1 and B2, H decreases with R_{bc} (Figures 3.6b and 3.6d). This happens because of the lateral load carrying capacity of the portal frame depends on column section properties, and because the column plastic moment capacity decreases with increase in R_{bc} in cases B1 and B2. The lateral force H in case C2 is lesser than that in case C1. This is attributed to the fact that the MRF softens when the compressive axial force in column increases. However, an increase in the lateral force H with increase in R_{jb} is observed in all cases when the joint panel zone is flexible. But, once the joint panel zone attains a certain degree of rigidity, the increase in lateral force is almost negligible. This is attributed to the increase in rigidity of joint panel zone causing an increase in the rotations in columns

and beams to attain the required lateral displacement. This ultimately causes the formation of plastic hinges first in beams and then in columns.

3.6.3 Normalized Energy Dissipation E_{dn}

The normalized energy dissipated E_{dn} shows the combined effect of E_d and the smooth variation of H (Figures 3.7a, 3.7b, 3.7c and 3.7d). When the joint panel zone becomes rigid, the change in E_d and H are marginal. Thus, E_{dn} follows the same trend.

3.7 Conclusions

The following are the broad observations of the parametric study presented above :

- (1) E_d increases with increase in R_{py} . But, when the joint panel zone attains certain degree of rigidity, the increase in E_d with increase in R_{py} is almost negligible.
- (2) E_d depends on R_{bc} . There is an optimum value of R_{bc} where the E_d is maximum.
- (3) The little effect of axial load P on E_d is little, but is considerable on lateral force H .
- (4) Since E_d depends on both R_{bc} and P , a more detailed study is required to arrive at ideal values of R_{bc} which maximises E_d without significantly increasing the lateral drift. It is, however, recognised that the axial load P in columns varies over a very large range during strong seismic energy shaking of the building.
- (5) E_d is controlled by the sequence of formation of hinges, which is in turn controlled by the stiffness and strength of the MRF components and the applied loads.

(6) There is no beneficial effect of increasing R_{jb} beyond 1.0 insofar as maximizing the energy dissipation is concerned. This implies that the joint panel zones must yield before the beams. Thus, *strong-column weak-beam and weaker joint* philosophy seems preferable.

• • •

Chapter 4

ENERGY CONSIDERATIONS IN DESIGN OF MRFs

4.0 General

The basic attempt in the seismic design of MRFs is to arrive at a structure that can withstand the lateral loads generated during expected seismic shaking and safely dissipate the seismic energy input to it without collapsing. Thus, both lateral strength and energy dissipation characteristics are important. Thus far, in the literature, very little research is actually devoted to the study of seismic response of steel planar MRFs *vis-a-vis* energy dissipation characteristics. In particular, the seismic energy dissipation characteristics of MRFs with different joint panel designs has not been addressed.

The nonlinear analysis of a complete frame is computationally intensive and time consuming, and hence cannot be used for investigating the above aspects. Since the complete frame consists of a number of storey sub-assemblages, the energy dissipation characteristics of the complete frame can instead be studied from the point of view of joint panel zone designs through these individual storey sub-assemblages. Since the number of joint panel zones and members in a storey sub-assemblage are few, the contribution of the joint panel zone to the overall energy dissipation characteristics can be pin pointed relatively easily. In the literature, typical joint sub-assemblages have been used in experimental studies as discussed in Chapter 2. And, for the purpose of the analytical studies, the use of storey sub-assemblages has been recommended [Fielding, 1994; Nagar and Murty, 1995]. They consist of the set of

beams, columns and joint panel zones present at a floor level. The interaction between these sub-assembly components plays a prominent role in its energy dissipation.

4.1 Storey Sub-Assemblages

Consider the planar frame of a typical multistorey building shown in Figure 4.1. A typical storey sub-assembly is highlighted in the figure. It consists of the columns of half the storey height from the storey above and below the floor under consideration, beams at that floor level, and the beam-column joint panel zones at that floor level.

Usually, in regular frames, the sizes of beams at different floor levels are reasonably similar. Thus, the rotational restraints offered by these beams to the columns at the floor levels are of the same order. Given this, it is reasonable to say that when the frame is subjected to lateral loads at the floor levels, the points of contraflexure are around the mid-heights of the columns. Thus, the storey sub-assembly is chosen to consist of only half the column from the storeys above and below (Figure 4.2), and the column stubs are taken as hinged at the far ends. Since the cyclic *relative* lateral response within the storey sub-assembly is of interest, the column stubs below the floor are taken to be restrained against translation at their base. The top ends of the column stubs above the floor are permitted lateral and vertical translation, and rotation degrees of freedom. However, these top ends of column stubs are imposed the condition of equal lateral translation. In the original complete frame, this may not be exactly true. Nodes at mid-heights of columns within a storey may translate by different amounts, depending on the extent of rigid diaphragm action of the floor slab and the rotational restraint offered by the beams.

4.2 Parameters Considered in Numerical Study

The present study concentrates on the cyclic behaviour of storey sub-assemblages under pseudo-static loading from the point of view of interior and exterior joint panel zone designs. Both in the literature, as well as in the codes, the design of exterior joint panel zones are not adequately addressed. As discussed in Chapter 2, the design provisions included in codes for joint panel zones are based on typical interior joint panel zone behaviour gathered from experimental and analytical studies.

The parameters considered in this study are discussed in Chapter 3. They are axial force P in columns, ratio R_{bc} of sums of beam and column moment capacities, and ratio R_{jb} of yield distortional joint moment capacity and sums of plastic moment capacity of beams. Amongst of these, the axial load in the column is not completely within the control of designer as depends on the level of seismic shaking. However, R_{bc} and R_{jb} can be controlled through the design of the columns, beams and joint panel zones (both interior and exterior).

4.3 Numerical Study through Example Storey Sub-assemblages

To demonstrate the influence of the strength and stiffness of the different components (*i.e.*, beams, columns and joint panel zones), three storey sub-assemblages from three different levels of a 20-storey planar MRF extensively used in literature (Figure 4.3), are considered. These three sub-assemblages, the geometries and section properties of which are shown in Figure 4.4, are taken from floors 19, 10 and 2, and will, hereinafter, be referred to as SSA-T, SSA-M and SSA-B, respectively. Table 4.2 gives the cross-section properties of the components in each of these sub-assemblages.

4.3.1 Specified Drift

In the analytical study, the lateral load that can be applied on the sub-assembly is arbitrary. However, in order to benchmark all studies to a common platform, the cyclic response of storey sub-assemblies are considered under a specified maximum lateral drift. For a storey height h of 3810 mm, the maximum design inter-storey displacements as per the different codes are given below:

(a) *UBC 94 and IS:1893-1984*

$$\text{Elastic maximum displacement limit } \Delta_{max} = 0.004h = 15\text{ mm} \quad (4.1)$$

(b) *AISC 91*

$$\begin{aligned} \text{Design maximum displacement limit under severe seismic conditions} \\ \Delta_{max} = 0.01h = 38\text{ mm} \end{aligned} \quad (4.2)$$

(c) *UBC 94*

$$\text{Design limit under ultimate condition } \Delta_{max} = \left(\frac{3}{8} R_w\right) 0.004h = 34\text{ mm} \quad (4.3)$$

assuming a Response Modification Factor R_w of 6 for ordinary MRFs.

However, in the sub-assemblies chosen, it may be difficult to achieve an inter-storey displacement of about 40 mm in for all joint designs. Some sub-assemblies may not possess enough lateral strength and/or ductility and may fail well before the above displacement is imposed. Keeping in view the sub-assemblies being studied, an inter-storey drift of 30 mm is chosen as the benchmark value.

4.3.2 Loads in Columns and Beams

The gravity load in a column of a storey sub-assembly under consideration is estimated (considering a UDL of 20 kN/m due to dead and live load on all beams) at

stories above the storey sub-assembly under consideration. The cyclic component of axial load on columns generated by the cyclic lateral seismic ground acceleration at the base of the MRF is taken arbitrarily, though guided by the literature [Goel, 1969]. The maximum fluctuating axial load on the exterior column is taken as 30% of its yield axial capacity. And, the fluctuating component of the axial load on the interior and exterior columns are taken in the proportion of 1:3, keeping in the mind their relative locations and axial stiffnesses. Table 4.1 shows these values. Figure 4.5 shows the various loads considered on the sub-assemblages studied.

4.3.3 Exterior and Interior Joint Panel Designs

In the present study, the energy dissipated E_d in one complete cycle by the storey sub-assembly is studied. The ratio R_{jb} of yield distortional joint moment capacity to the sum of the plastic moment capacities of the beams meeting at that joint is a critical factor representing the joint panel design. The minimum value of R_{jb} is calculated based on available column web thickness. However, for the purpose of analytical study, the minimum value of R_{jb} is taken as 0.5, which may in some cases imply a value of the joint panel zone plate which is much below the available column web thickness. This case helps in considering alternate column sections with web thickness smaller than the ones chosen.

4.4 Analysis

The analysis of the storey sub-assemblages carried out as explained in section 3.2, except that *Fibre Model* beam-column elements are used for time history analysis

instead of the *Plastic Hinge Model* beam-column elements [Murty and Hall, 1995]. This choice of beam-column element is made to include the trend of gradual plastification of the beam and column section due to bending moments.

4.5 Responses of Interest

The results of the analysis of these sub-assemblages are presented in the form of graphs of energy dissipation E_d , lateral force H , normalized energy dissipation E_{dn} and normalized lateral force H_n , drawn as a function of R_{jb} . E_d , E_{dn} and H have been discussed earlier in section 3.4. The lateral force is normalized as per

$$H_n = \frac{H}{\sum V_{yj}} \quad (4.4)$$

where

H = Lateral force required for a specified drift in a storey sub-assemblage;
and $\sum V_{yj}$ = Sum of yield distortional shear capacity of all joint panel zones present in the storey sub-assemblage. The effect of joint panel zone design, of both interior and exterior joints, on the response quantities are obtained for each of the sub-assemblage.

4.6 Results and Discussions

The salient observations of the study on storey sub-assemblages are as under.

4.6.1 Energy Dissipation E_d

In the three sub-assemblages, the energy dissipation E_d (Figures 4.6, 4.7 and 4.8) increases as $(R_{jb})_E$ gets closer to 0.5 and $(R_{jb})_I$ gets closer to 1.0. Figure 4.9

shows the hysteresis loops of H vs Δ curves for the extreme combinations of exterior and interior joint panel zone designs of SSA-T. The above observation, that weak exterior joint panel zone design together with strong interior joint panel zone design produce large E_d , is graphically presented.

In storey sub-assemblages, the variation of energy dissipation is not smooth as in case of portal frames discussed in Chapter 3. This may be due to the complex interaction of various factors which are not possible to control in storey sub-assemblages, like unequal amount of axial force present in the columns due to the various loads applied on the sub-assemblage and unequal values of R_{bc} at interior and exterior joints.

4.6.2 Lateral Force H

In case of storey sub-assemblages, the lateral force capacity H increases with increase in joint panel thickness (Figures 4.10, 4.11 and 4.12). But, the increase is more with increase in $(R_{jb})_E$ than with increase in $(R_{jb})_I$. However, the increase in H is marginal once the joint panel zone attains sufficient rigidity. This is true individually for both exterior and interior joint panel zones, and also in the combined case. In some cases of rigid joint panel zone designs, it is observed that the storey sub-assemblage forms a mechanism even before achieving the specified drift.

4.6.3 Normalized Energy Dissipation E_{dn}

In the three sub-assemblages, the normalized energy dissipation E_{dn} (Figures 4.13, 4.14 and 4.15) show a similar trend as in E_d , but the trend is more gradual. This

is attributed to the smooth variation of lateral force H with respect to the exterior and internal joint designs.

4.6.4 Normalized Lateral Force H_n

The normalized lateral force H_n (Figures 4.16, 4.17 and 4.18) in the three sub-assemblages show a marginal increase with a decrease in the flexibility of exterior joint panel zone. It is, however, interesting to note that the normalized lateral force H_n in the maximum energy dissipation region, *i.e.*, $(R_{jb})_E = 0.6$ and $(R_{jb})_I = 0.8$ to 1.0, takes a constant value of about 0.21 to 0.23 in all the three cases of sub-assemblages.

4.7 Design Implications

The storey sub-assemblage study recommends that $(R_{jb})_E$ should be around 0.6, whereas $(R_{jb})_I$ should be around 0.8 to 1.0 for increased energy dissipation of MRF under cyclic load conditions. This observation is based on both energy as well as strength points of view. But, currently the codes recommend $(R_{jb})_E$ and $(R_{jb})_I$ as 0.8 based on only strength consideration. As mentioned earlier, the decrease in the lateral force capacity of storey sub-assemblage is very small by making exterior joint panel zone flexible. It is important to note that the normalized lateral force H_n is observed to be in the range of 0.21 to 0.23. Understandably, for higher range of ductility in the joint panel zone this could be marginally larger, say 0.25.

From the limited study conducted on the storey sub-assemblages, the following modification may be considered in the joint panel design based on energy as well as

strength considerations. The required design yield distortional shear strength V_{yj} of the joint panel zones at a particular floor can be calculated as

$$V_{yj} = \begin{cases} \frac{V_s}{H_n} \left(\frac{(R_{jb})_I}{N_i (R_{jb})_I + 2(R_{jb})_E} \right) & \text{for an interior joint panel zone} \\ \frac{V_s}{H_n} \left(\frac{(R_{jb})_E}{N_i (R_{jb})_I + 2(R_{jb})_E} \right) & \text{for an exterior joint panel zone} \end{cases} \quad (4.5)$$

where

V_s = Design storey shear,

H_n = Normalized lateral force factor to be used in design of joint panel zone

N_i = Number of interior joint panels present in a storey,

$(R_{jb})_E = 0.6$, and

$(R_{jb})_I = 0.8$ to 1.0 .

Here, the recommended value of H_n is based on normalized lateral force study, whereas the values of $(R_{jb})_E$ and $(R_{jb})_I$ based on energy dissipation study. Thus, this approach includes both strength and energy considerations.

4.8 Seismic Behaviour of 20-Storey Steel Planar MRF

The above design recommendations for joint panel zone design are based on pseudo-static cyclic loading. Since the earthquake ground motion is random and not cyclic, it is necessary to study these recommendations under dynamic earthquake-type loading. In this section, a 20-storey steel planar MRF (Figure 4.3) is subjected through four types of ground motions, three recorded and one synthetic. These ground motions are :

- (1) Elcentro 1940,
 - (2) Elcentro 1940 scaled by a factor of 1.5,
 - (3) San Fernando (Pacoima Dam) 1970,
- and (4) Synthetic Pulse (Figure 4.19).

Details of these ground motions are given in Table 4.3. The response spectra of these time histories are shown in Figure 4.20. The 20-storey MRF is analysed under each ground motion for four combinations of joint panel zone designs. These combinations are shown in Table 4.3. In the first three designs, the thickness of the joint panel is taken as the column web thickness, if the calculated thickness of the joint panel is less than the available column web thickness. However, for the purpose of analytical study, a fourth design is also studied. This design 4 is similar to design 2, except that the joint panel thickness is provided as per calculations, even though this value is sometimes less than the column web thickness. The loading and displacement boundary conditions of the 20-storey frame are taken from literature.

4.8.1 Results and Discussions

The salient points of time history responses of 20-storey steel planar MRF under each ground motion are presented in this section.

4.8.1.1 *El Centro*

The floor displacement response of design 1 (Figure 4.21a) and design 2 (Figure 4.21b) are more or less similar. But, the ductility demand on exterior joint panel zones at upper storey levels is larger in design 2. The design 4, the floor

displacement profile (Figure 4.21c) shows a small drop in the maximum roof displacement. The ductility demand on exterior joint panel zones (Figure 4.22) is considerably larger than that on interior joint panel zones throughout the MRF.

4.8.1.2 1.5 El Centro

The floor displacement response is more or less similar trend in design 1 (Figure 4.23a) and design 2 (Figure 4.23b) as observed under in El Centro ground motion. However, the displacements are understandably larger in case of design 2. And, the ductility demands for joint panel zones (Figure 4.24) are also increased considerably larger. But, in design 4, the maximum roof displacements (Figure 4.23d) decreases considerably with a marginal increase in ductility demands on exterior joint panel zones throughout the MRF. In design 3, the displacements at all floors (Figure 4.23c) of MRF are considerably larger.

4.8.1.3 San Fernando (Pacoima Dam)

For all designs of the joint panel zones, the complete MRF vibrated about non-zero mean displacement position. This plastic drift may be due to large velocity pulse in this earthquake. The designs 1, 2 and 4, gave more or less similar floor displacement responses (Figures 4.25a, 4.25b and 4.25d). In all the these three designs, the ductility demands on joint panels are very high (Figure 4.26), especially in the interior joint panel zones of the lower stories. But, in design 3, the maximum floor displacements decreased considerably (Figure 4.26c). This reduction may be due to the decrease in high ductility demands in the interior joint panels, especially in the lower stories of the

MRF. The number of plastic excursions of the MRF are fewer during the initial duration of motion, when compared to other combinations. The plastic excursions in the exterior and interior joint panel are shown in Figure 4.27

4.8.1.4 Synthetic Pulse

In synthetic pulse record the similar trend of response observed in all designs of joint panel zones (Figures 4.28a, 4.28b, 4.28c, 4.28d and 4.29) as in San Fernando record. This is because of the more or less similar characteristics of ground motion in both cases.

4.9 Conclusions

The following are some salient conclusions drawn from the above study:

- (1) The energy dissipation in an MRF depends strongly on the relative strength and stiffness of the structural members present in MRF.
 - (2) The effects of interior and exterior joint panels on energy dissipation are different.
 - (3) The procedure for the design of joint needs to be modified to include both energy dissipation as well as strength considerations.
 - (4) The joint design ratios $(R_{jb})_E$ and $(R_{jb})_I$ which cause maximum energy dissipation are about 0.6 and 0.8-1.0, respectively.
 - (5) In the design of MRFs, column sections which satisfy the strength requirements for both exterior and interior joint panel zones with minimum web thickness are preferable. Doubler plates, if required can be added without much difficulty. And such design of MRFs is also economical.
-

- (6) The design provisions given in various codes seems inadequate from the combined consideration of energy and as well as strength, especially in case of exterior joint panel zones.

• • •

Chapter 5

SUMMARY AND CONCLUSIONS

5.1 Summary

This thesis attempts to provide a design criteria for joint panel zones of steel planar moment-resisting frames (MRFs) under seismic loading conditions from energy dissipation as well as strength considerations. The following is a summary of the contributions of this thesis :

- (1) The importance of joint panel zones of a moment-resisting frame under cyclic loading conditions is understood from the literature. The factors that effect the cyclic behaviour are identified. Various models proposed in the literature for analytically simulating joint panel zones are studied. The *Ellipsoidal Joint Hysterisis Model* is identified for use in the present study.
 - (2) The influences of the various parameters that effect the energy dissipation in MRFs are studied through simple portal frames with different designs subjected to pseudo-static but cyclic loading conditions. The variation in energy dissipation in one complete hysteresis loop is observed with different joint panel designs.
 - (3) The energy dissipation characteristics of storey sub-assemblages are studied *vis-a-vis* exterior and interior joint panel designs, under pseudo-static but cyclic loading conditions. Again, the energy dissipation in one complete hysteresis cycle of the different exterior and interior joint panel zone designs are presented in the form of energy surfaces.
-

- (4) A new design approach for the design of exterior and interior joint panel zones based on energy dissipation and strength consideration is proposed.
- (5) The recommended design approach is evaluated through dynamic time history analyses of an example 20-storey steel planar moment-resisting frame under some recorded and synthetic ground motions.

5.2 Conclusions

The following are the salient conclusions drawn from the present study :

- (1) The design of joint panel zones based on energy dissipation as well as strength consideration is more realistic.
 - (2) The energy dissipation in MRFs depends very much on the relative strength and stiffness of its members, *i.e.*, columns, beams and joint panel zones. *Strong-column weak-beam weaker-joint* philosophy seems appropriate from energy considerations also.
 - (3) The sequence of formation of plastic hinges is identified as the key controlling factor for the energy dissipation of MRFs. •
 - (4) The influence of exterior joint panel zones are different from that of interior joint panel zones in MRFs from energy considerations.
 - (5) The drop in the lateral strength and stiffness of MRFs by employing the flexible exterior joint panel zones than currently proposed in the design codes is insignificant. These flexible exterior joint panel zones significantly increase the energy dissipation in MRFs under cyclic loading conditions.
 - (6) The ductility demand is significantly lower in the columns and beams of the frames if relatively more flexible exterior joint panels are used.
-

- (7) The design provisions in codes for joint panel zones are incomplete for exterior joint panel zones. Further, the code provisions need to be revised to include both strength as well as energy dissipation consideration.

5.3 Recommendations for Future Work

Based on this limited numerical study, the following specific issues seem significant for consideration as future work in this area:

- (1) The influence of the various parameters namely component strength and stiffness in the energy dissipation of MRFs needs to be studied in greater detail by considering wide range of frames.
- (2) The energy dissipation characteristics of storey sub-assemblages *vis-a-vis* exterior joint panel zones need to be studied for different number of bays in the parent MRFs.
- (3) The behaviour of corner joint panel zones in a multi-bay MRF needs to be studied from energy dissipation as well as strength point of view.
- (4) The range of values of the normalized lateral force and normalized energy dissipation with the joint panel zone designs can be more precisely estimated by studying more number of storey sub-assemblages in an MRF.
- (5) The performance of the proposed design recommendations can be ascertained through time history analysis for more types of MRFs under a large spectrum of recorded as well as synthetic ground motions.

• • •

REFERENCES

- AISC 1991, "Seismic Provisions for Structural Steel Buildings," American Institute of Steel Construction, Inc., Illinois, 1991.
- Becker, R., "Panel Zone Effect on the Strength and Stiffness of Steel Rigid Frames," *Engineering Journal*, AISC, Inc., New York, No.1, 1975, pp 19-29.
- Bertero, V.V., "Seismic Behaviour of Steel Beam-to-Column Connection Subassemblages," *Proceedings of Fourth World Conference on Earthquake Engineering*, Santiago, Chile, 1969.
- Bertero, V.V., Popov, E.P., and Krawinkler, H., "Beam-Column Subassemblages under Repeated Loading," *Journal of Structural Division*, ASCE, Vol.98, No.ST5, May 1972, pp 1137-1159.
- Fielding, D.J., "Frame Response Considering Plastic Panel Hinges," *Engineering Journal*, AISC, 1994, pp 31-37.
- Fielding, D.J., and Chen, W.C., "Steel Frame Analysis and Connection Shear Deformation," *Journal of Structural Division*, ASCE, Vol.99, No.ST1, January, 1973, pp 1-18.
- Fielding, D.J., and Huang, J.S., "Shear in Beam-To-Column Connections," *Welding Journal*, Welding Research Supplement, Vol.50, No.7, July, 1971, pp 313-326.
- Fukumoto, Y., and Lee, G.C., "Stability and Ductility of Steel Structures Under Cyclic loading," CRC Press, Inc., Boca Raton, 1992, pp 325-334.
- Goel, S.C., " $P-\Delta$ and Axial Column Deformation in Aseismic Frames," *Journal of Structural Division*, ASCE, Vol.95, No.ST8, August, 1968, pp 1693-1702.
- Hall, J.F., and Murty, C.V.R., "Beam-Column Behaviour," *Journal of Engineering Mechanics*, ASCE, Vol.121, No.12, December 1995, pp 1284-1291.
- Hanson, R.D., "Comparison of Static and Dynamic Hysteresis Curves," *Journal of Engineering Mechanics*, ASCE, Vol.92, No.EM5, October, 1966, pp 87-113.
- IS:1893-1984, "Indian Standard Criteria for Earthquake Resistant Design of Structure," *Bureau of Standards*, New Delhi, 1984.
- IS:800-1984, "Indian Standard Code for Practice for General Construction in Steel," *Bureau of Standards*, New Delhi, 1984.
- IS:4326-1993, "Indian Standard Earthquake Resistant Design and Construction of Buildings-Code of Practice," *Bureau of Standards*, New Delhi, 1993.
- Kato, B., "Beam-to-Column Connection Research in Japan," *Journal of Structural Division*, ASCE, Vol.108, No.ST2, February, 1982, pp 343-359.
- Kato, B., and Nakao, M., "The Influence of the Plastic Deformation of Beam-To-Column Connections on the Stiffness, Ductility and Strength of Open Frames," *Proceedings of Fifth World Conference on Earthquake Engineering*, Vol.1, Rome, Italy, 1973, pp 825-828.
- Krawinkler, H., "Shear in Beam-Column Joints in Seismic Design of Steel Frames," *Engineering Journal*, AISC., No.3, 1978, pp 82-91.
- Krawinkler, H., Bertero, V.V., and Popov, E.P., "Shear Behaviour of Steel Frame Joints," *Journal of Structural Division*, ASCE, Vol.101, No.ST11, November, 1975, pp 2315-2325.
-

- Krawinkler, H., and Popov, E.P., "Seismic Behaviour of Moment Connections and Joints," *Journal of Structural Division*, ASCE, Vol.108, No.ST2, February, 1982, pp 373-391.
- Lui, E.M., and Chen, W.F., "Analysis and Behaviour of Flexibly-Jointed Frames," *Engineering Structures Journal*, Butterworth & Co Ltd., Vol.8, April 1986, pp 107-118.
- Marsh, J.M., "Earthquakes: Steel Structures Performance and Design Code Developments," *Engineering Journal*, AISC, 1993, pp 56-65
- Murty, C.V.R., "Nonlinear Seismic Behaviour of Steel Planar Moment-Resisting Frames," *Report No. EERL 92-01*, California Institute of Technology, Pasadena, California, USA, 1992
- Murty, C.V.R., and Hall, J.F., "Earthquake Collapse Analysis of Steel Frames," *Earthquake Engineering and Structural Dynamics*, Vol.23, 1994, pp 1199-1218.
- Nader, M.N., and Astaneh, A., "Proposed Code Procedures for Seismic Design of Steel Semi-Rigid Frames," *Proceedings of Fifth U.S. National Conference on Earthquake Engineering*, Chicago, Illinois, Vol.2, July 1994, pp 381-391
- Nader, M.N., and Astaneh, A., "Seismic Behaviour and Design of Semi-Rigid Steel Frames," *Report No. UCB/EERC-92/06*, University of California at Berkeley, USA, 1992.
- Nagar, A., and Murty, C.V.R., "Joint Panel Zones as Seismic Fuses In Dissipation of Seismic Energy," *Bulletin of The Indian Society of Earthquake Technology*, Roorkee, Vol.32, No.1, March 1995, pp 17-32.
- Naka, T., Kato, B., Watabe, M., and Nakao, M., "Research on the Behaviour of Steel Beam-to-Column Connections in the Seismic-Resistant Structure," *Proceedings of The Fourth World Conference on Earthquake Engineering*, Santiago, Chile, 1969.
- NIST 1995, "A Survey of Steel Moment-Resisting Frame Buildings Affected by the 1994 Northridge Earthquake," *Report No. NISTR 5625*, United States Department of Commerce Technology Administration, Gaithersburg, USA, 1995.
- NZS 3404, "Code for Design of Steel Structures," *Standards Association of New Zealand*, Wellington, New Zealand, 1988.
- Popov, E.P., Bertero, V.V., and Krawinkler, H., "Moment-Resisting Steel Sub-assemblages under Seismic loadings," *Proceedings of Fifth World Conference on Earthquake Engineering*, Vol.2, Rome, Italy, 1973, pp 1481-1490.
- Popov, E.P., and Englehardt, M.D., "On Seismic Steel Joints and Connections," *Engineering Structures Journal*, Butterworth & Co Ltd., Vol.11, July, 1989, pp 148-162.
- Popov, E.P., and Pinkey, R.B., "Reliability of Steel Beam-To-Column Connections Under Cyclic Loading," *Proceedings of Fourth World Conference on Earthquake Engineering*, Santiago, Chile, 1969.
- SEAOC 1988, "Recommended Lateral Force Requirements and Commentary," Seismology Committee, Structural Engineers Association of California, San Francisco, California 1988.

- Tabuchi, M., Kanatani, H., Kamba, T., Yamanari, M., and Uemori, H., "Effect of joint zonels on elastic-plastic behaviour of moment resisting frames," *Proceedings of Tenth World Conference on Earthquake Engineering*, Madrid, Spain, 1992, pp 4491-4494.
- Tsai, K.C., and Popov, E.P., "Seismic Panel Zone Design Effect on Elastic Storey Drift in Steel Frames," *Journal of Structural Engineering*, ASCE, Vol.116, No.12, December, 1990, pp 3285-3301.
- Tsai, K.C., Shun, W., and Popov, E.P., "Experimental Performance of Seismic Steel Beam-Column Moment Joints," *Journal of Structural Engineering*, ASCE, Vol.121, No.6, June, 1995, pp 925-931.
- UBC 1994, Uniform Building Code, International Conference of Building Officials, Whittier, California, 1991.
- Vann, W.P., Thompson, L.E., Whally, L.E., and Ozier, L.D., "Cyclic Behavior of Rolled Steel Members," *Proceedings of Fifth World Conference on Earthquake Engineering*, Vol.1, Rome, Italy, 1973, pp 1187-1193.
- Vasquez, J., Popov, E.P., and Bertero, V.V., "Earthquake Analysis of Steel Frames with Non-Rigid Joints," *Proceedings of Fifth World Conference on Earthquake Engineering*, Vol.1, Rome, Italy, 1973, pp 1752-1756.
- Wakabayashi, M., Matsui, C., Minami, K., and Mitani, I., "Inelastic Behavior of Steel Frames Subjected to Constant Vertical and Alternating Horizontal Loads," *Proceedings of Fifth World Conference on Earthquake Engineering*, Vol.1, Rome, Italy, 1973, pp 1194-1197.

Table 3.1: Details of cross section properties of beams and columns in structure cases C1 and C2.

Member	EA (10^5 kN)	EI (kN m ²)	P_y (kN)	M_p (kN m)	R_{bc}
Column	9.66	10070	1210	115.3	--
Beam	11.62	8000	1453	115.3	1.00
	10.52	7350	1315	104.6	0.90
	9.36	6420	1170	91.7	0.80
	8.50	5710	1063	82.0	0.70
	7.91	5200	989	75.0	0.65
	7.34	4760	918	68.8	0.60
	6.32	3900	790	57.1	0.50

Table 3.2: Details of cross section properties of beams and columns in structure cases B1 and B2.

Member	EA (10^5 kN)	EI (kN m ²)	P_y (kN)	M_p (kN m)	R_{bc}
Beam	6.32	3900	790	57.1	--
Column	5.70	4610	713	57.1	1.00
	6.13	5220	767	63.5	0.90
	6.53	5930	828	70.9	0.80
	7.35	6940	919	81.7	0.70
	7.77	7510	972	87.8	0.65
	8.29	8180	1036	95.1	0.60
	9.56	10010	1195	114.2	0.50

Table 3.3: Details of joint panel zone plate considered in the study.

Joint Dimensions (mm)			M_{jy} (kN m)
d_c	d_b	t	
250	200	8	57.7
250	200	10	72.2
250	200	12	86.6
250	200	14	101.0
250	200	16	115.5
250	200	18	129.9
250	200	20	144.3

Table 3.4: Details of vertical nodal load P in each structure case studied.

Case	Vertical Nodal Load	
	$P(kN)$	P/P_{yc}
C1	350	0.29
C2	424	0.35
B1	350	*
B2	*	0.29

* Column sections change

Table 4.1: Details of loading and strength parameters of the sub-assemblages studied

Sub- assemblage		R_{bc}	R_{jb}	Axial Load ($\%P_{yc}$)			Bending Moment (kN m)
				Gravity		Earth quake	
				P_{top}	P_{floor}		
SSA-T	I	0.86	0.40-1.35	4.2	2.1	8.9	0.0
	E	0.73	0.47-1.35	2.4	1.2	30.0	62.0
SSA-M	I	0.81	0.40-1.15	17.5	1.6	15.9	0.0
	E	0.39	0.50-1.20	5.5	0.5	30.0	62.0
SSA-B	I	0.56	0.50-1.00	25.6	1.4	19.4	0.0
	E	0.26	0.50-1.60	6.6	0.4	30.0	62.0

Table 4.2: Details of members cross sectional properties of the sub-assemblage studied

Sub-assemblage	Section	EA (kN)	EI (kN m ²)	P_y (kN)	M_p (kN m)
SSA-T	W14X132	5006400	127370	6258	958.64
	W24X146	5548400	381270	6936	1712.45
	W14X109	4129000	103230	5161	786.58
	W21X122	4632000	246410	5790	1257.71
	W30X99	3755000	332150	4694	1278.19
SSA-M	W14X257	9755000	283080	12194	1995.12
	W24X162	6154800	430380	7694	1917.29
	W30X116	4412900	410400	5516	1548.59
SSA-B	W14X370	14064500	452860	17581	3015.22
	W30X191	7238700	763370	9048	2757.12
	W30X116	4418900	410410	5516	1548.58

Table 4.3: Details of earthquake ground motions and the interior and exterior joint panel designs used in the storey

No.	Earthquake Ground Motion	R_{jb}		Peak Parameters			Duration (sec)
		I	E	PGA (g)	PGV (m/sec)	PGD (m)	
EC1 EC2 EC3	El Centro	0.8 0.8 0.8*	0.8 0.6 0.6*	0.348	0.334	0.109	50
1.5EC1 1.5EC2 1.5EC3 1.5EC4	1.5 El Centro	0.8 0.8 1.0 0.8*	0.8 0.6 0.6 0.6*	0.522	0.501	0.164	50
SF1 SF2 SF3 SF4	Pacoima Dam (San Fernando)	0.8 0.8 1.0 0.8*	0.8 0.6 0.6 0.6*	1.170	-1.132	0.377	20
SP1 SP2 SP3 SP4	Synthetic Pulse	0.8 0.8 1.0 0.8*	0.8 0.6 0.6 0.6*	0.410	2.000	2.000	20

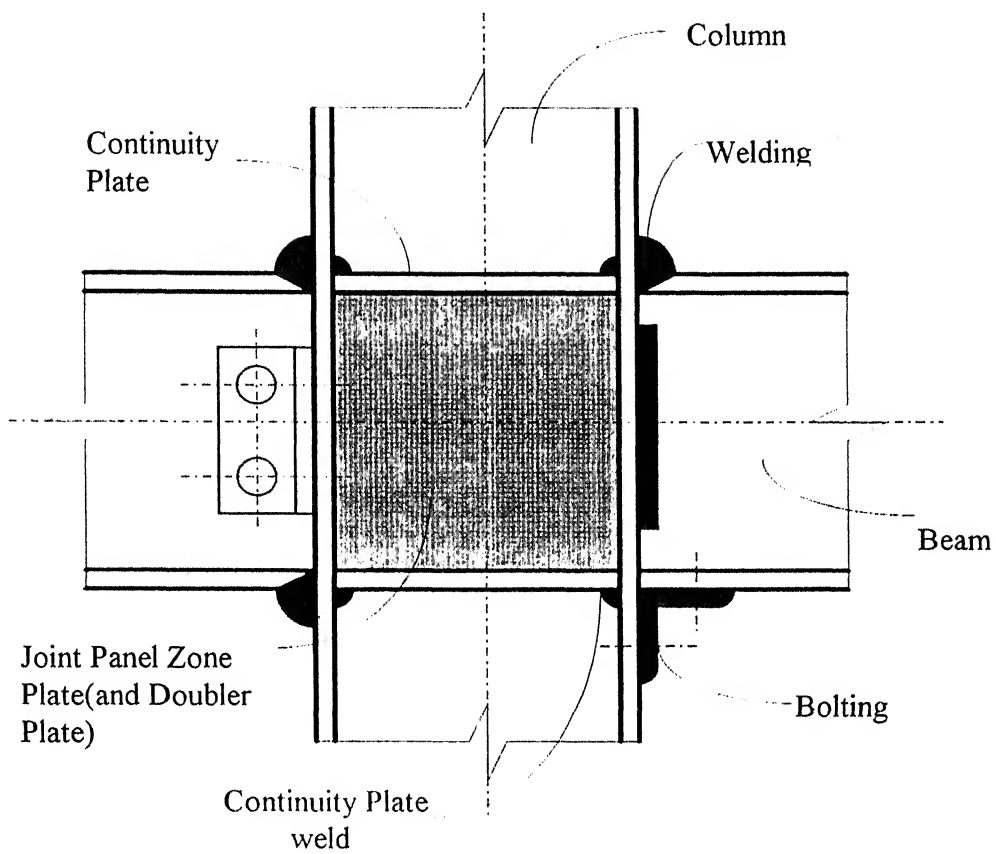


Figure 1.1: A schematic view of a typical interior joint panel zone region of a steel MRF.

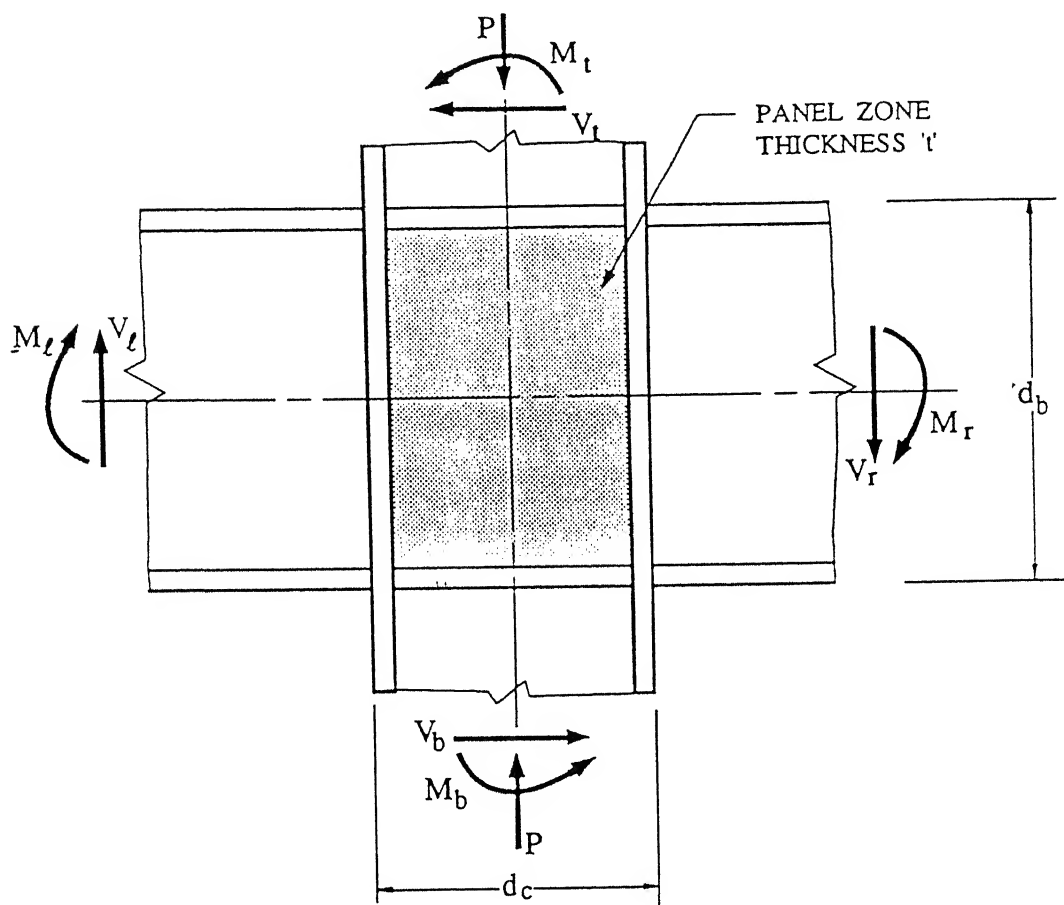


Figure 2.1 : Loads transferred through a planar joint panel zone.

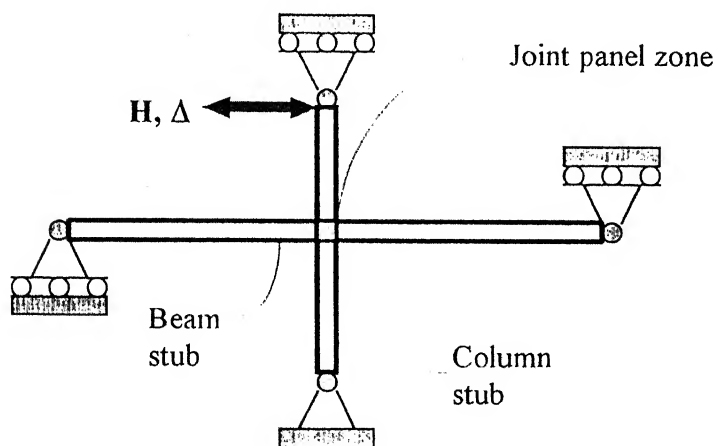


Figure 2.2: Typical joint sub-assemblages experimentally tested by past researchers.

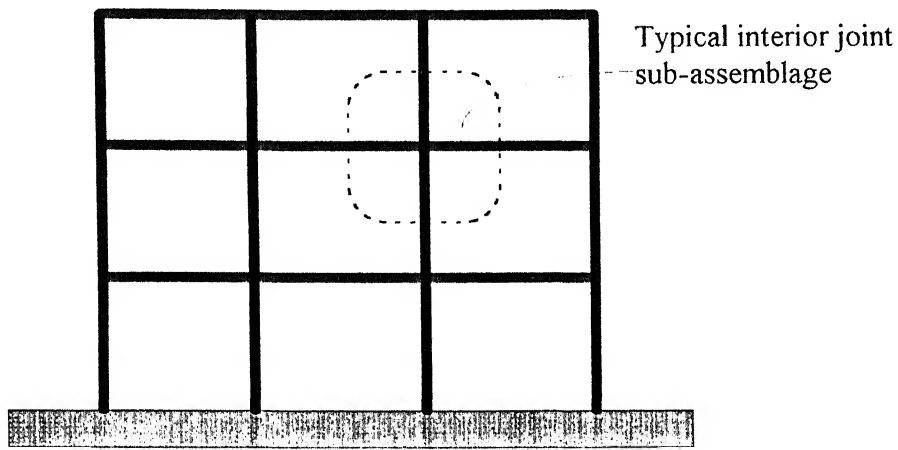


Figure 2.3: Typical interior sub-assembly of a frame structure considered in experimental and analytical studies by various researchers.

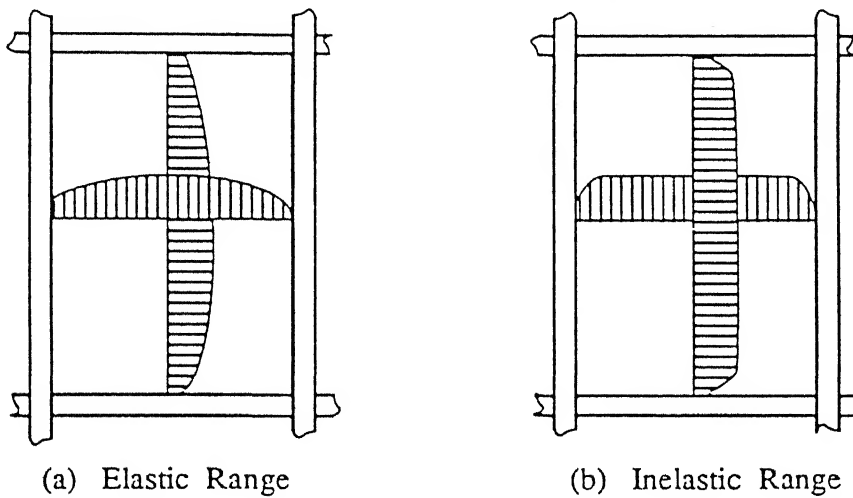


Figure 2.4: Shear distribution in a planar joint in the (a) elastic range, and (b) inelastic range.

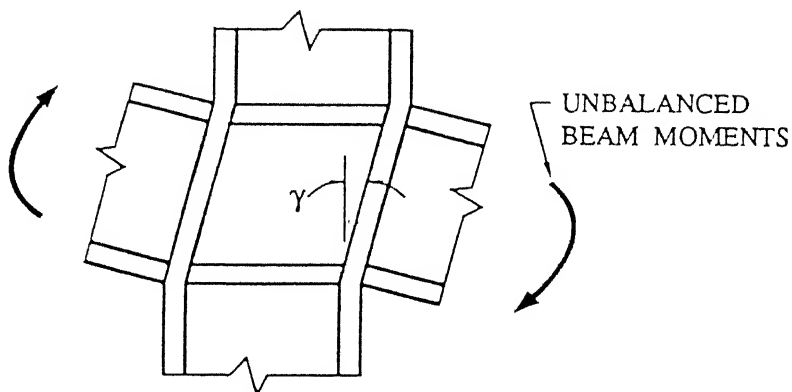
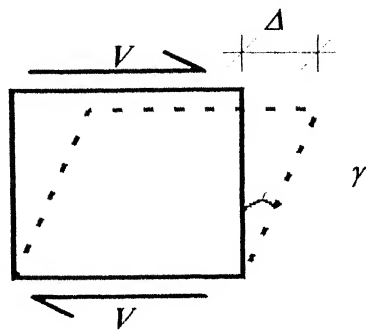
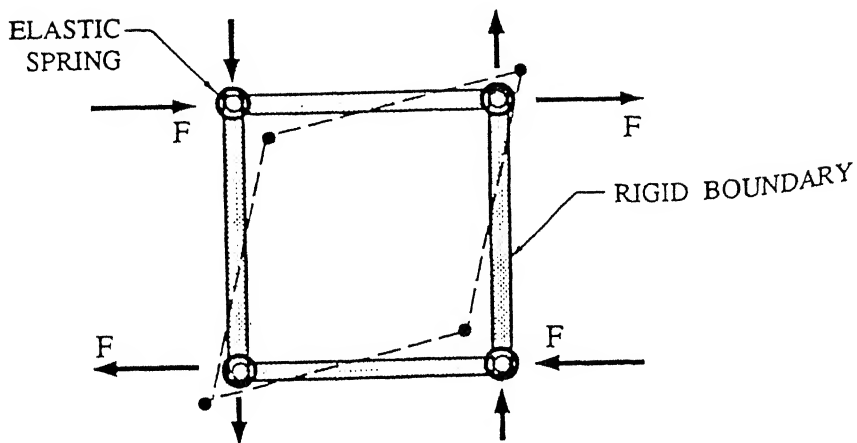


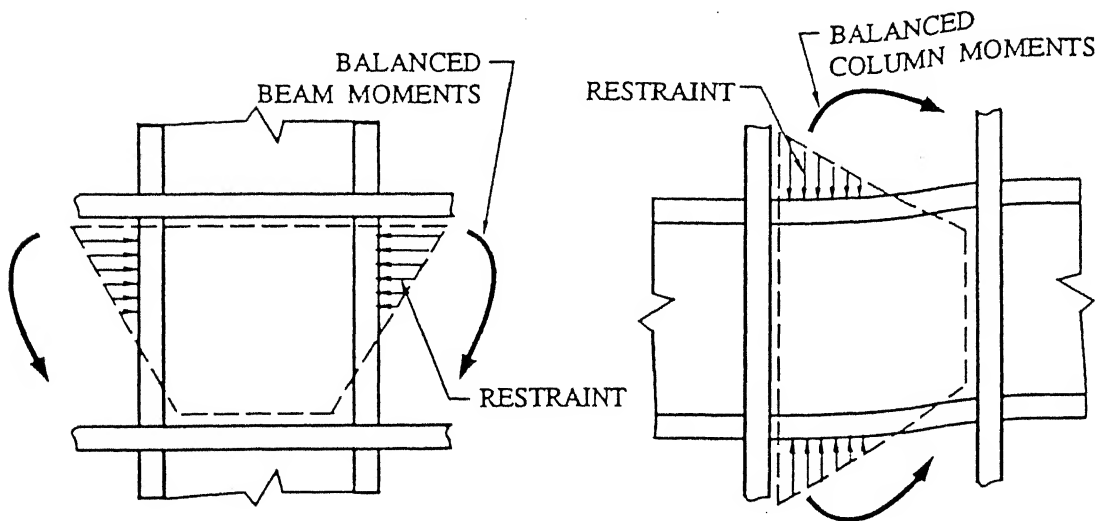
Figure 2.5: Shear behaviour caused by unbalanced moments.



(a)



(b)



(c)

Figure 2.6: Shear resistance due to (a) panel zone plate (b) joint panel boundary elements and (c) restraint to flexural deformation by the adjacent beams and columns.

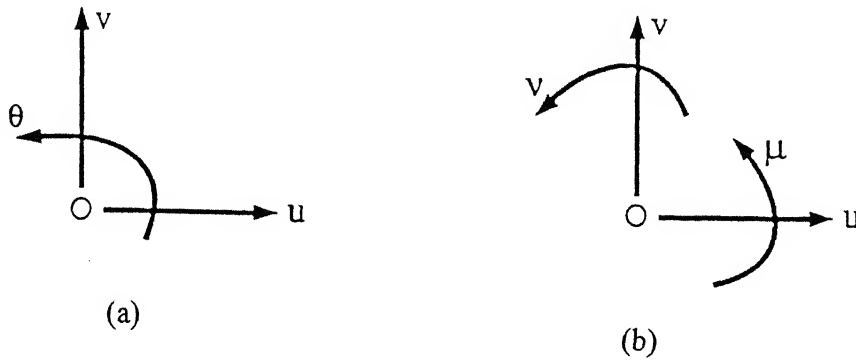


Figure 2.7: Degrees of freedom considered at each global node in the description of planar steel MRF (a) frame without joint elements (b) frame with joint elements.

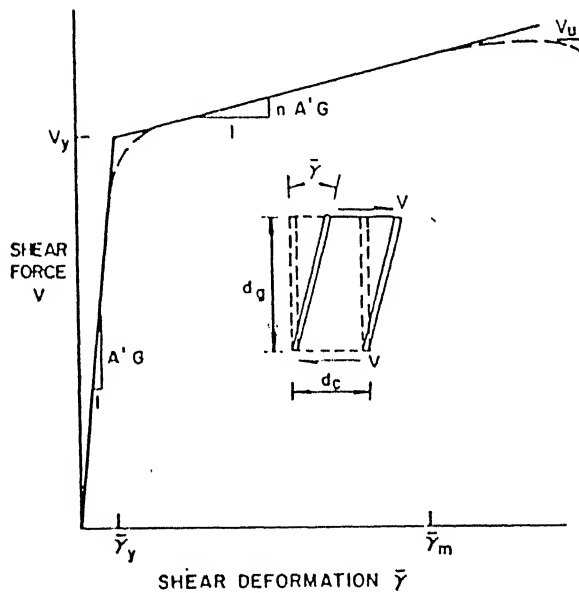


Figure 2.8: Bilinear Model for monotonic joint panel zone behaviour [Fielding and Chen, 1973].

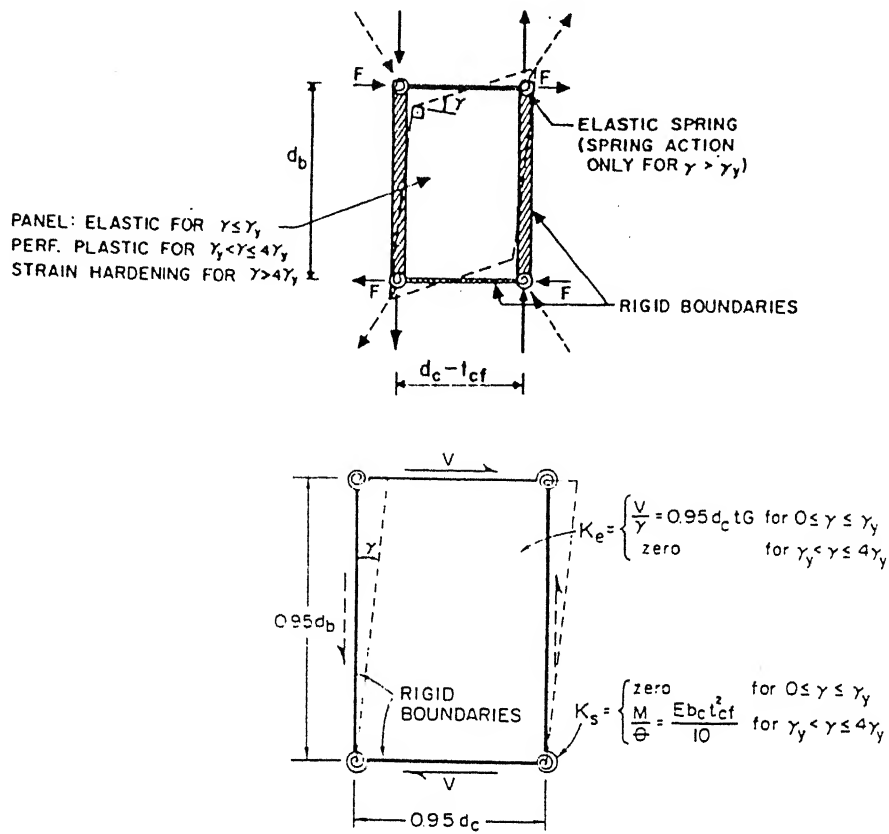


Figure 2.9: Trilinear Model for monotonic joint panel zone behaviour [Krawinkler *et al*, 1978].

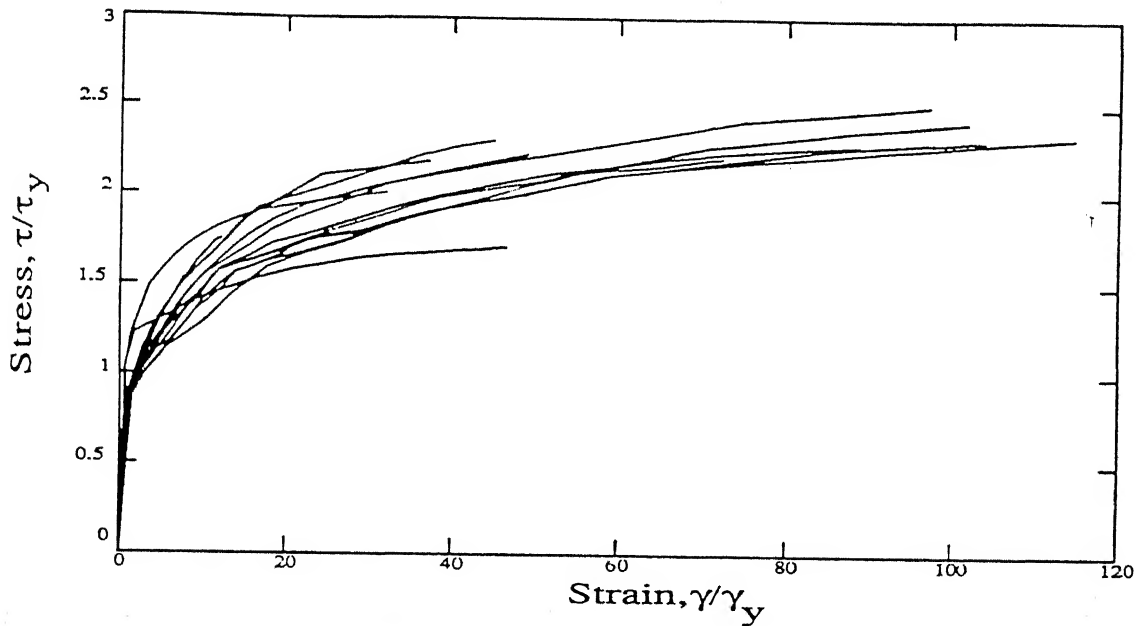


Figure 2.10: Summary of experimental data [Kato and Nakao, 1973] of the monotonic stress-strain curves of the joint shear response from steel beam-column sub-assemblages test.

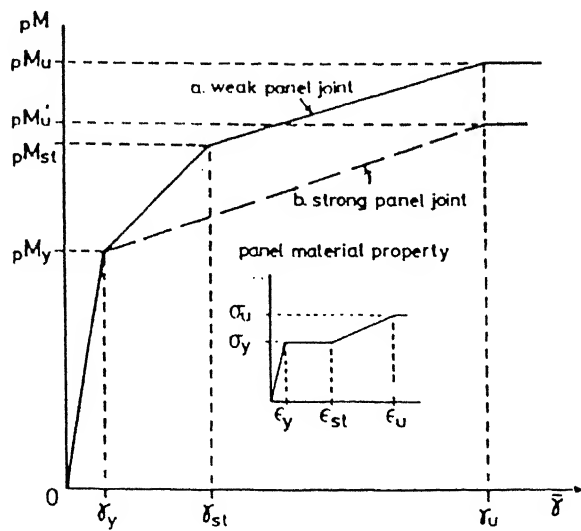


Figure 2.11: Trilinear Model for monotonic joint panel behaviour [Kato, 1982].

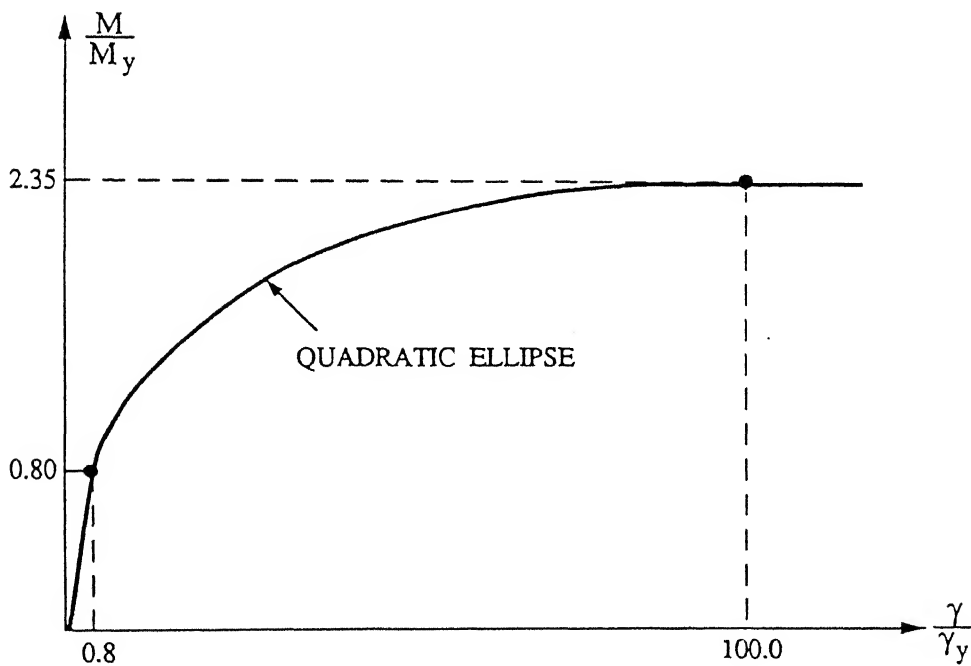


Figure 2.12: Joint moment *versus* joint shear strain curve for Ellipsoidal Hysteresis Joint Model [Hall and Murty, 1994].

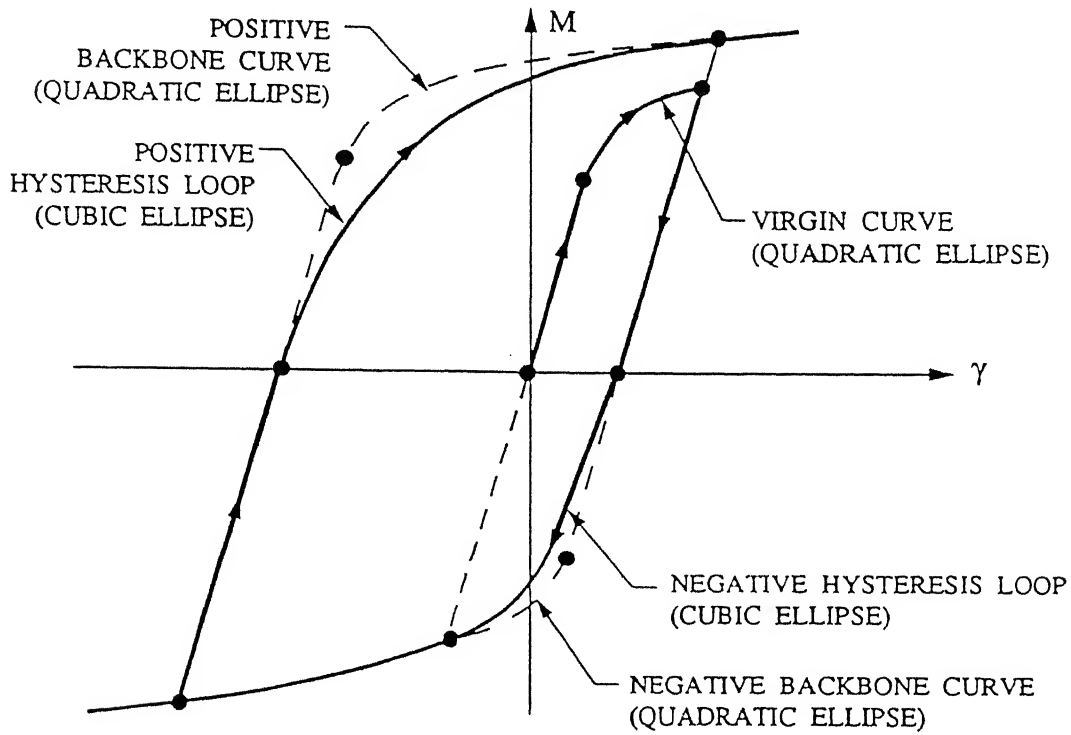


Figure 2.13: Quadratic ellipses for virgin curves and backbone curves, and cubic ellipses for positive and negative hysteresis loops in the ellipsoidal joint hysteresis model [Hall and Murty, 1994].

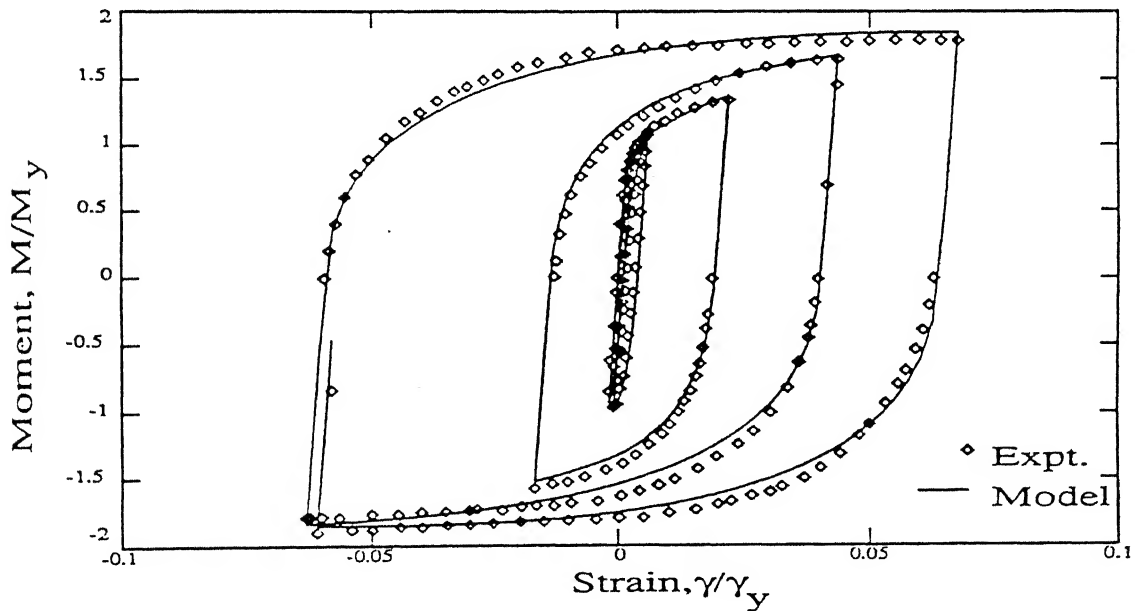


Figure 2.14: Comparison of experimental hysteresis loops [Krawinkler, *et al* 1975] of the shear response of a steel joint sub-assembly test with the theoretical prediction using ellipsoidal joint hysteresis model [Hall and Murty, 1994].

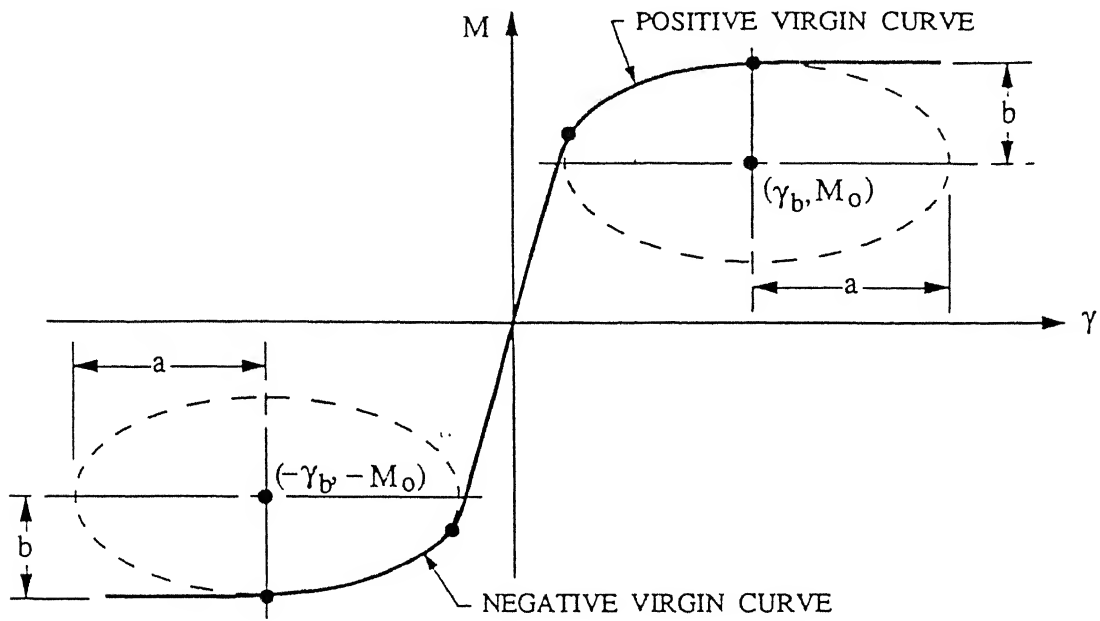


Figure 2.15: Geometry of the quadratic ellipses modeling the nonlinear virgin curve in the ellipsoidal joint hysteresis model [Hall and Murty, 1994].

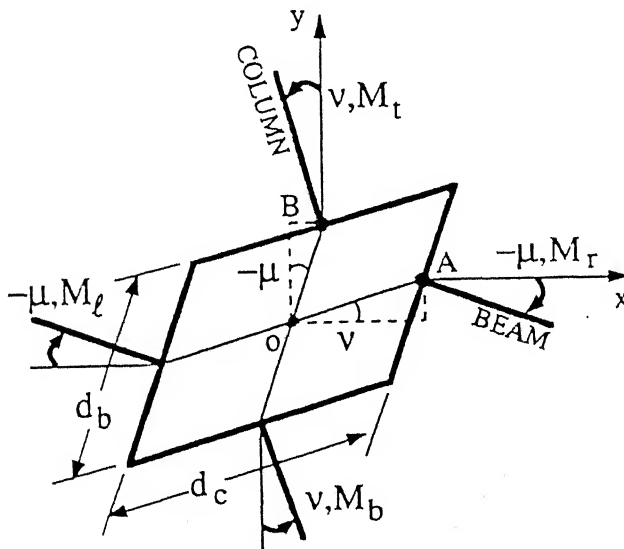


Figure 2.16: Forces and deformations at the degrees of freedom of the planar joint element.

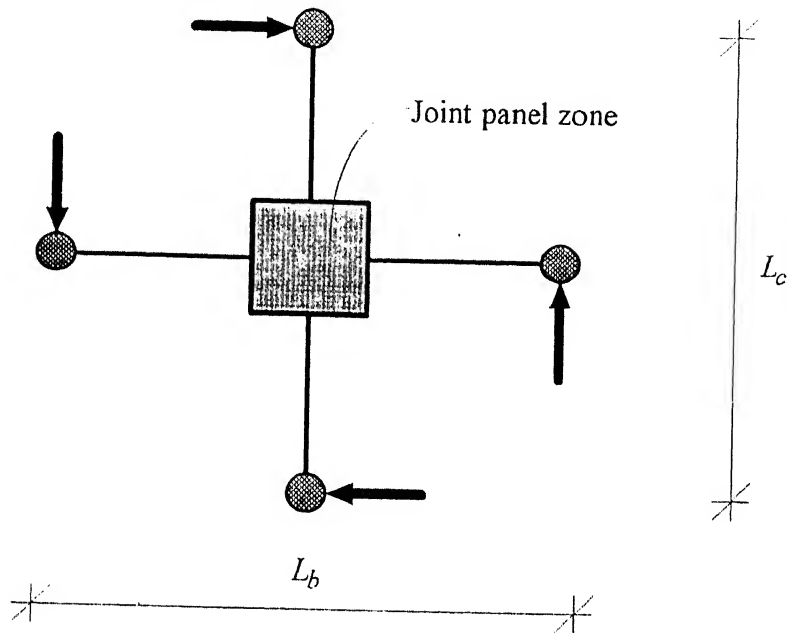


Figure 2.17: Interior joint panel referred to in the design specification [Tabuchi, *et al*, 1992].

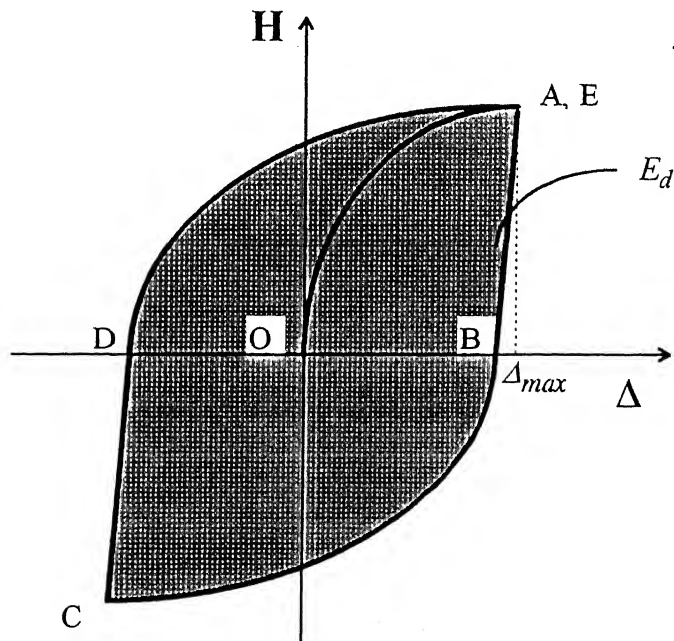


Figure 3.1: A typical hysteresis loop formation under one complete cycle of application of lateral load.

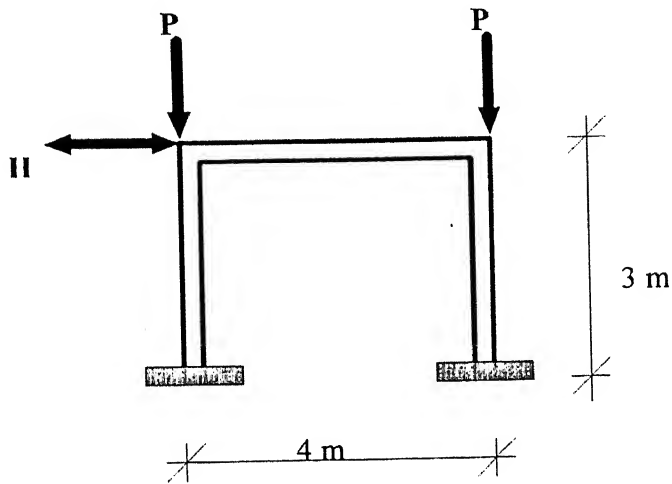


Figure 3.2: Geometry and loading on the Portal Frame used in the study.

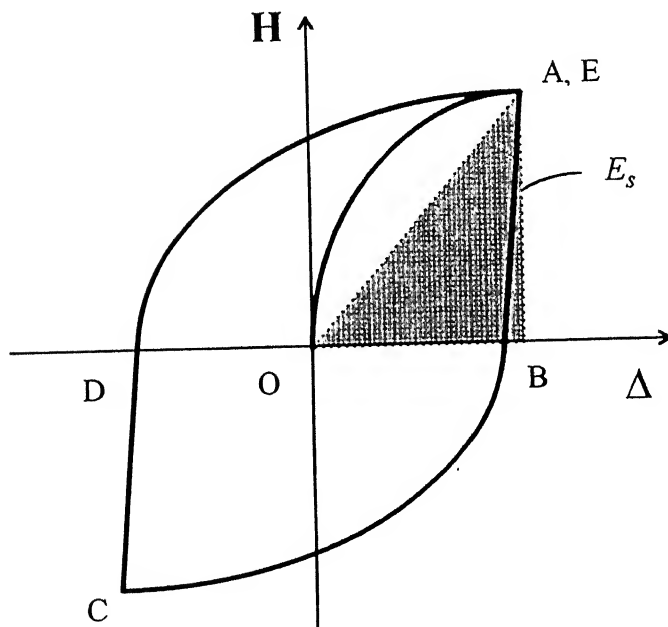
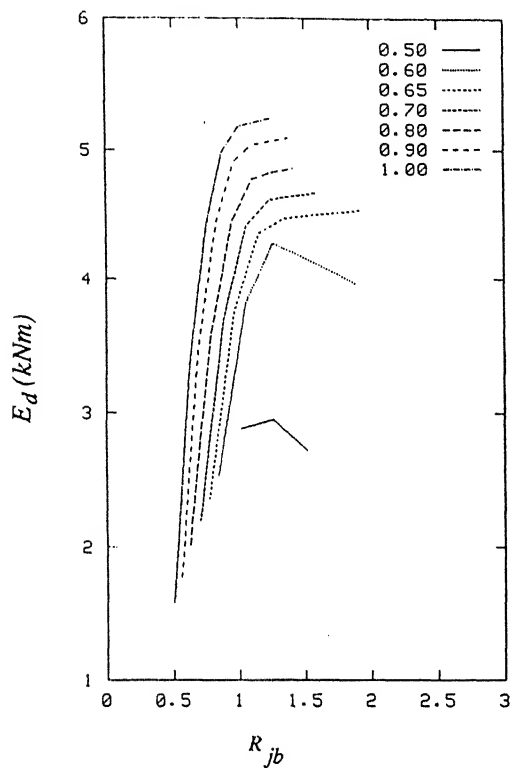
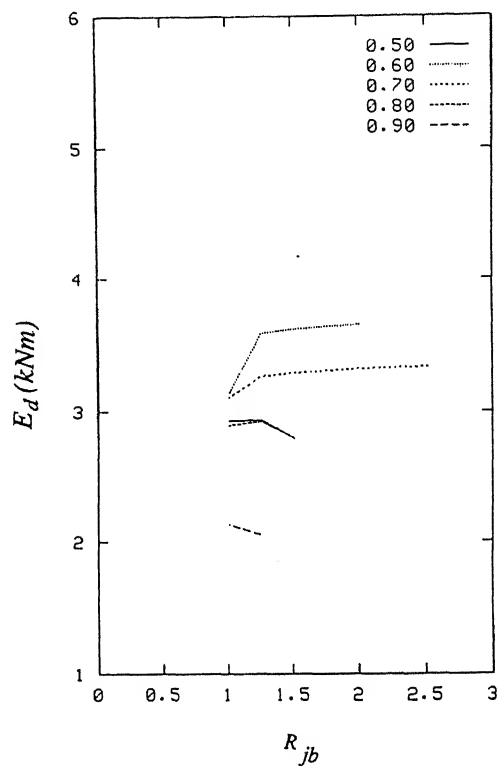


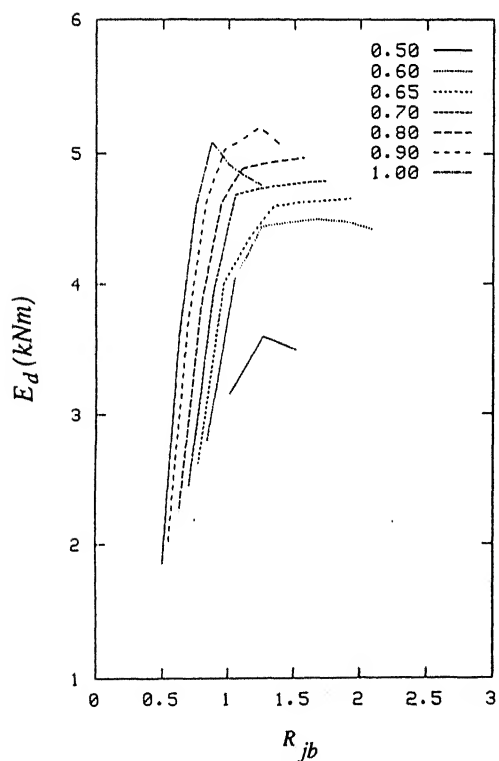
Figure 3.3: Geometric description of the static energy associated with the initial loading path OA in the lateral load H versus lateral displacement Δ curve.



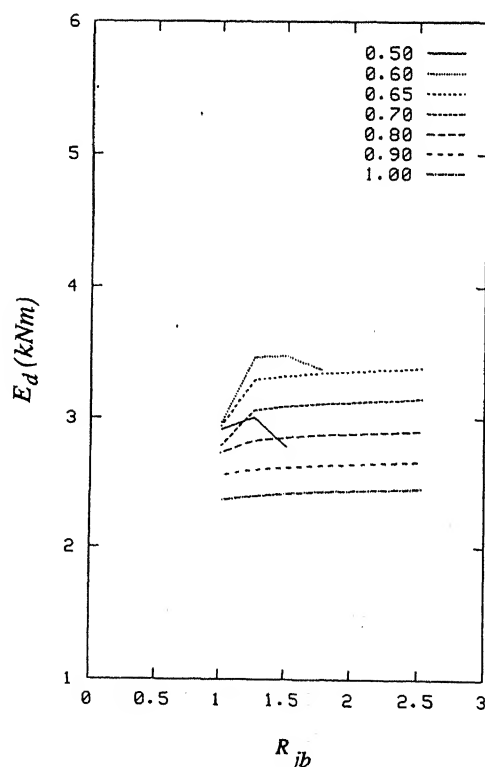
(a)



(b)



(c)



(d)

Figure 3.4: Effect of joint panel zone design on the energy dissipation E_d in the example portal frames with different R_{bc} values (a) C1, (b) B1, (c) C2 and (d) B2.

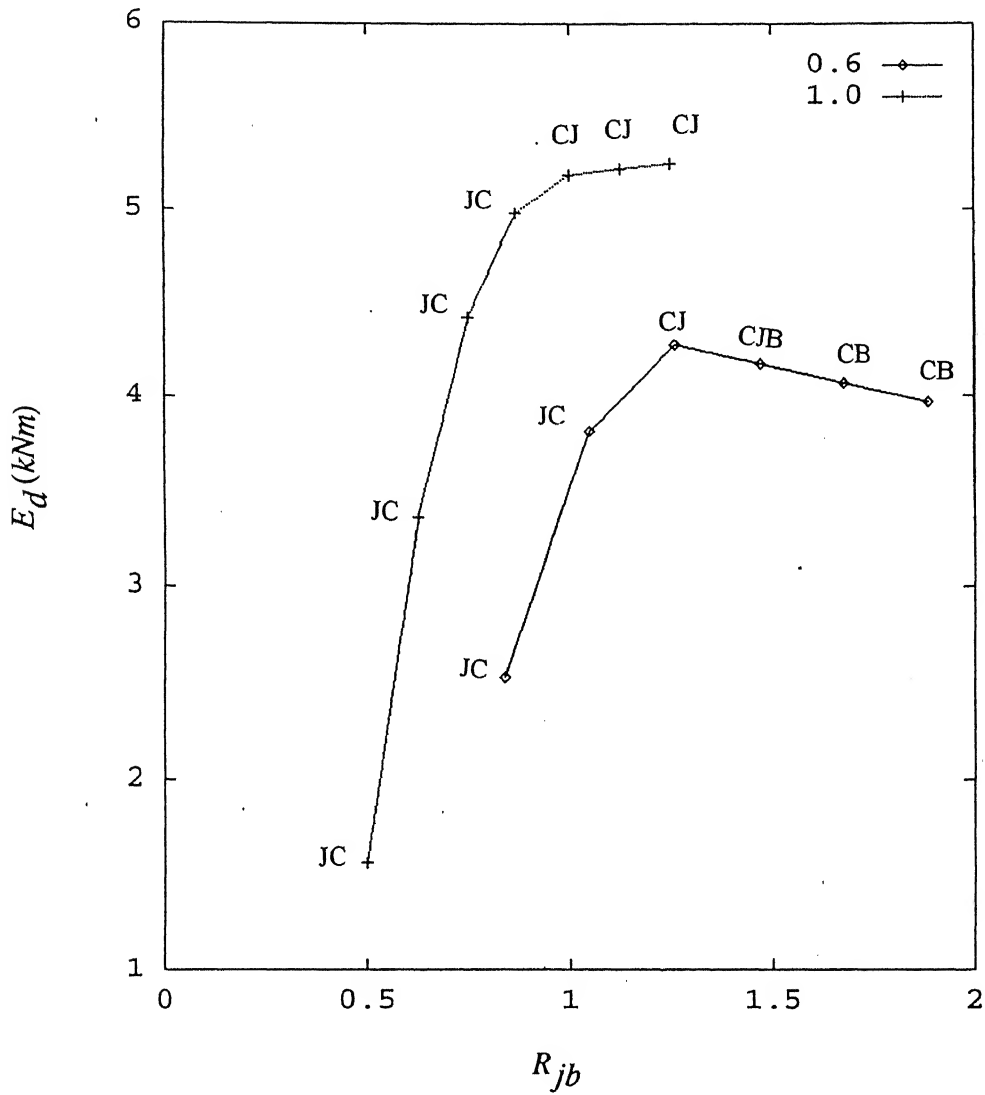
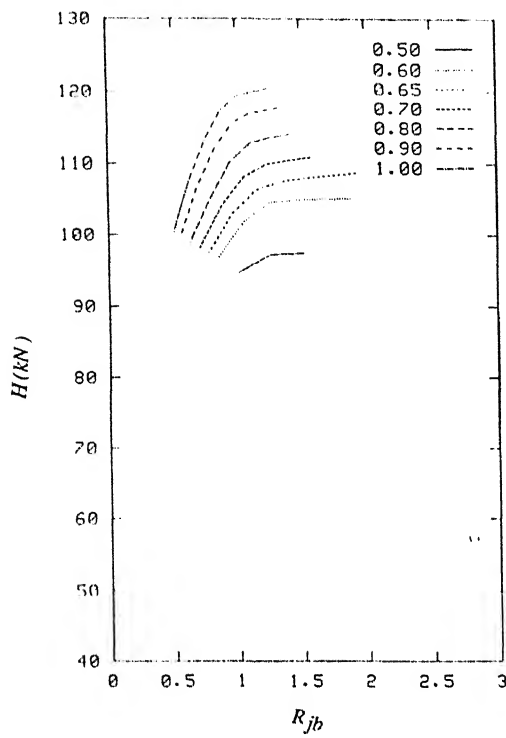
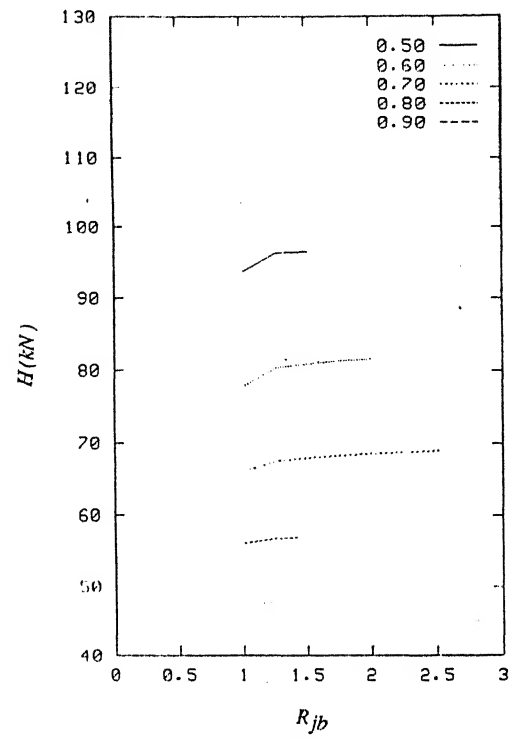


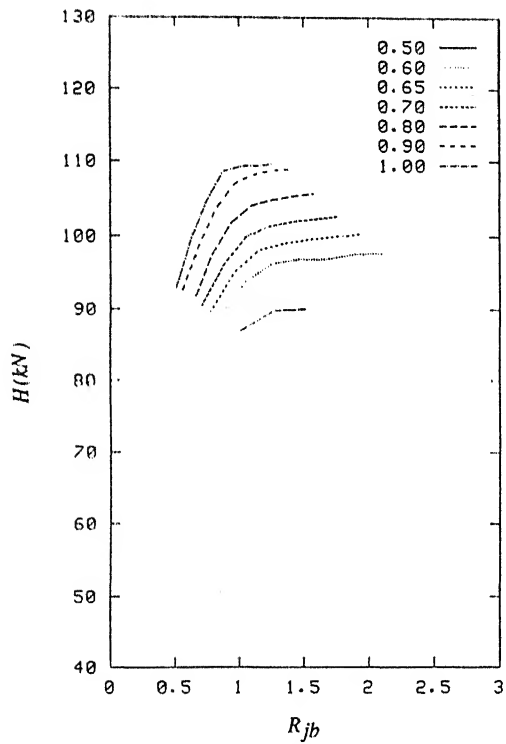
Figure 3.5: Effect of joint panel zone design on the energy dissipation E_d in the example portal frames with two separate values of R_{bc} , showing the sequence of formation of hinges in each frame. The sequence of formation of plastic hinges is indicated by letters J, C, B, corresponding to joint panel zone, column and beam, respectively. For example, CJB refers to first hinge in column, next in joint panel zone followed by that beam.



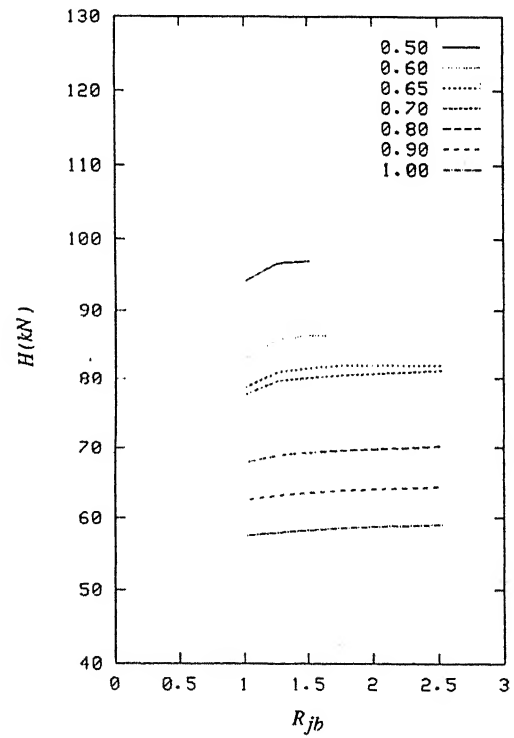
(a)



(b)



(c)



(d)

Figure 3.6: Effect of joint panel zone design on the lateral force H in the example portal frames with different R_{bc} values (a) C1, (b) B1, (c) C2, and (d) B2.

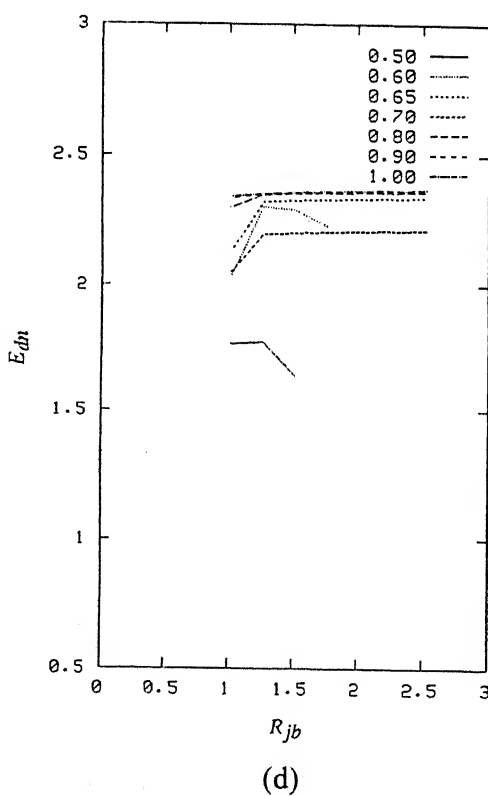
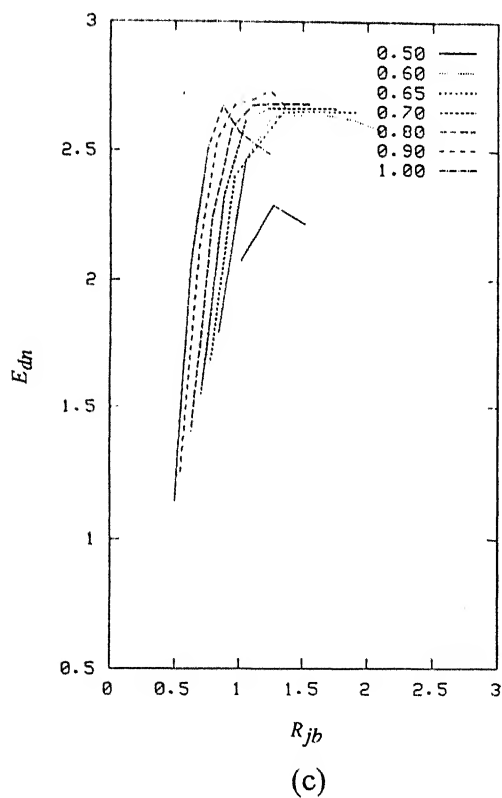
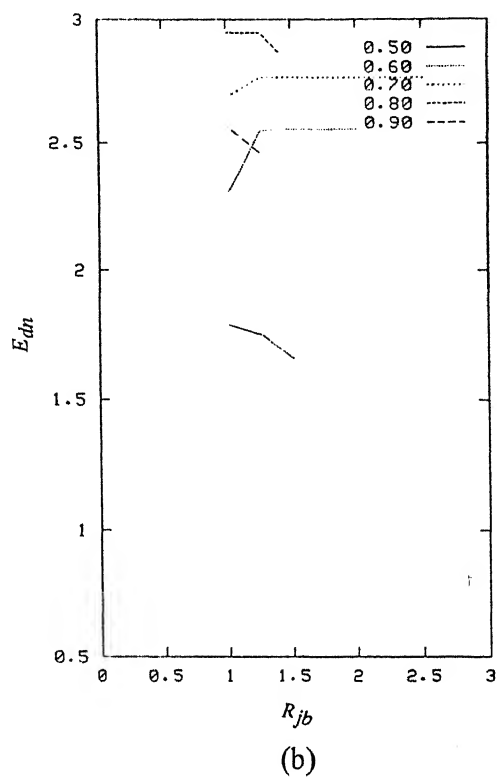
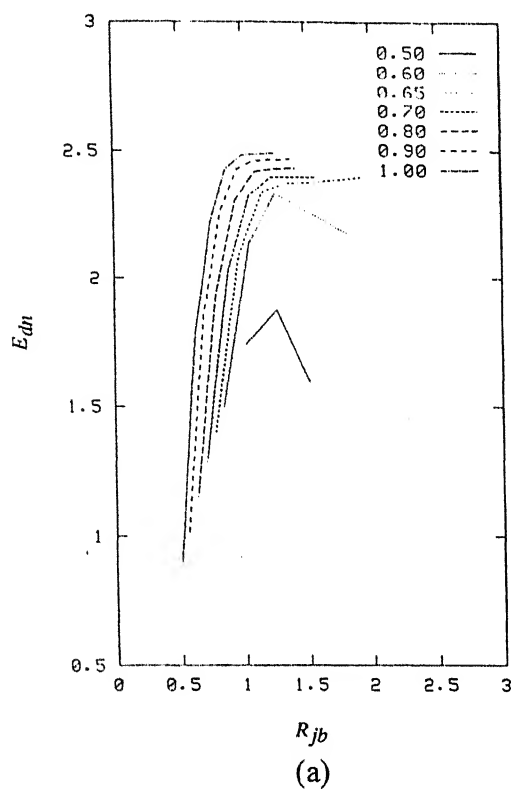


Figure 3.7: Effect of joint panel zone design on the normalized energy dissipation E_{dn} in the example portal frames with different R_{hc} values (a) C1, (b) B1, (c) C2, and (d) B2.

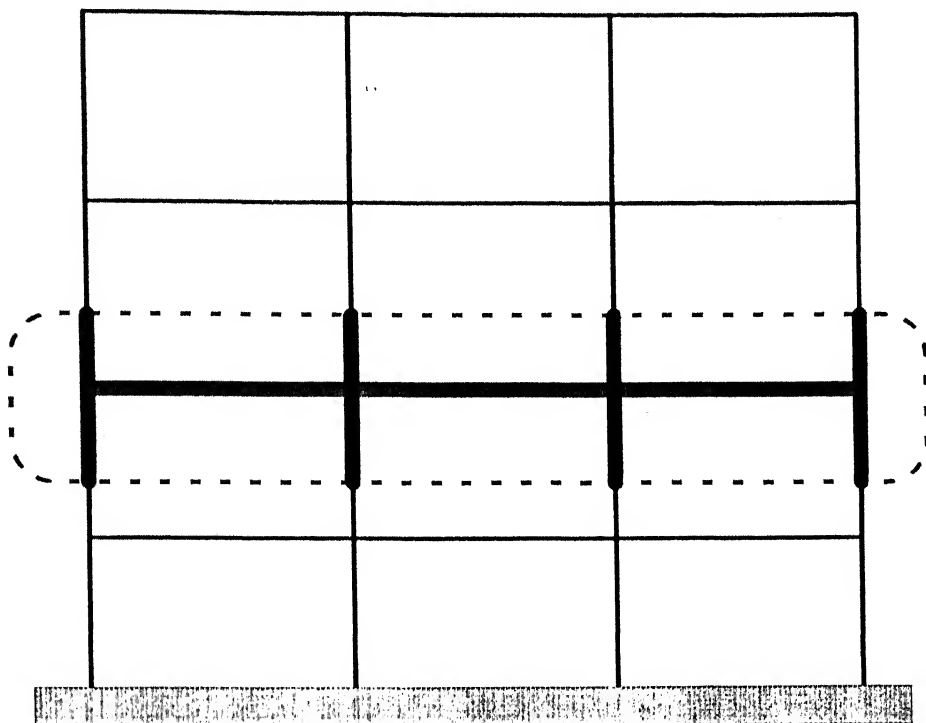


Figure 4.1: A storey sub-assemblage of a three-bay three storey MRF.

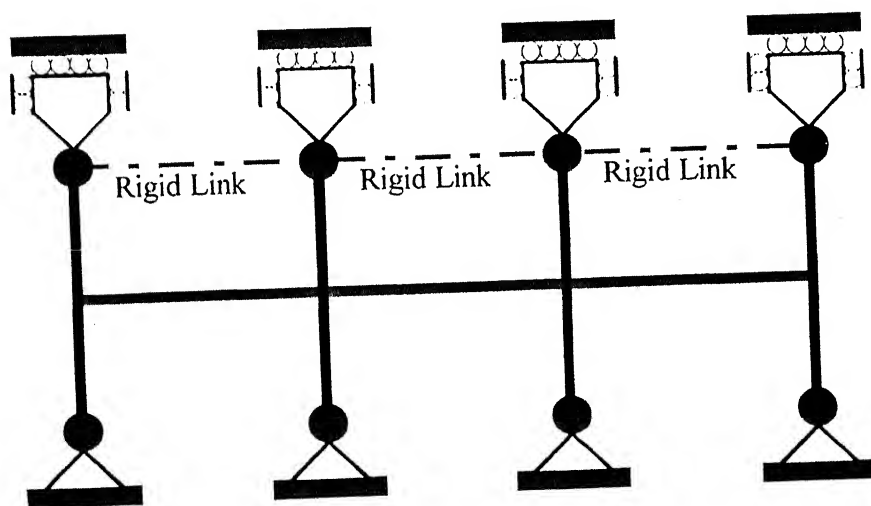


Figure 4.2: Boundary condition employed in the analysis of the storey sub-assemblage extracted from a three-bay three-storey MRF.

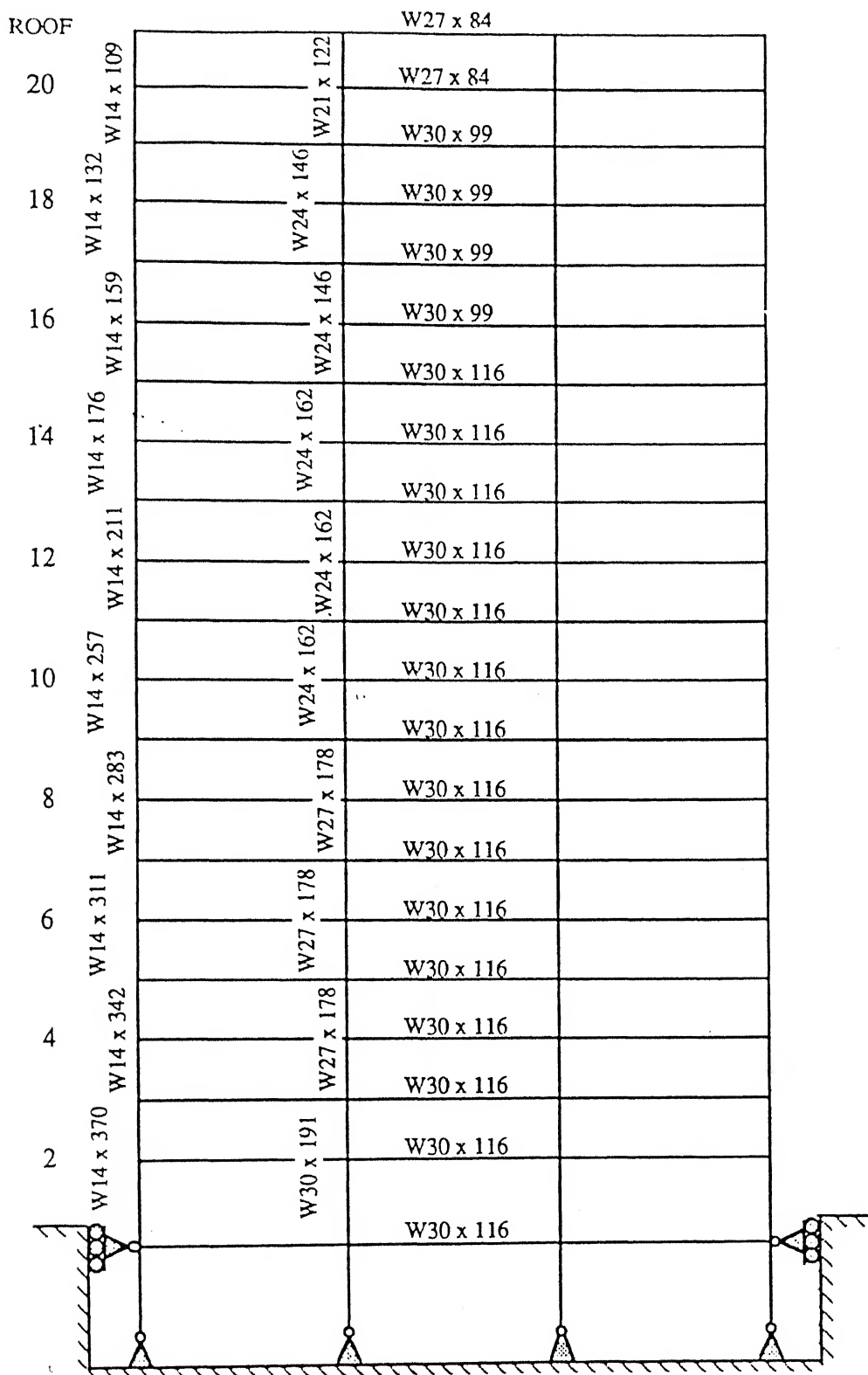
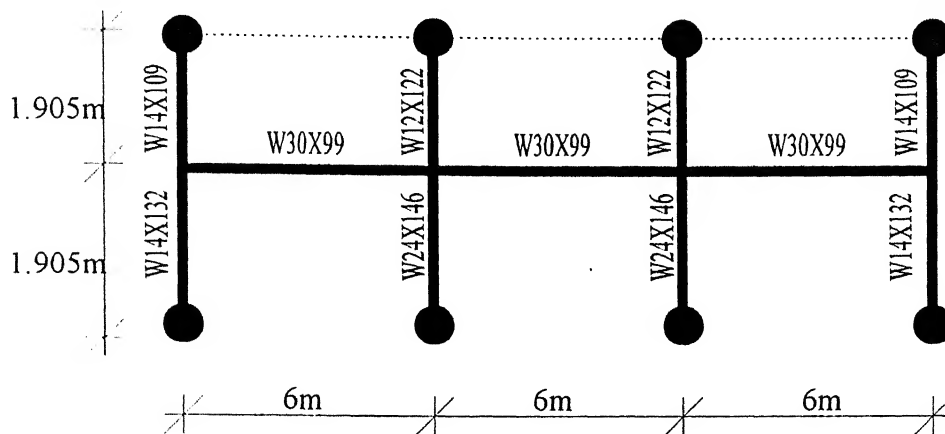
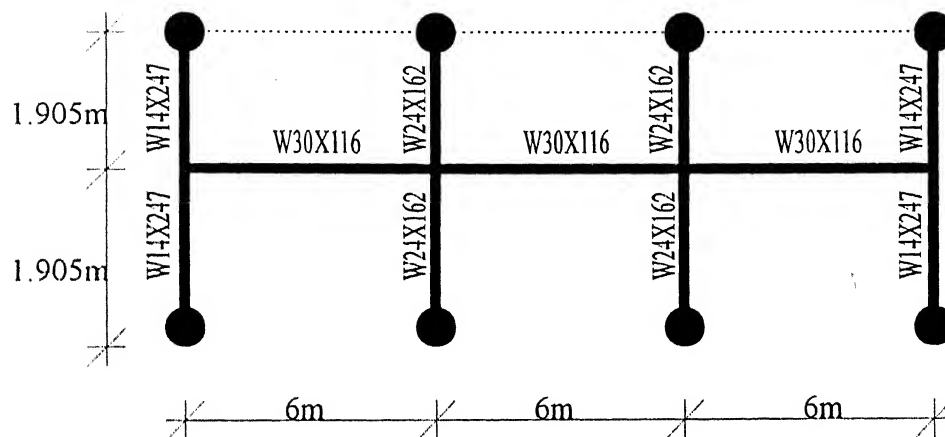


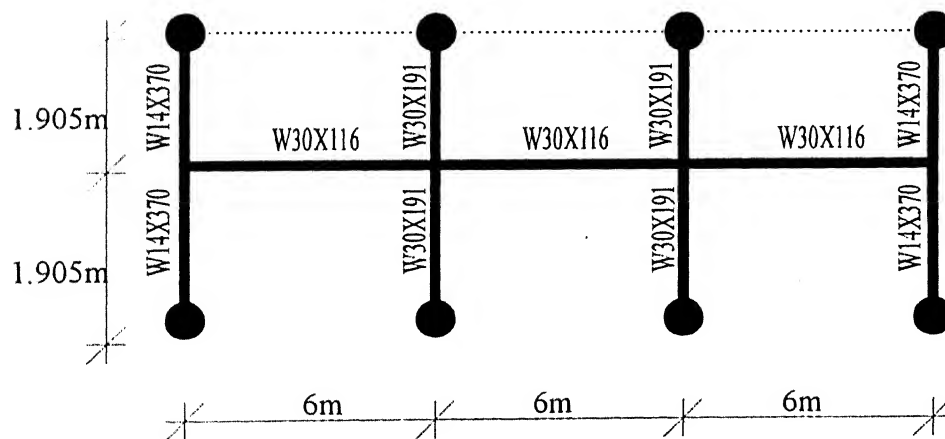
Figure 4.3: Member cross-section sizes of the planar MRF studied.



(a) SSA-T



(b) SSA-M



(c) SSA-B

Figure 4.4: Storey sub-assemblages used in the analytical study.

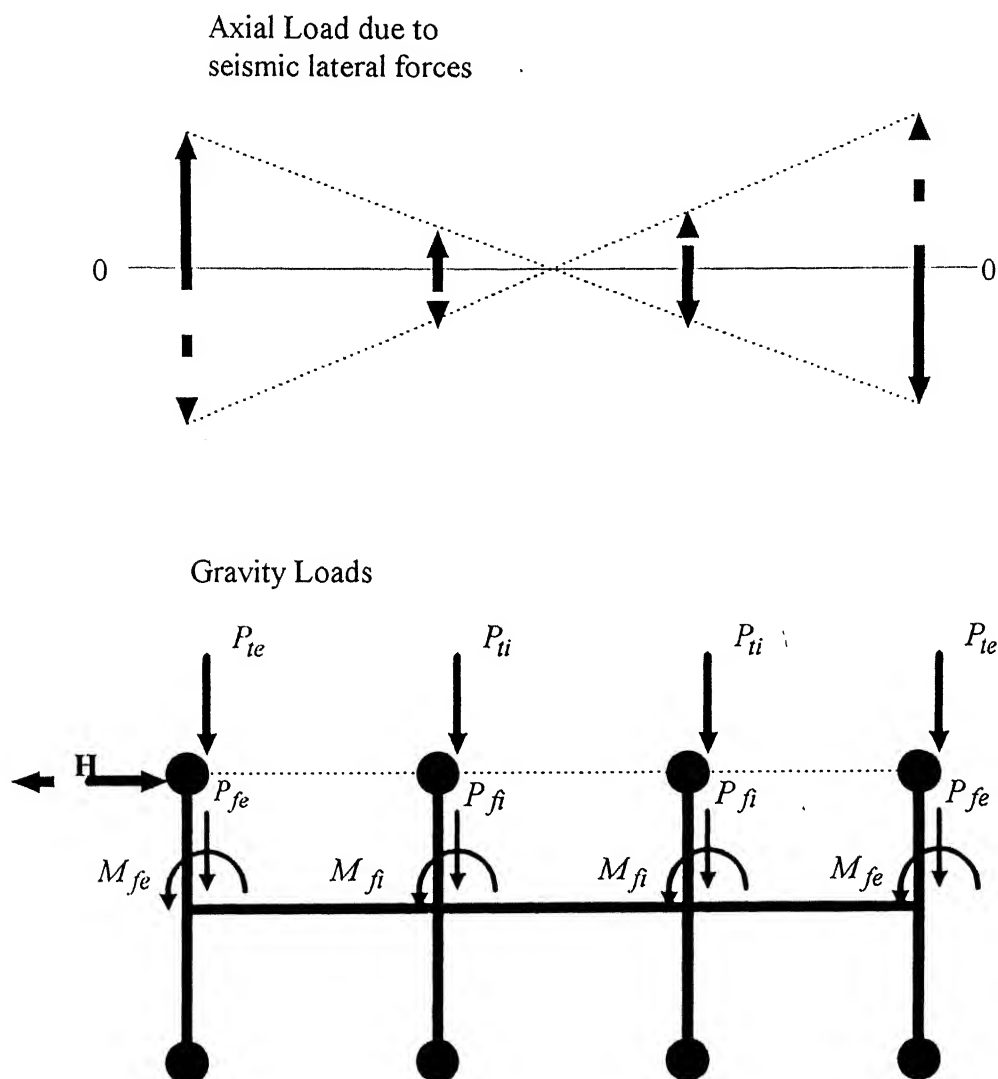
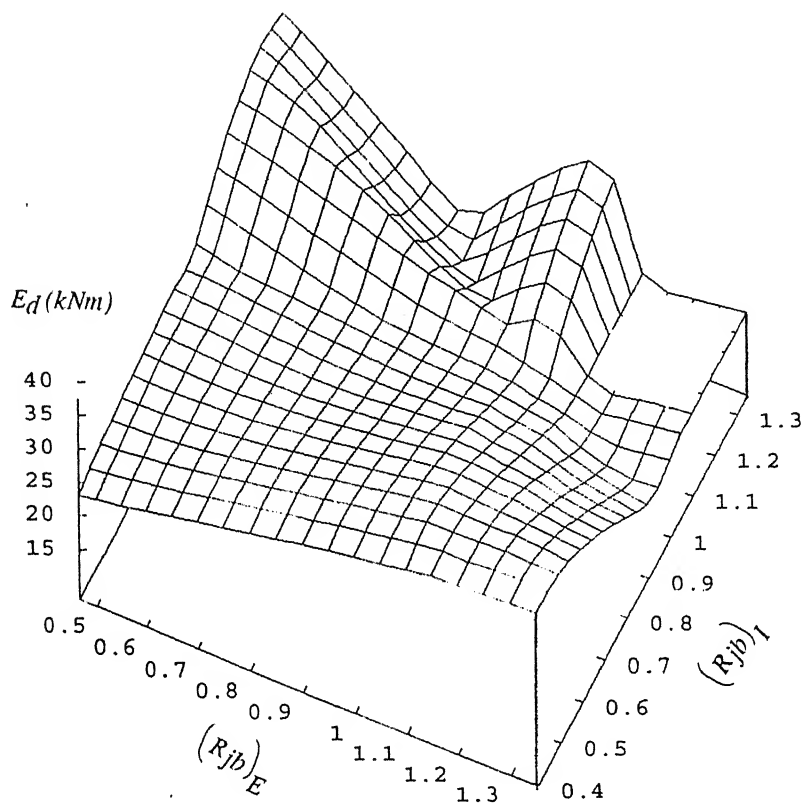
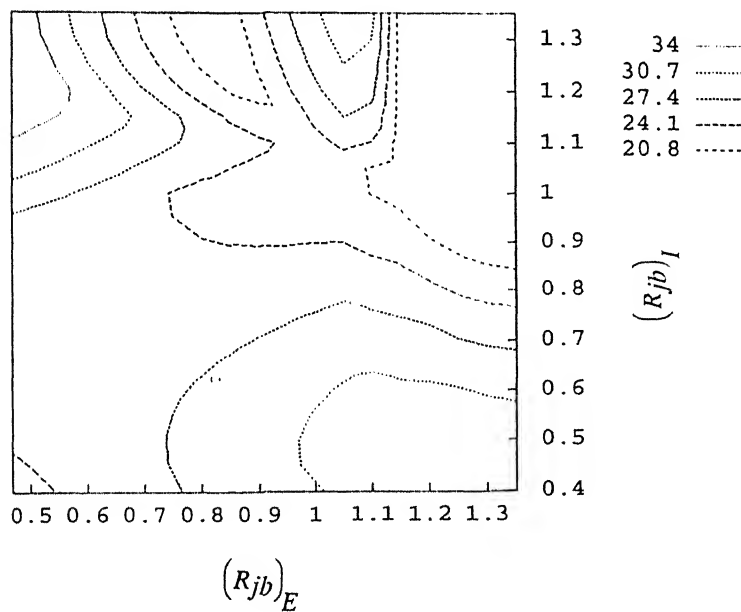


Figure 4.5: Gravity and fluctuating loads applied in the analysis of the sub-assembly of a three-bay MRF.

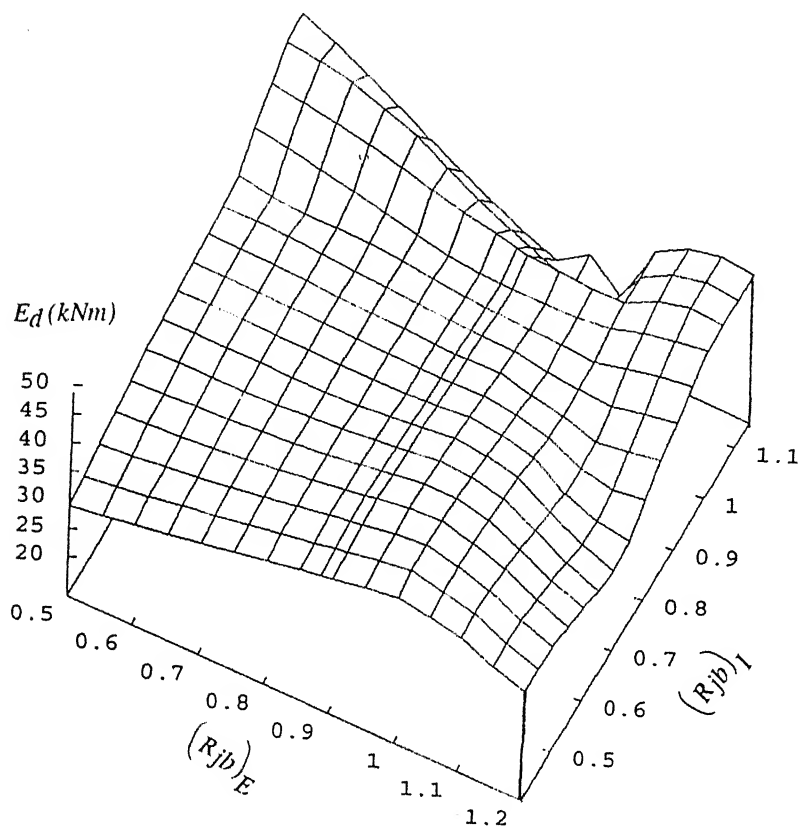


(a) Energy surface

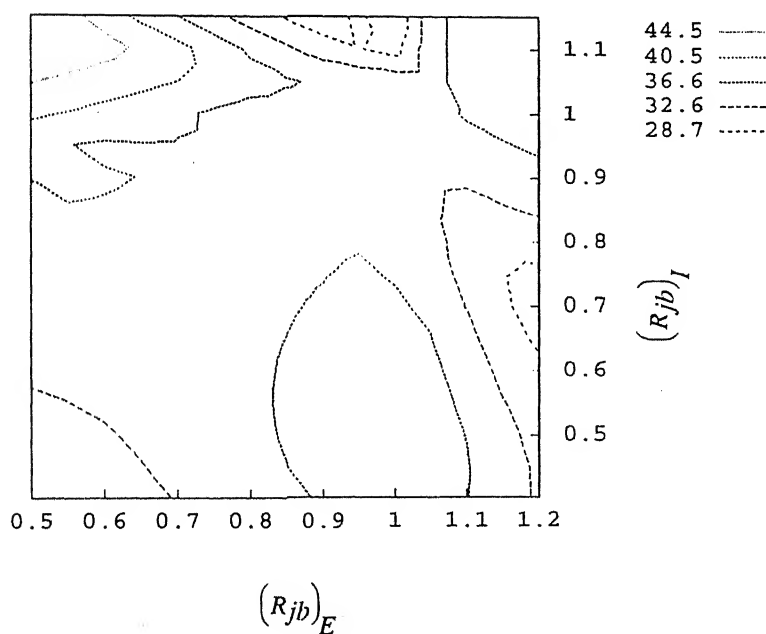


(b) Energy contours

Figure 4.6: Effect of joint panel zone designs on the energy dissipation in the storey sub-assembly SSA-T.

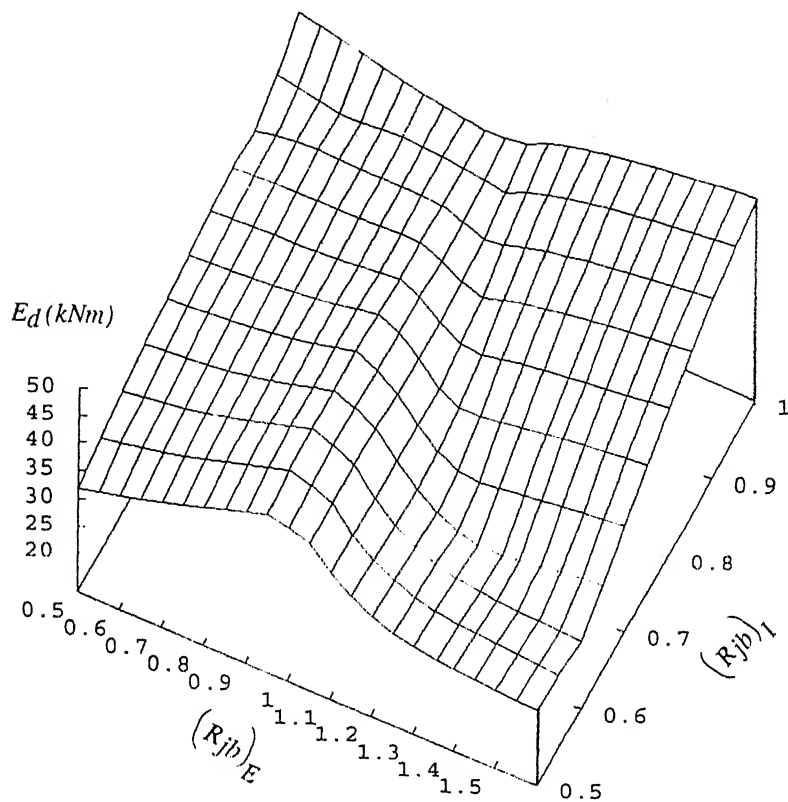


(a) Energy surface

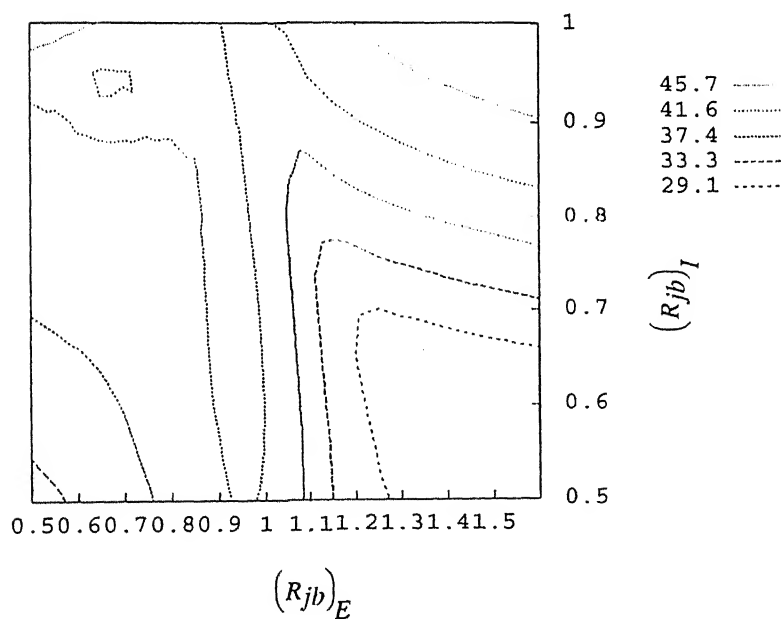


(b) Energy contours

Figure 4.7: Effect of joint panel zone designs on the energy dissipation in the storey sub-assembly SSA-M.

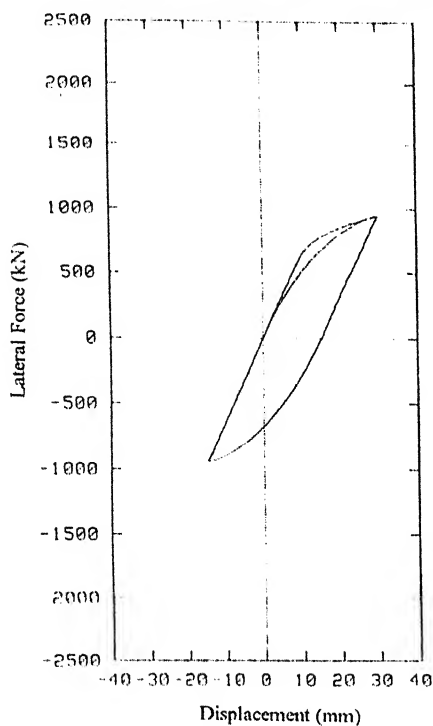


(a) Energy surface

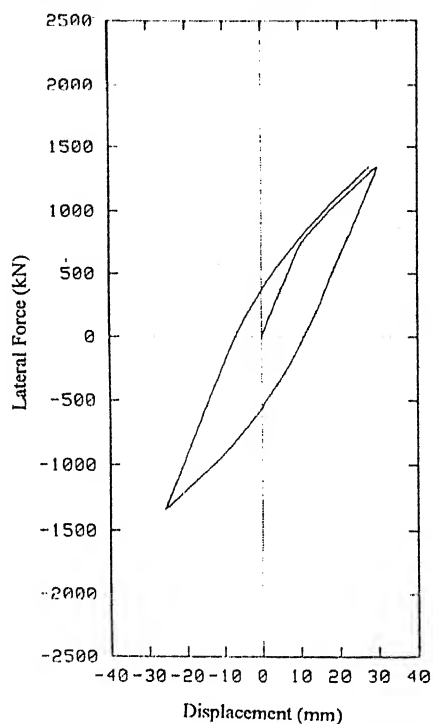


(b) Energy contours

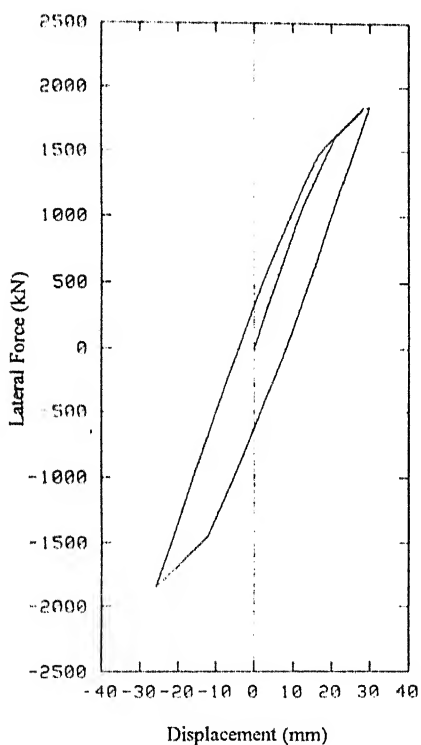
Figure 4.8: Effect of joint panel zone designs on the energy dissipation in the storey. sub-assembly SSA-B.



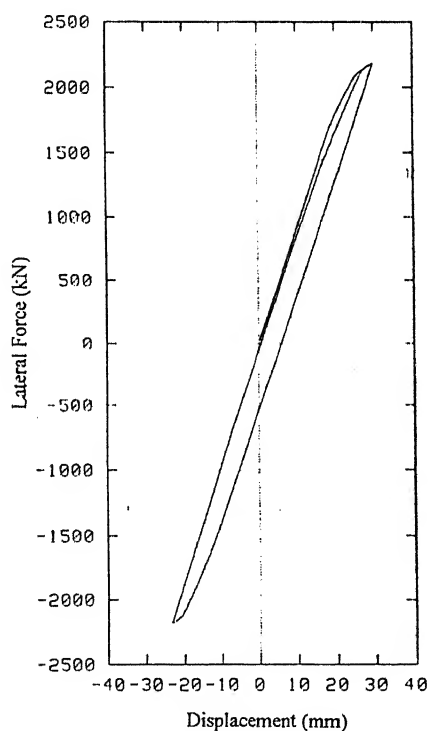
$$(a) \left(R_{jb}\right)_E = 0.47 \quad \left(R_{jb}\right)_I = 0.40$$



$$(b) \left(R_{jb}\right)_E = 0.47 \quad \left(R_{jb}\right)_I = 1.35$$

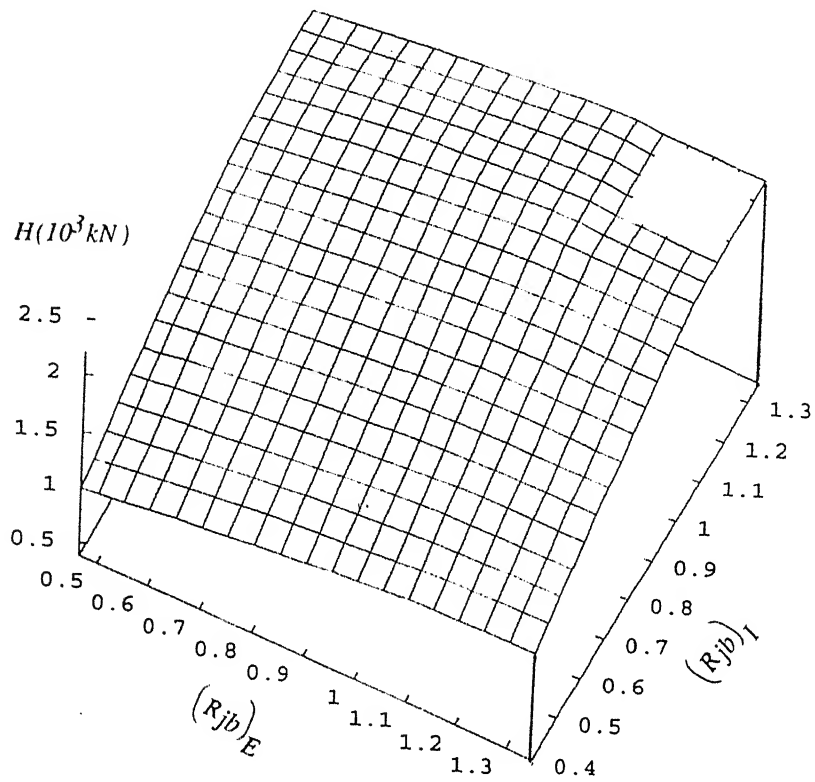


$$(c) \left(R_{jb}\right)_E = 1.35 \quad \left(R_{jb}\right)_I = 0.40$$

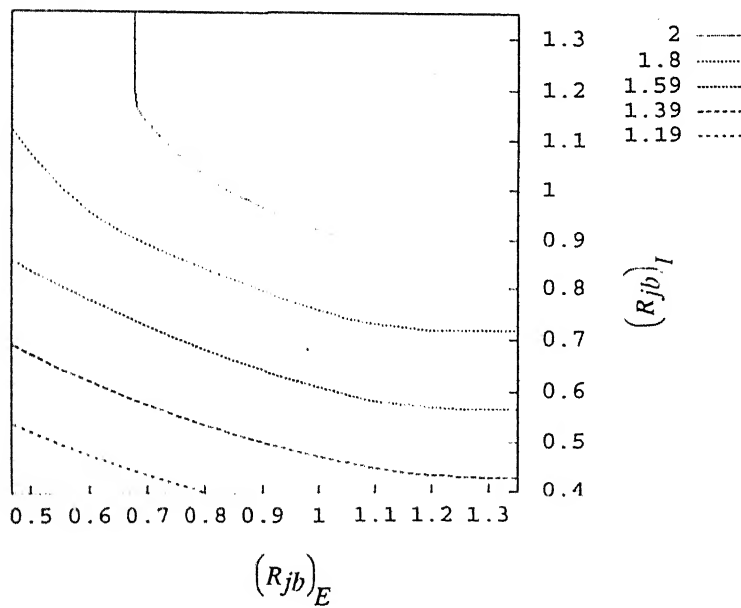


$$(d) \left(R_{jb}\right)_E = 1.35 \quad \left(R_{jb}\right)_I = 1.05$$

Figure 4.9: Typical Hysteresis Loops of the lateral force H versus lateral displacement Δ curves for the extreme cases of joint panel zone designs in storey sub-assembly SSA-T.

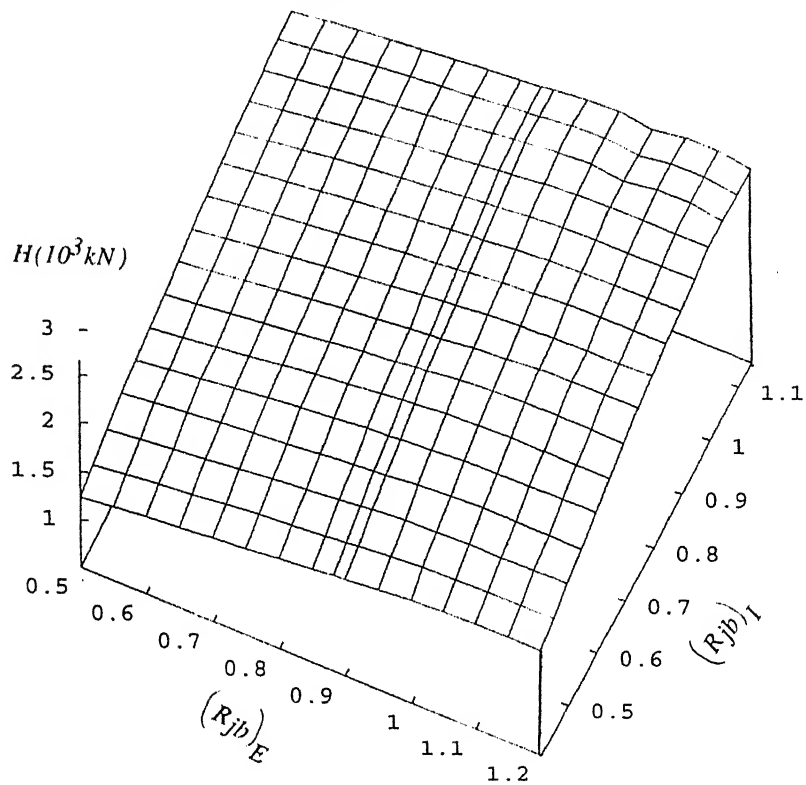


(a) Lateral force surface

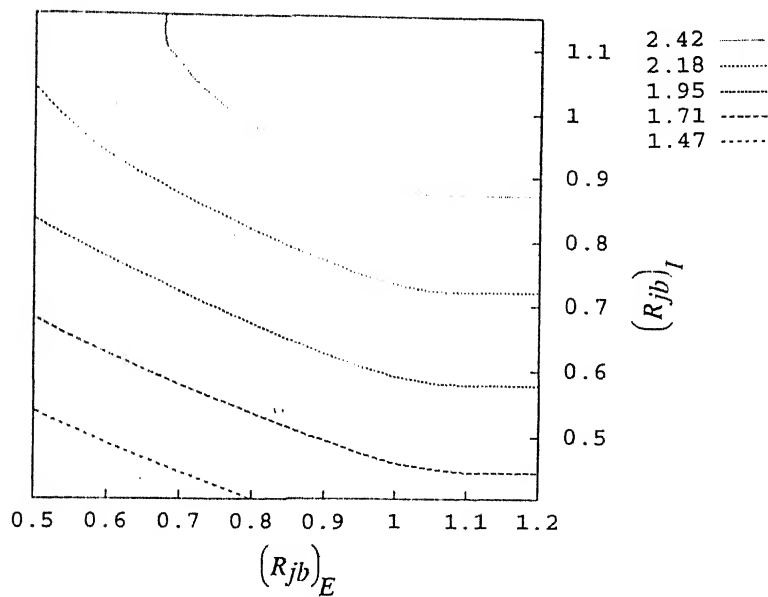


(b) Lateral force contours

Figure 4.10: Effect of joint panel zone designs on the lateral force H carrying capacity in sub-assembly SSA-T.

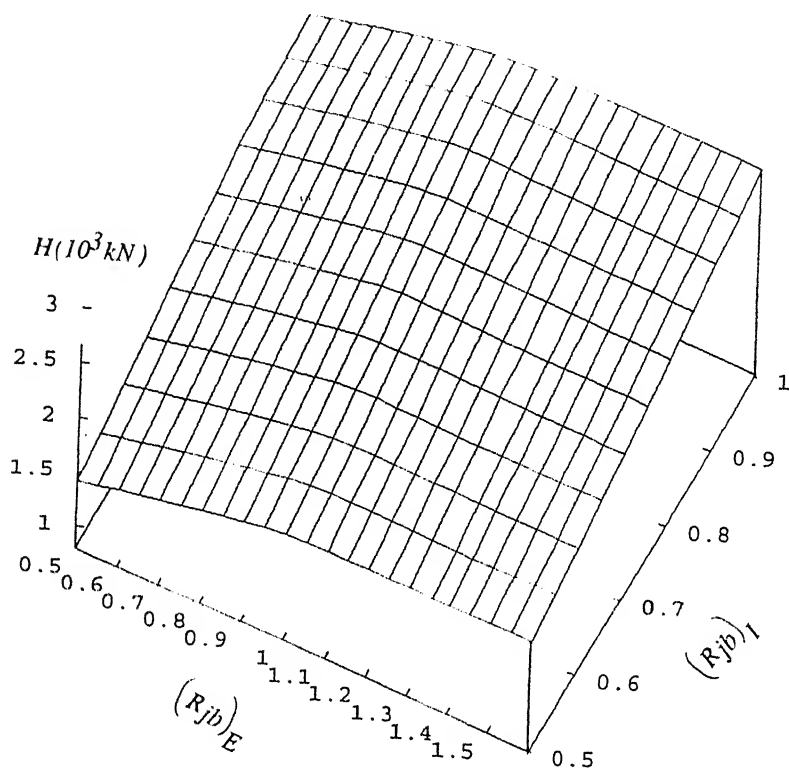


(a) Lateral force surface

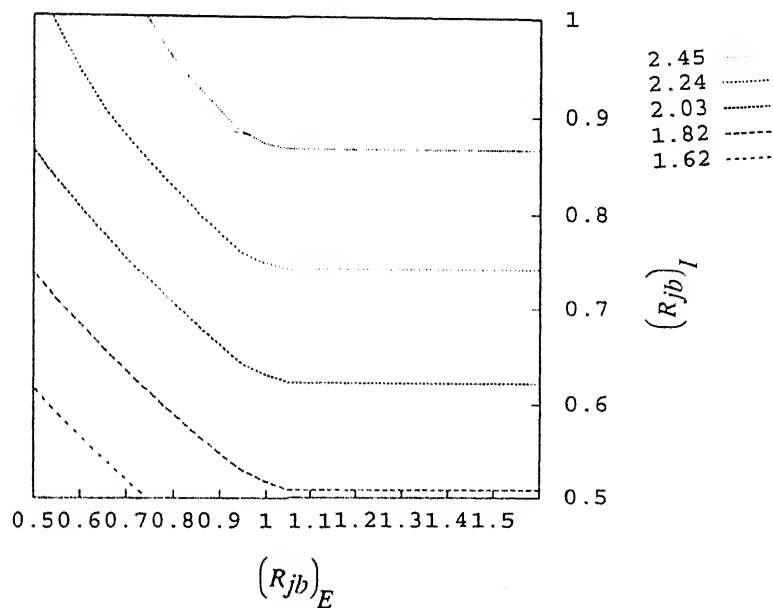


(b) Lateral force contours

Figure 4.11: Effect of joint panel zone designs on the lateral force H carrying capacity in sub-assembly SSA-M.

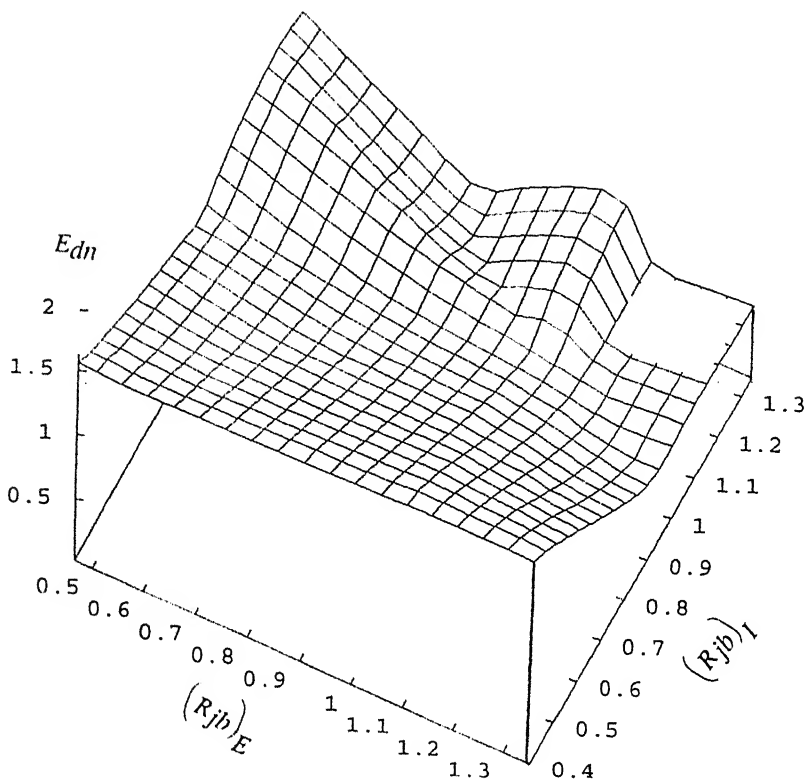


(a) Lateral force surface

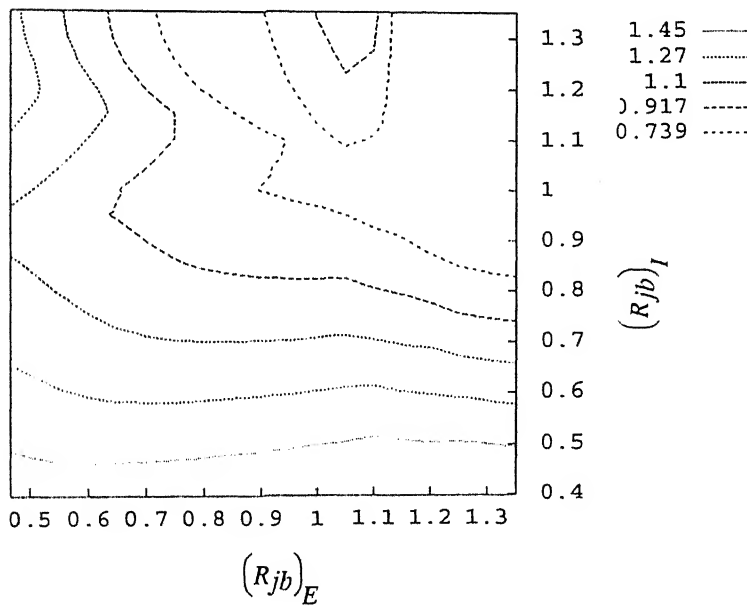


(b) Lateral force contours

Figure 4.12: Effect of joint panel zone designs on the lateral force H carrying capacity in sub-assembly SSA-B.

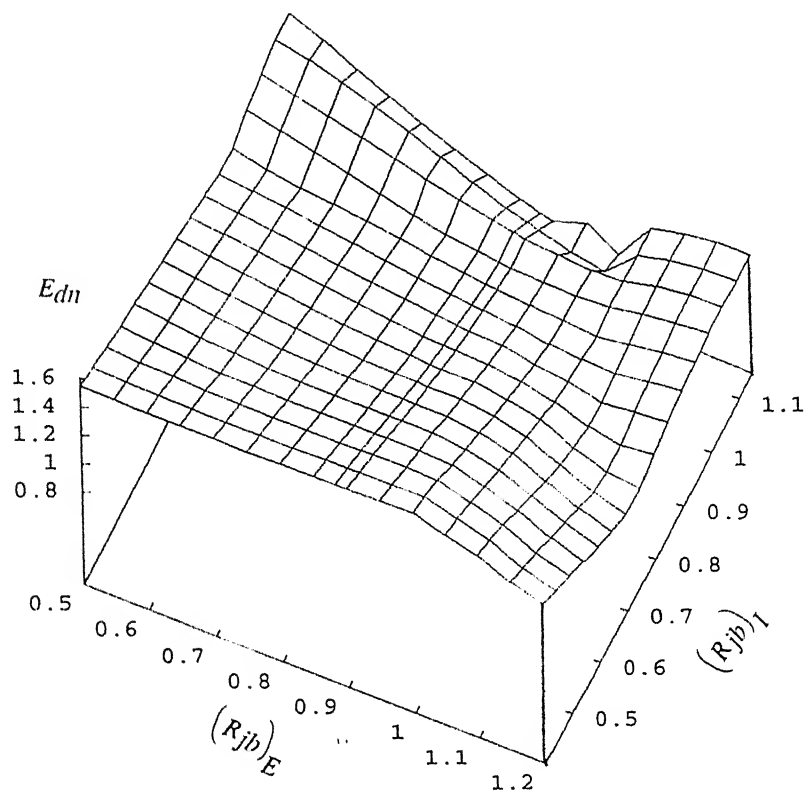


(a) Normalized energy surface

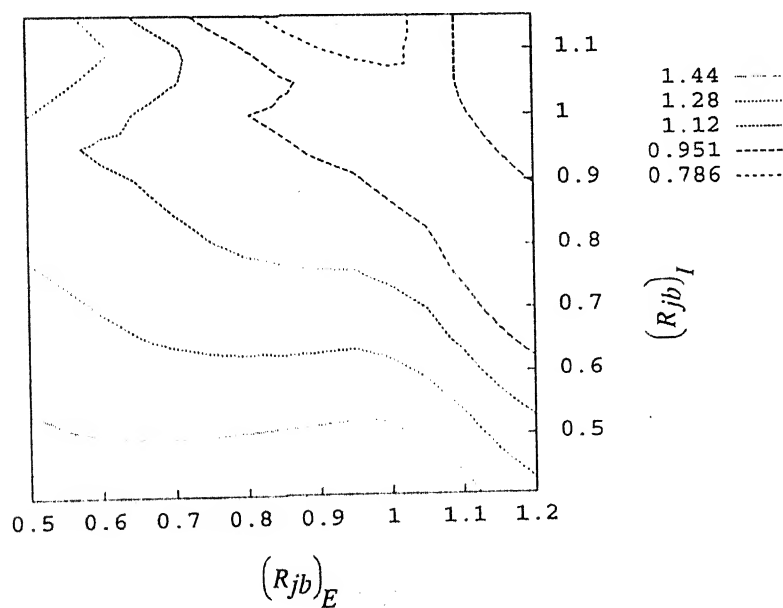


(b) Normalized energy contours

Figure 4.13: Effect of joint panel zone designs on normalized energy dissipation in storey sub-assembly SSA-T.

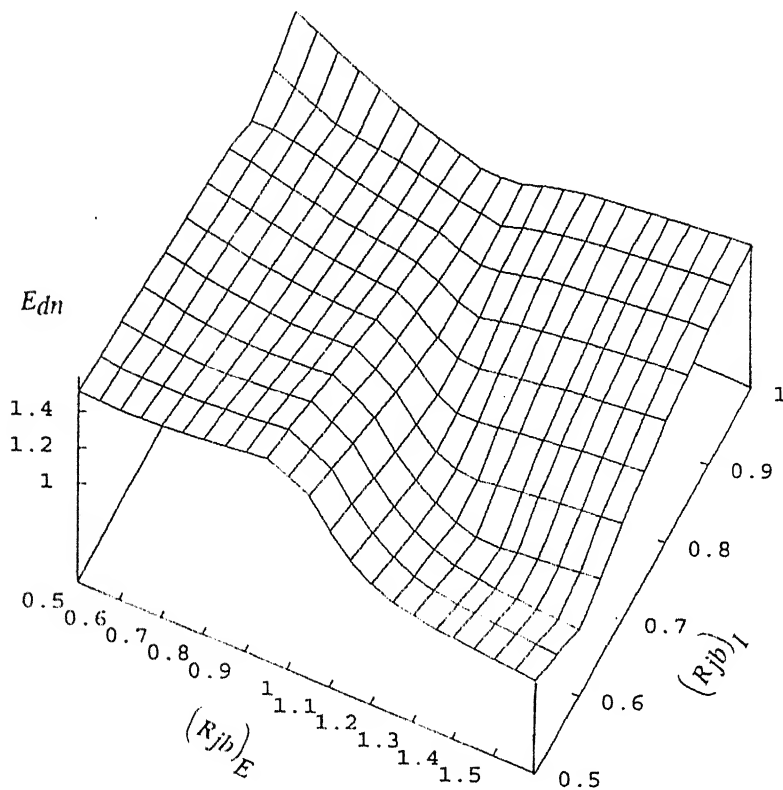


(a) Normalized energy surface

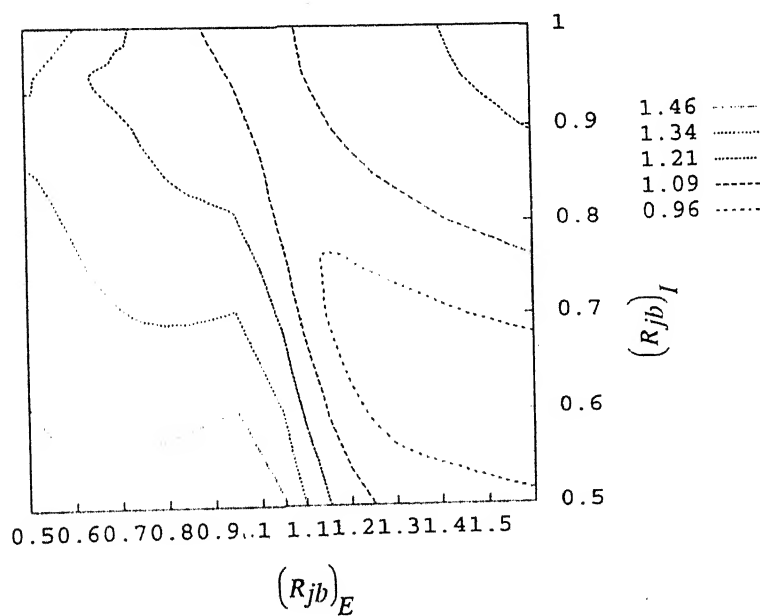


(b) Normalized energy contours

Figure 4.14: Effect of joint panel zone designs on normalized energy dissipation in storey sub-assembly SSA-M.

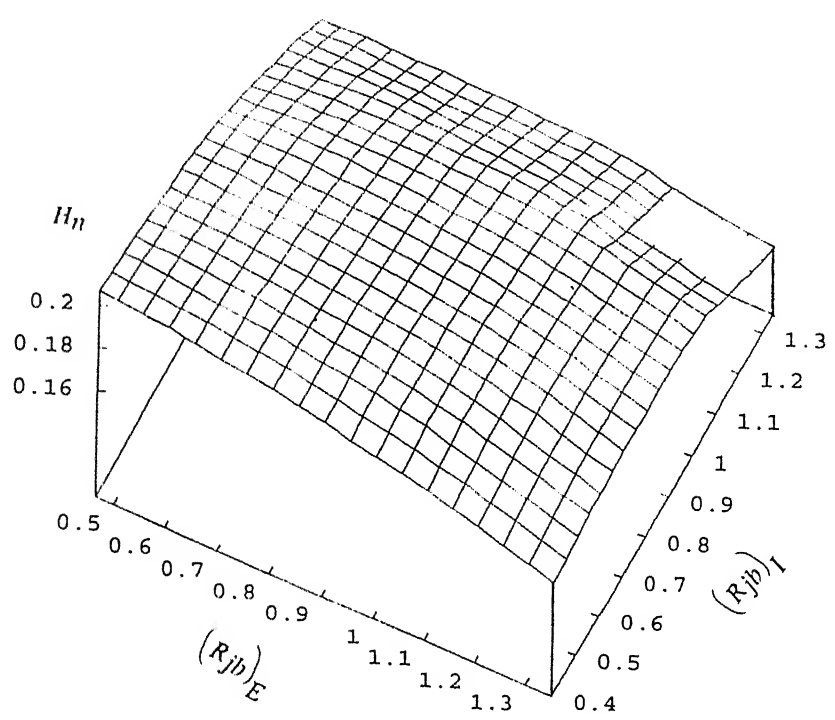


(a) Normalized energy dissipation surface

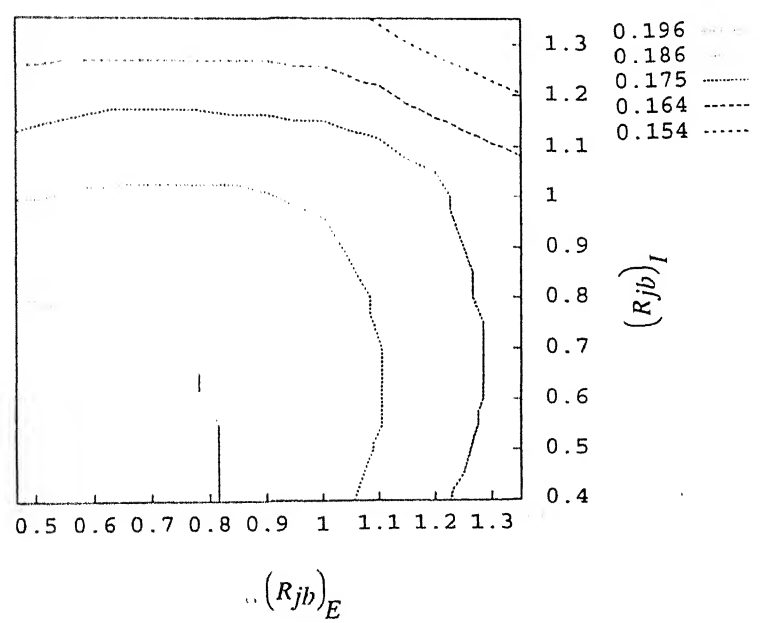


(b) Normalized energy dissipation contours

Figure 4.15: Effect of joint panel zone designs on normalized energy dissipation in storey sub-assembly SSA-B.

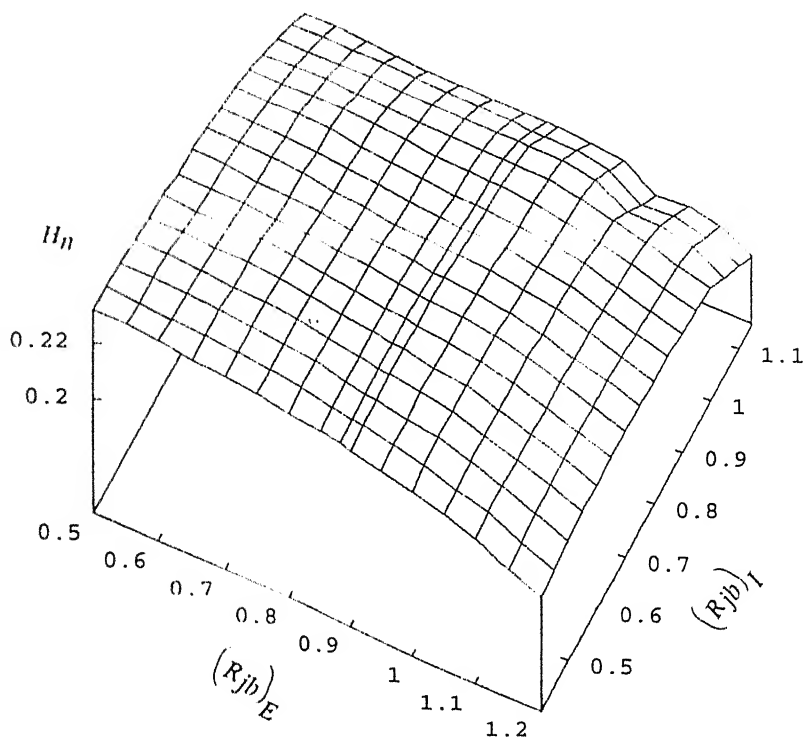


(a) Normalized lateral force surface

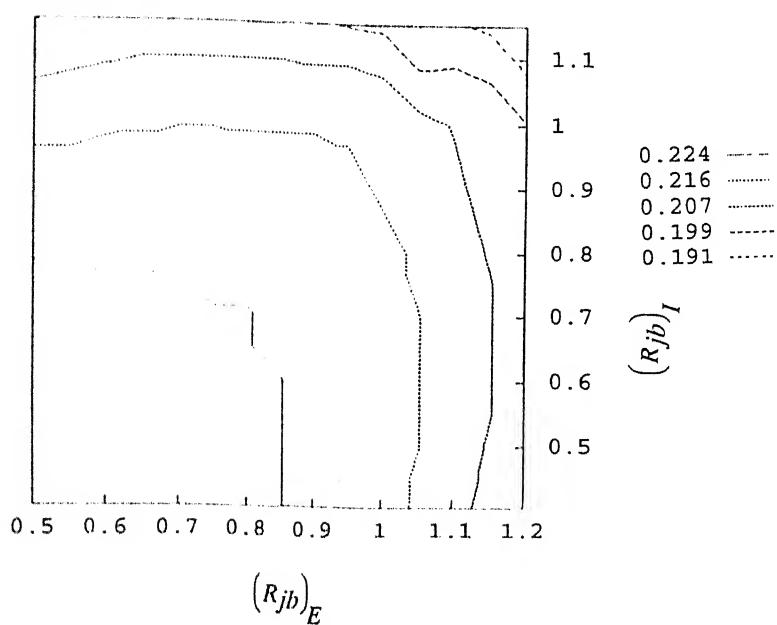


(b) Normalized lateral force contours

Figure 4.16: Effect of joint panel zone designs on normalized lateral force in storey sub-assemblages SSA-T.

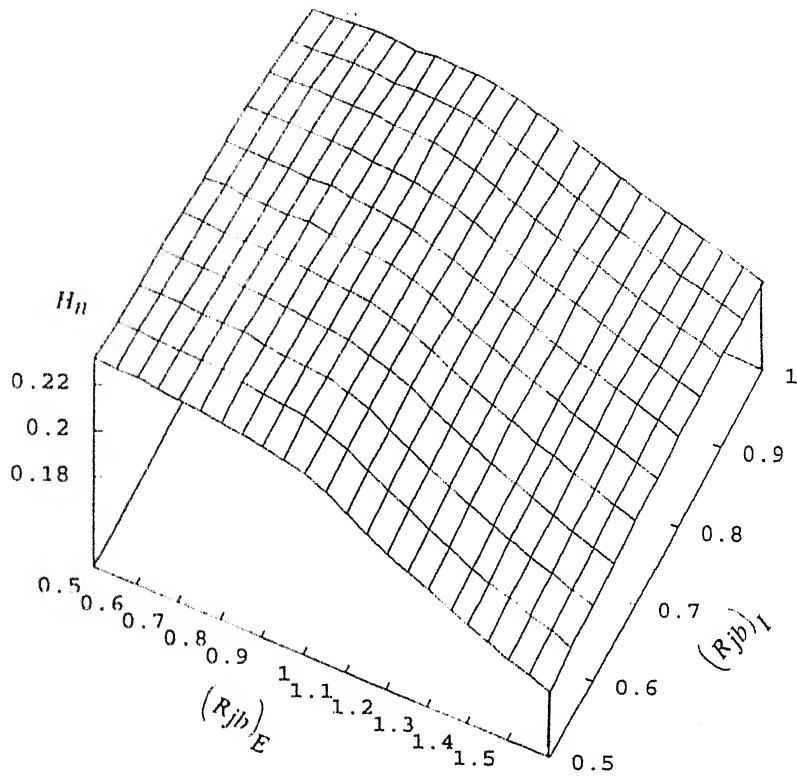


(a) Normalized lateral force surface

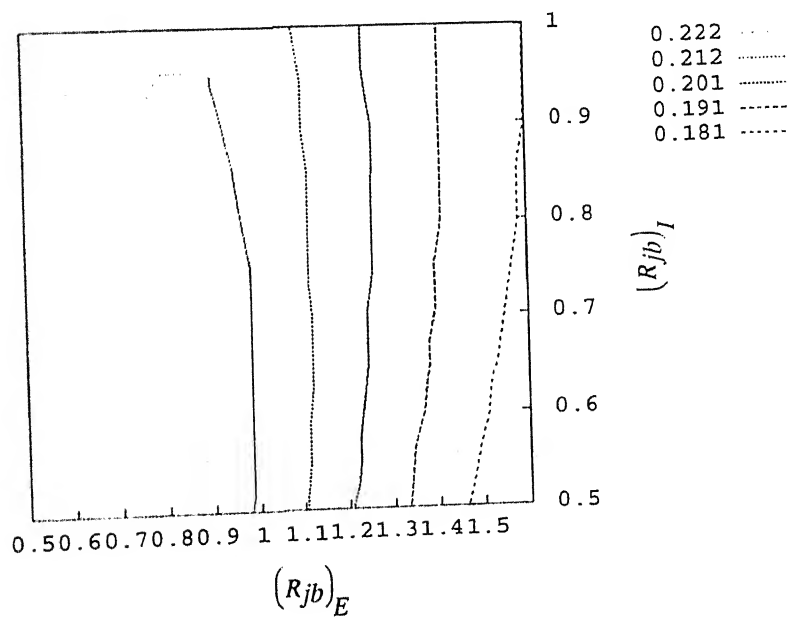


(b) Normalized lateral force contours

Figure 4.17: Effect of joint panel zone designs on normalized lateral force in storey sub-assemblages SSA-M.



(a) Normalized lateral force surface



(b) Normalized lateral force contours

Figure 4.18: Effect of joint panel zone designs on normalized lateral force in storey sub-assemblages SSA-B.

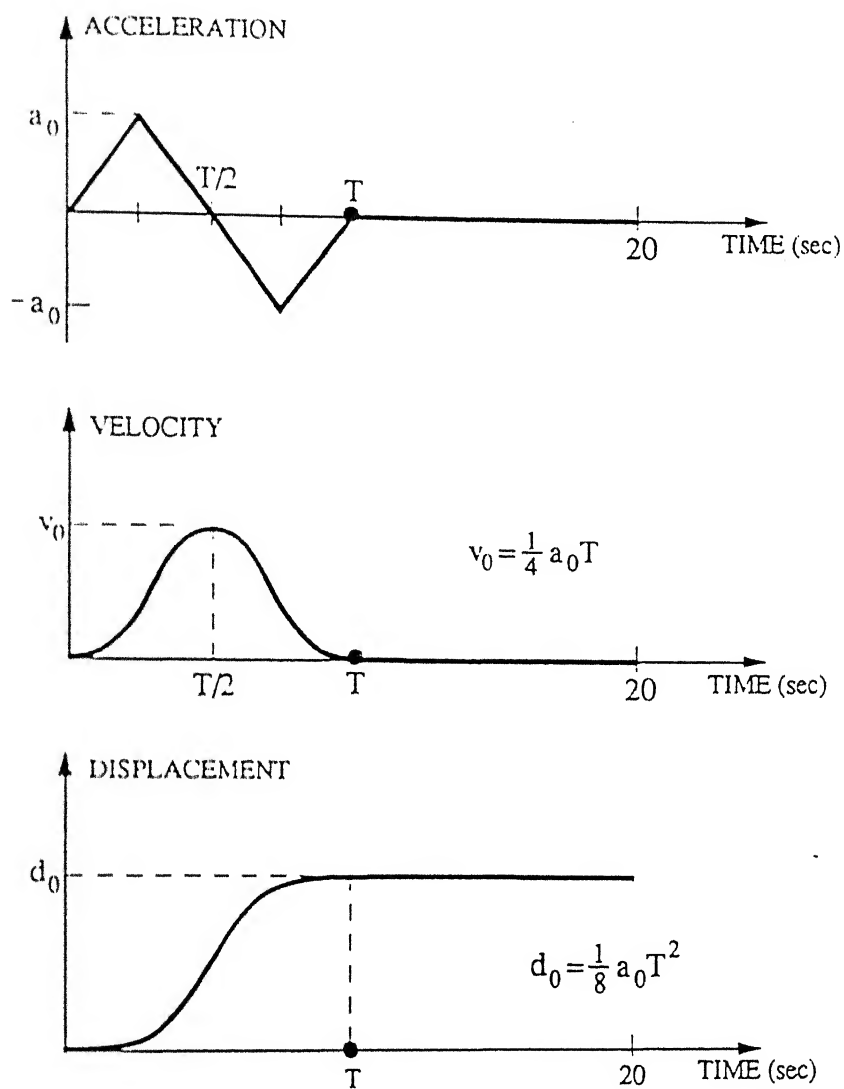


Figure 4.19: Synthetic ground motion with large velocity pulse.

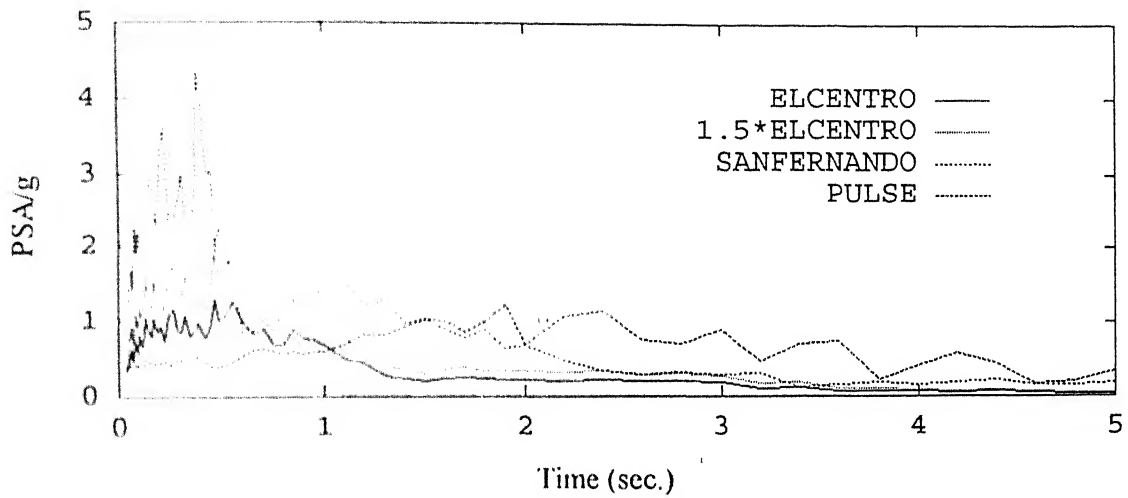
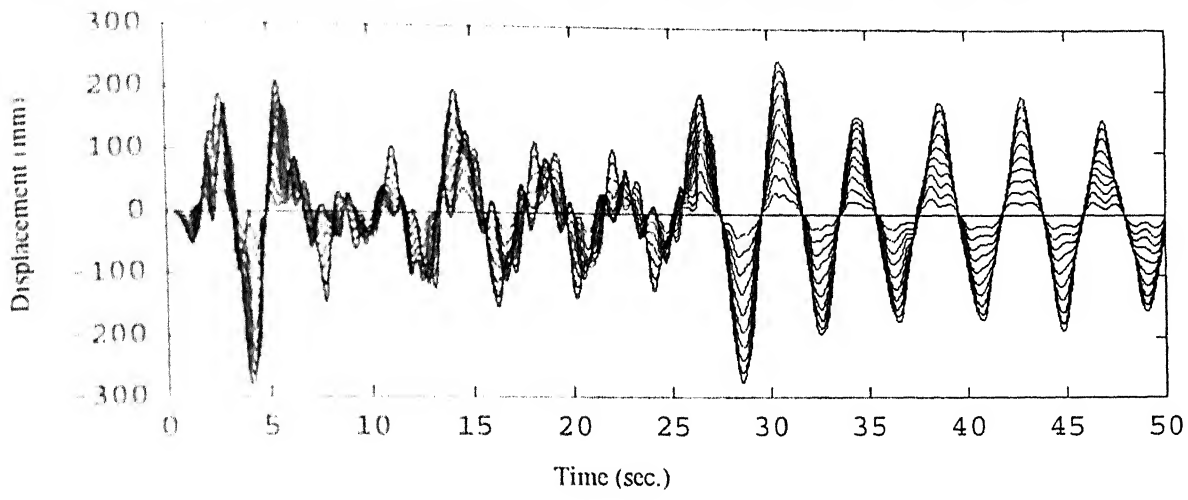
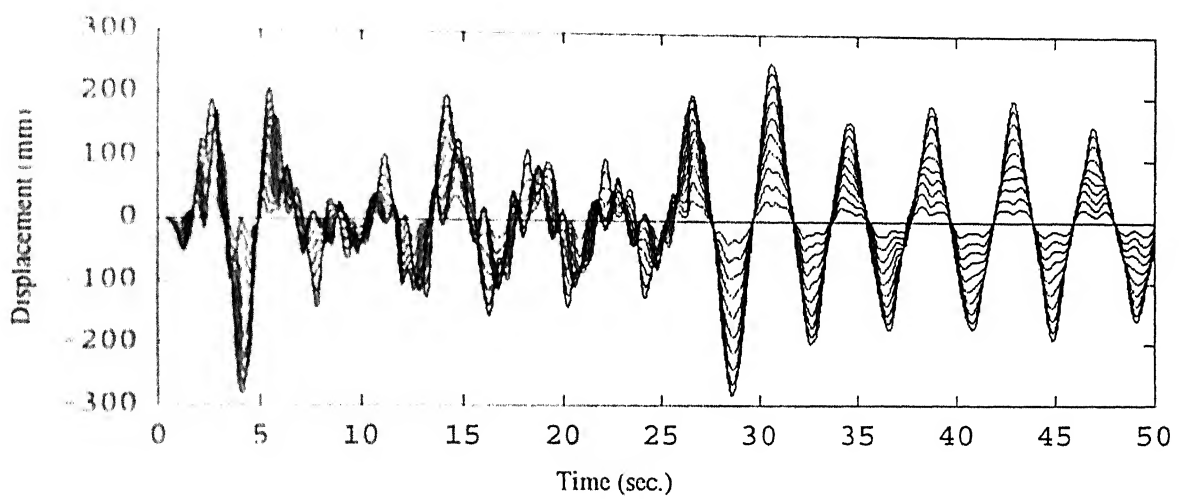


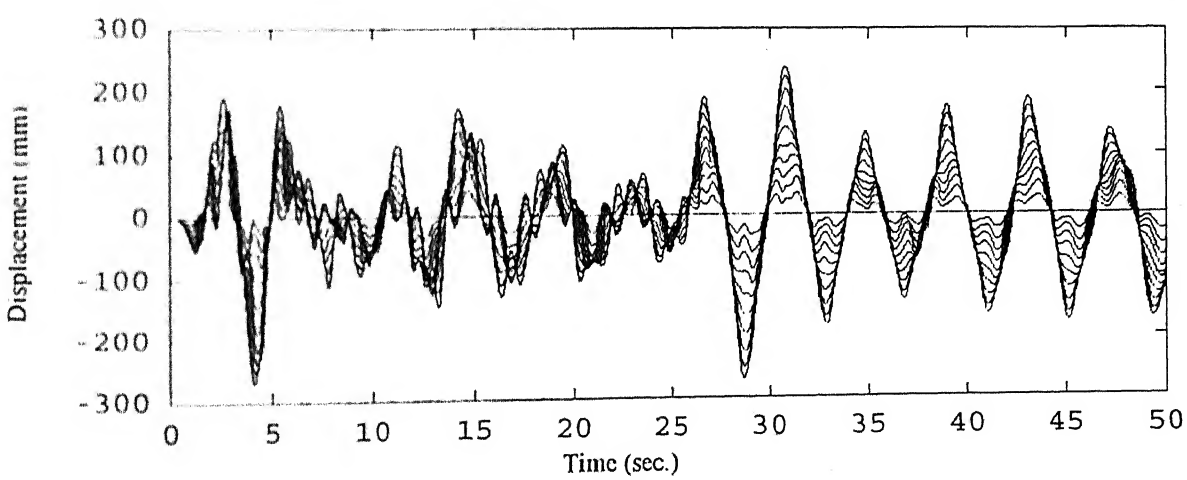
Figure 4.20: Response spectra of the ground motion used in the study.



(a)

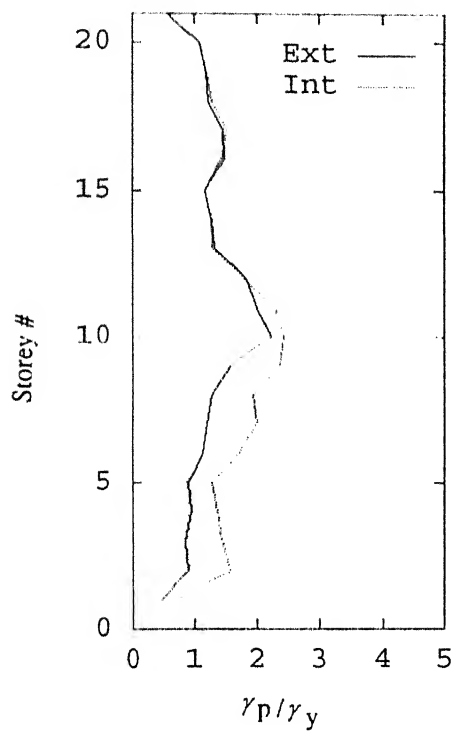


(b)

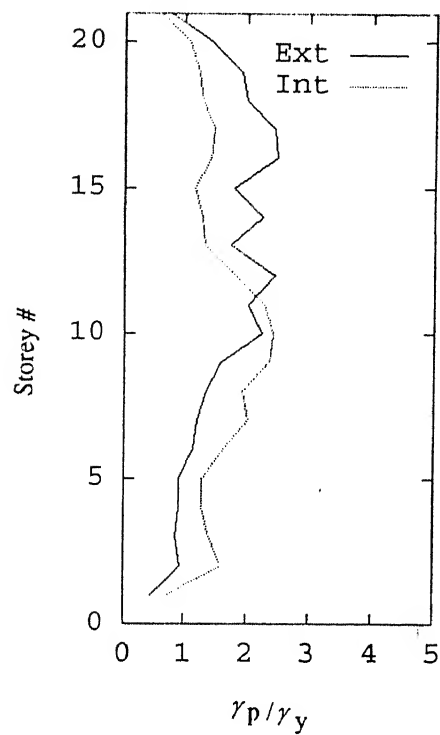


(c)

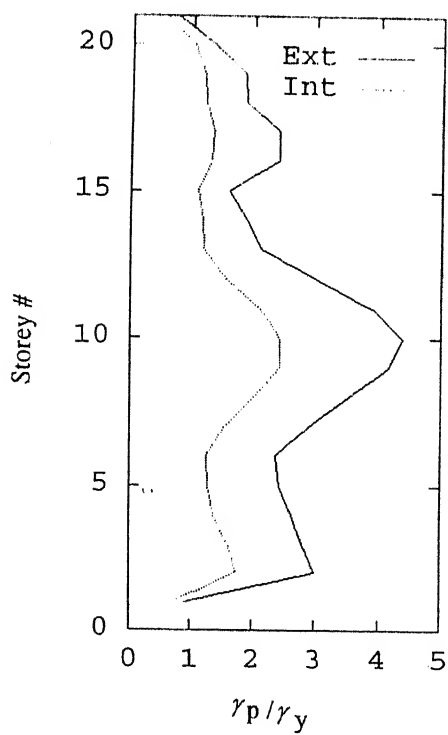
Figure 4.21: Floor responses of the 20-storey MRF with (a) Design 1, (b) Design 2, and (c) Design 4.



(a)

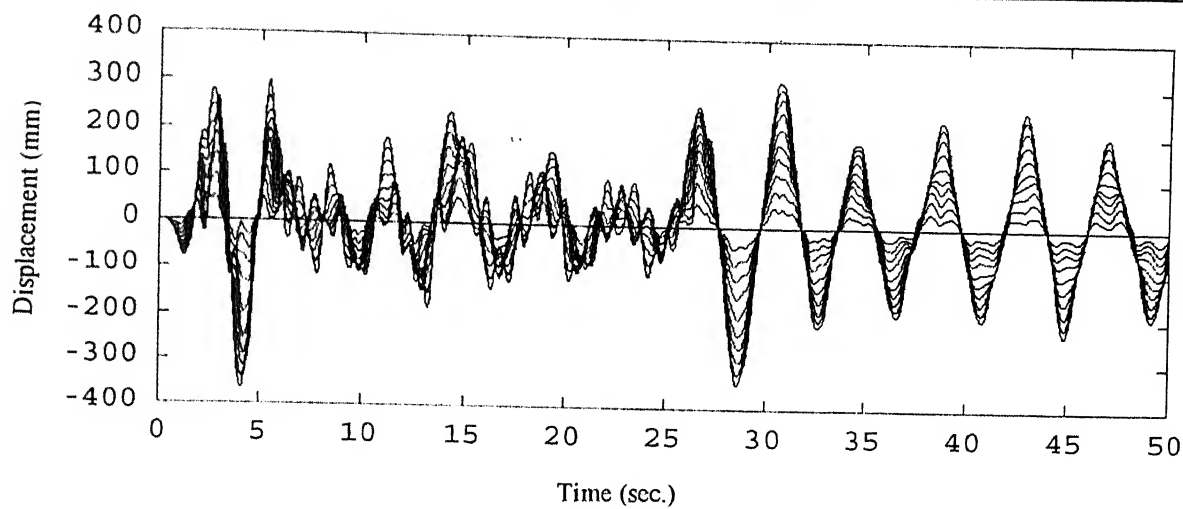


(b)

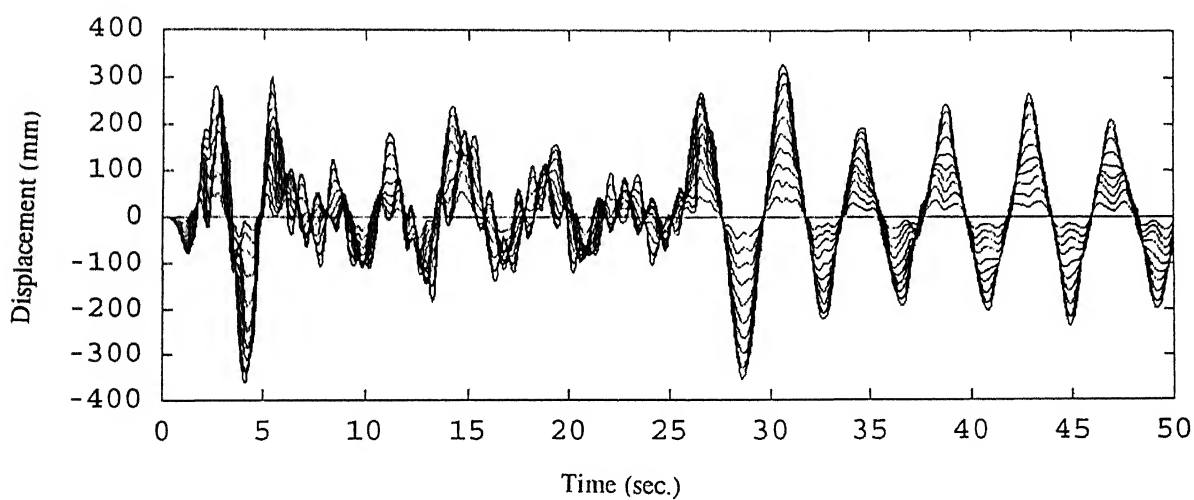


(c)

Figure 4.22: Ductility factors of interior and exterior joint panels of 20-storey MRF with (a) Design 1, (b) Design 2, and (c) Design 4.



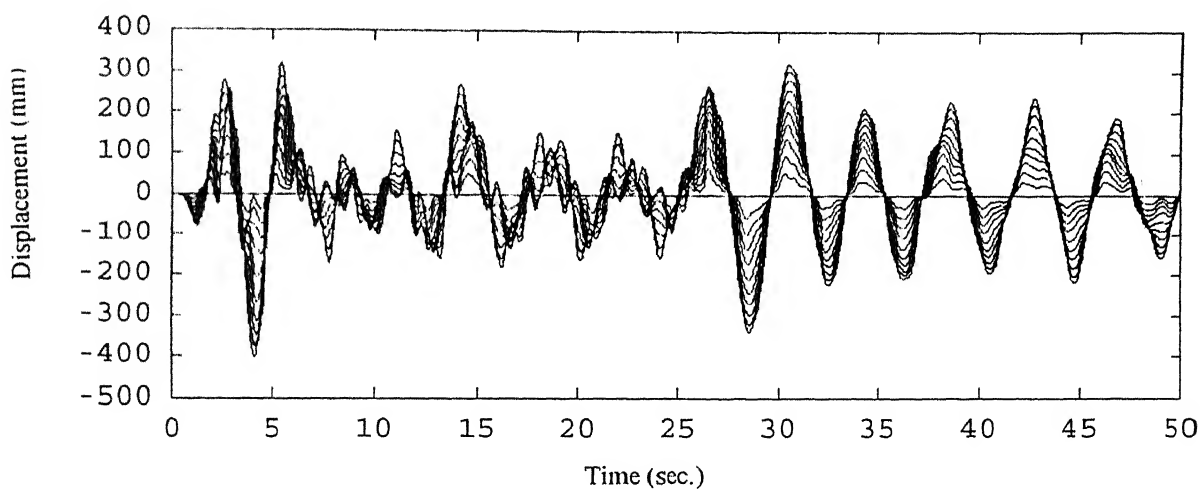
(a)



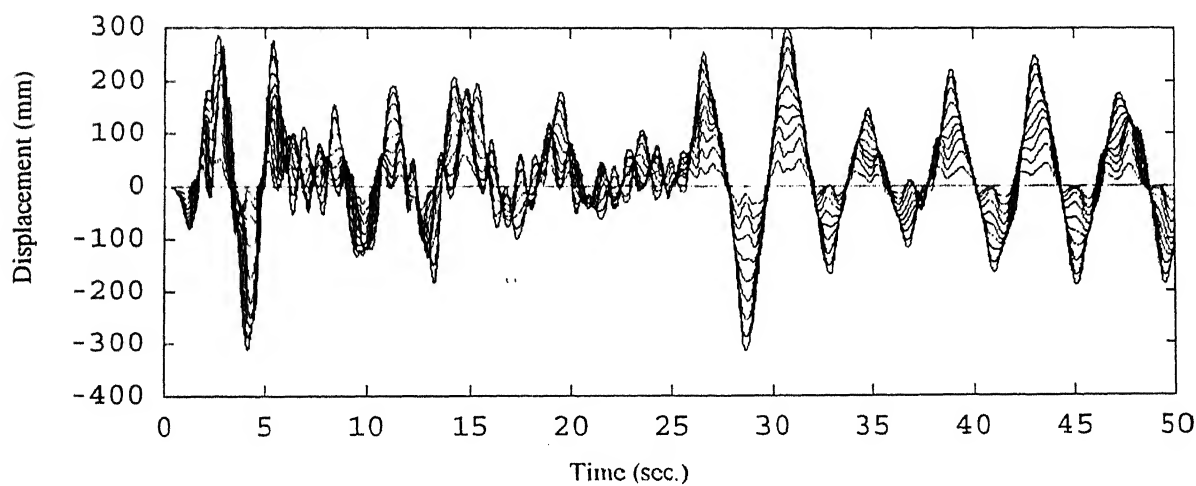
(b)

Figure 4.23: Floor responses of the 20-storey MRF with (a) Design 1, (b) Design 2, (c) Design 3, and (d) Design 4.

contd.....



(c)



(d)

Figure 4.23: Floor responses of the 20-storey MRF with (a) Design 1, (b) Design 2, (c) Design 3, and (d) Design 4.

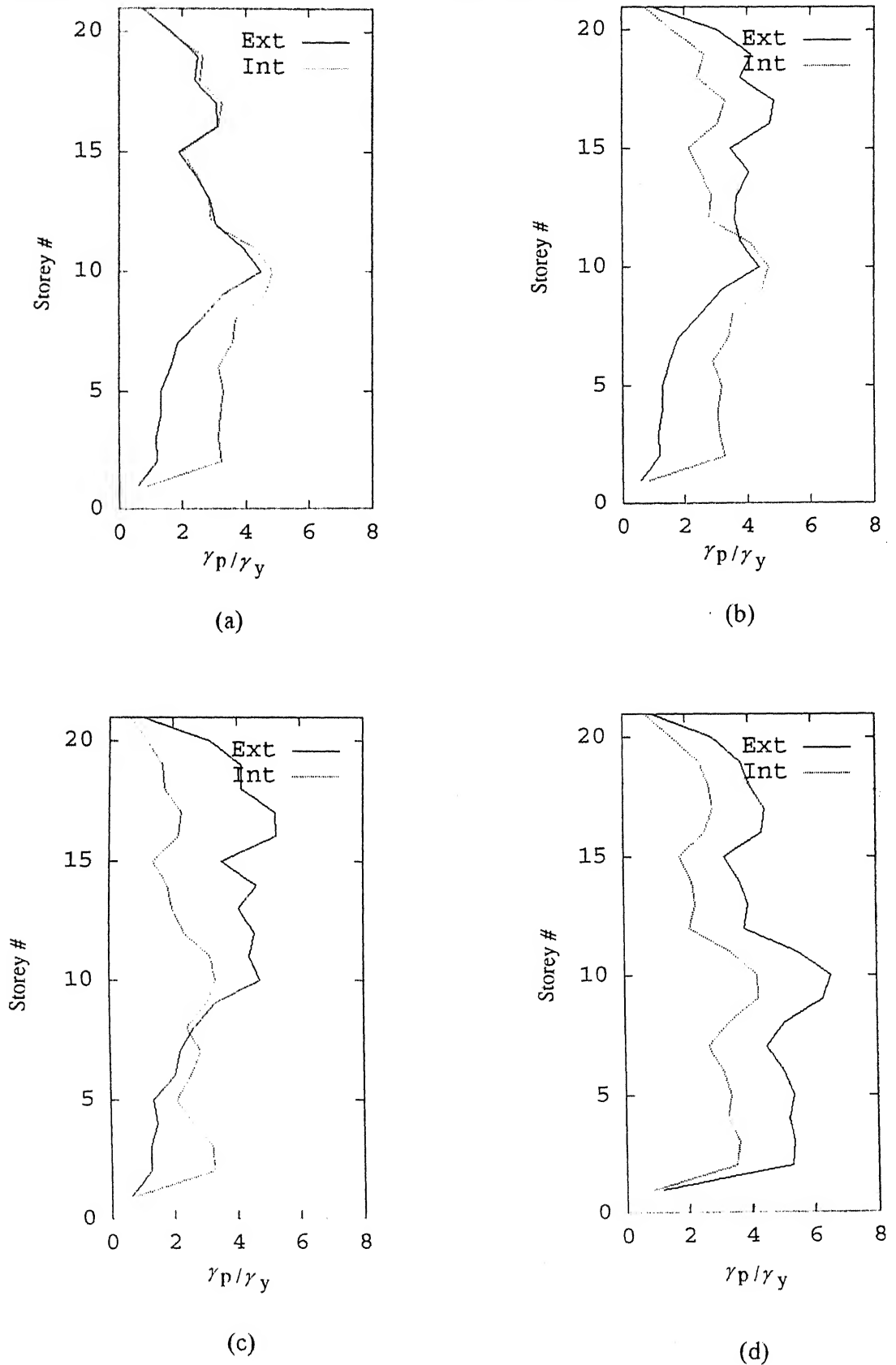
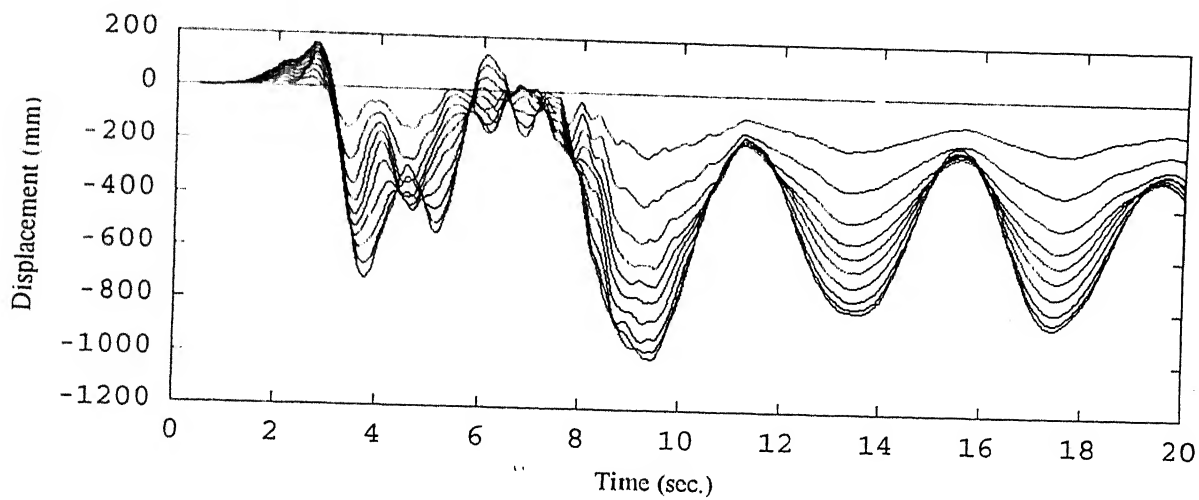
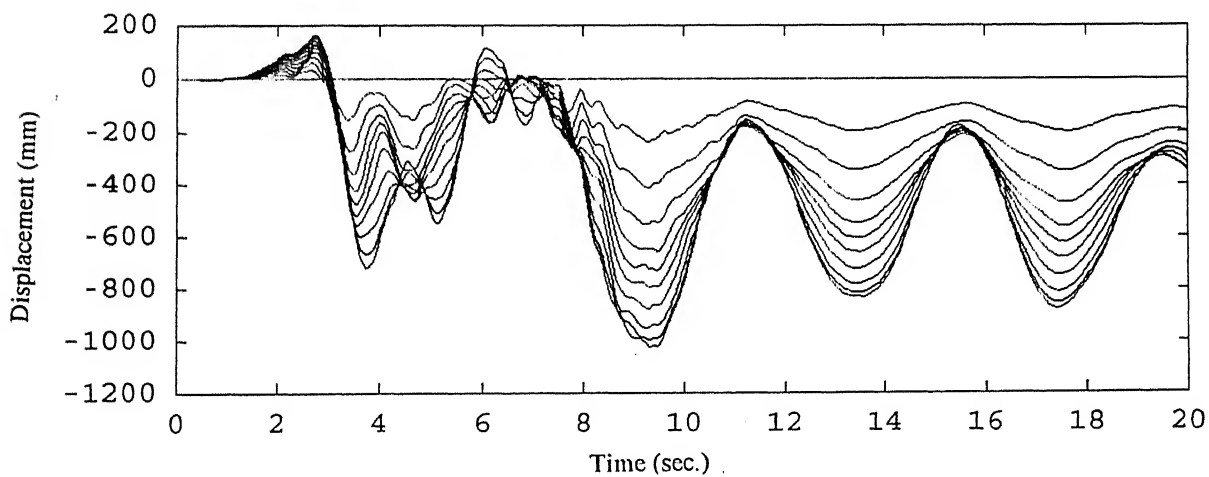


Figure 4.24: Ductility factors of interior and exterior joint panels of 20-storey MRF with (a) Design 1, (b) Design 2, (c) Design 3, and (d) Design 4.



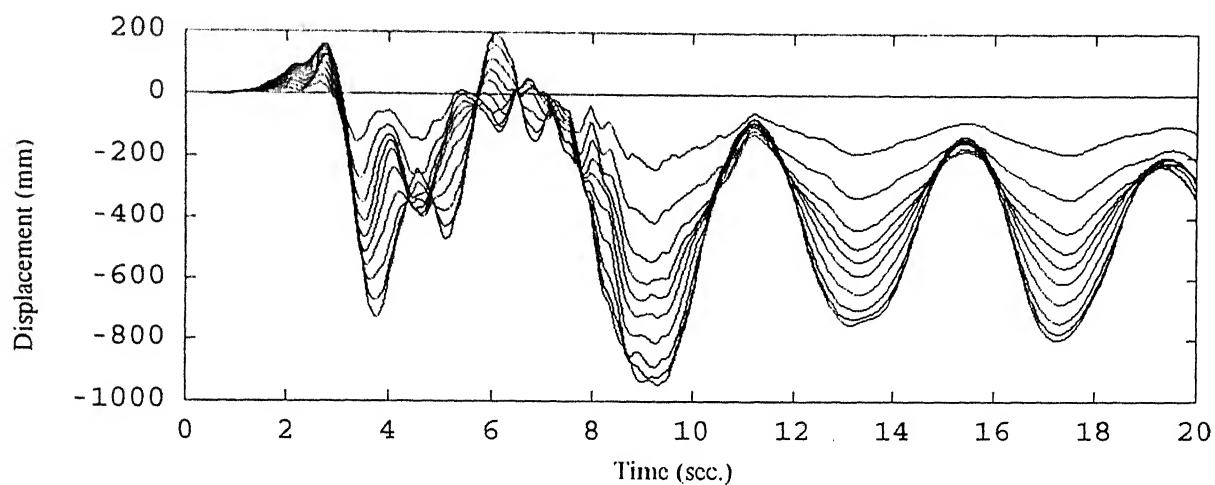
(a)



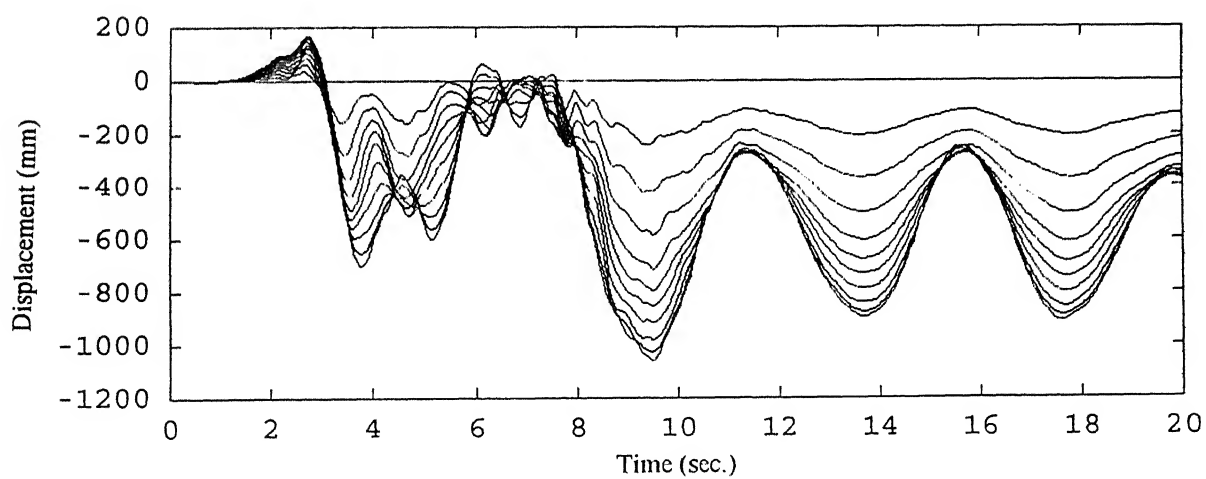
(b)

Figure 4.25: Floor responses of the 20-storey MRF with (a) Design 1, (b) Design 2, (c) Design 3, and (d) Design 4.

contd.....

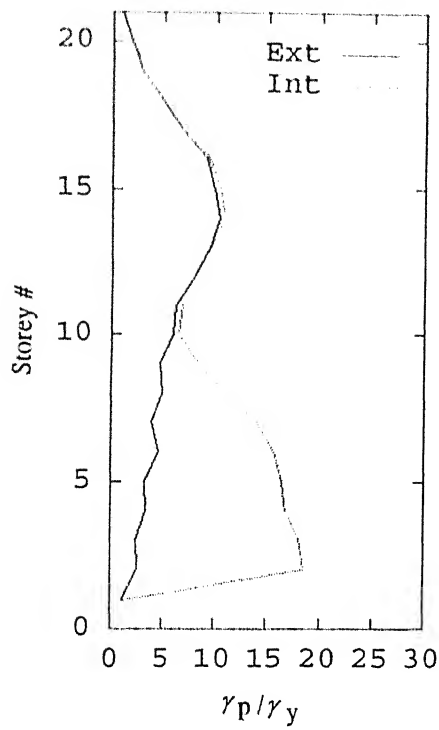


(c)

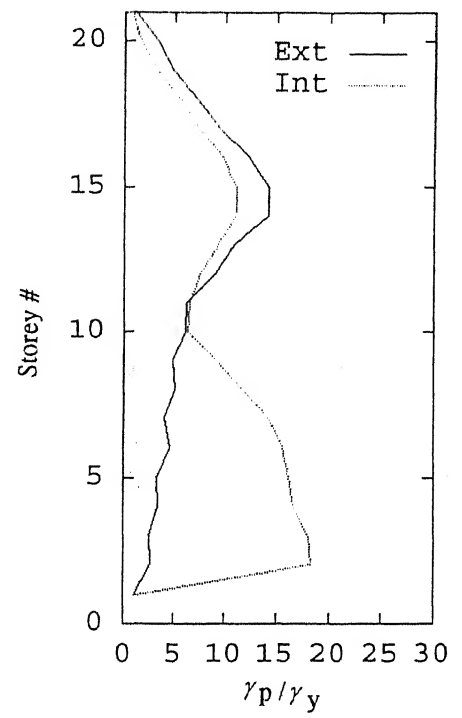


(d)

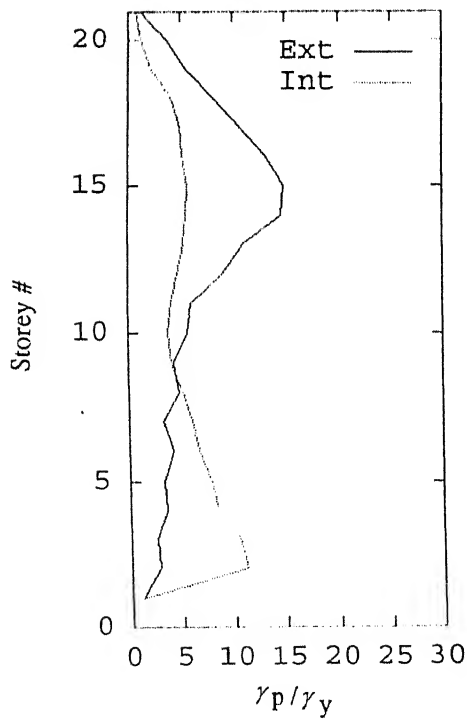
Figure 4.25: Floor responses of the 20-storey MRF with (a) Design 1, (b) Design 2, (c) Design 3, and (d) Design 4.



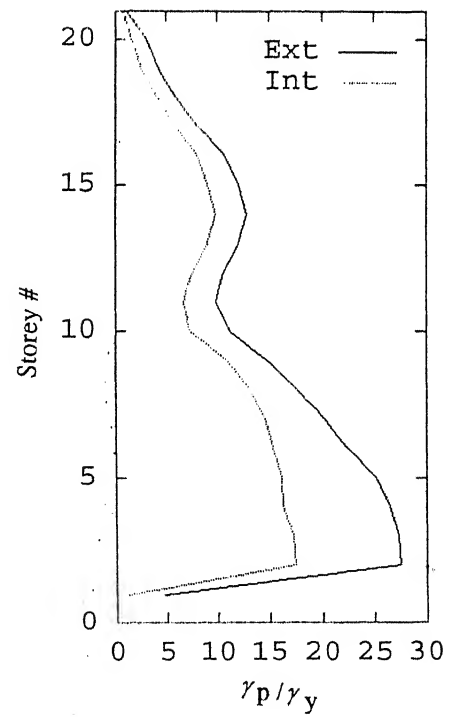
(a)



(b)

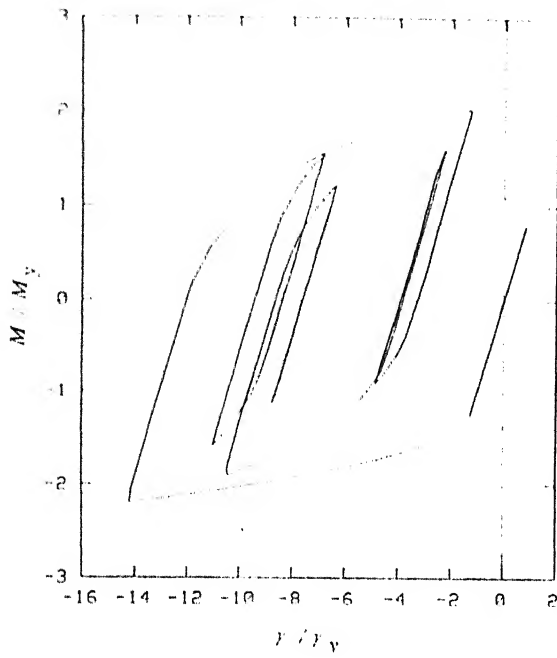


(c)

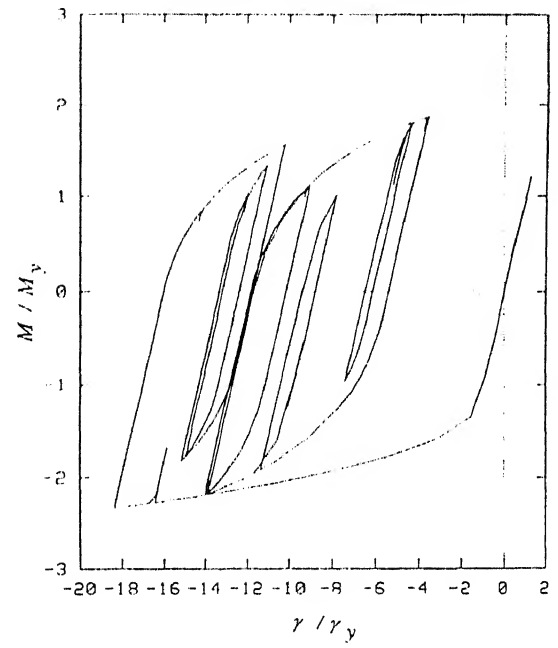


(d)

Figure 4.26: Ductility factors of interior and exterior joint panels of 20-storey MRF with (a) Design 1, (b) Design 2, (c) Design 3, and (d) Design 4.

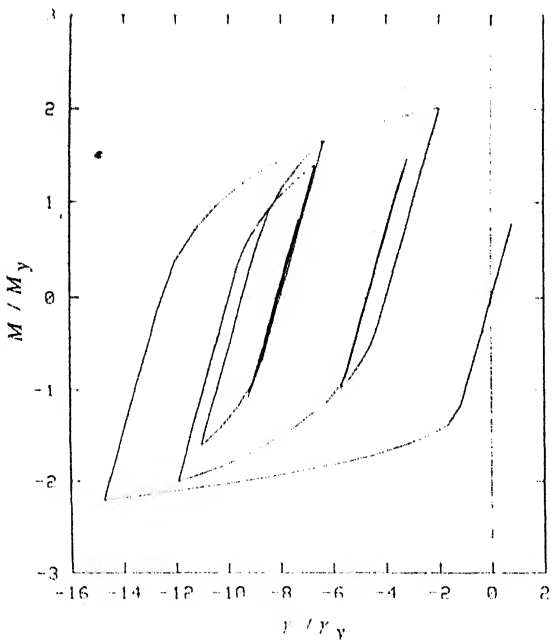


Exterior

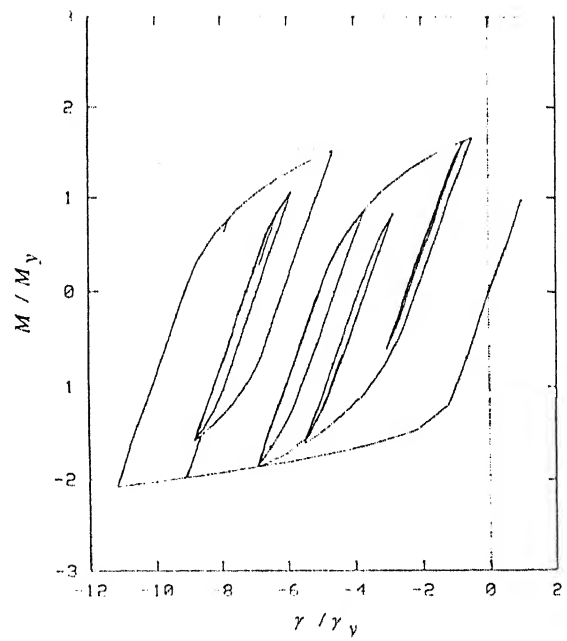


Interior

(a) Design 2



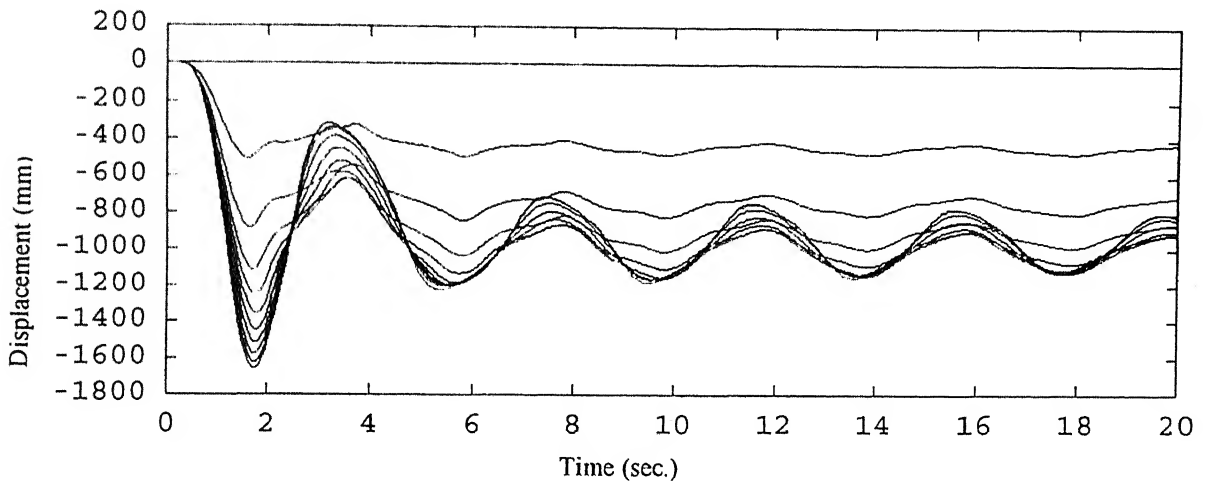
Exterior



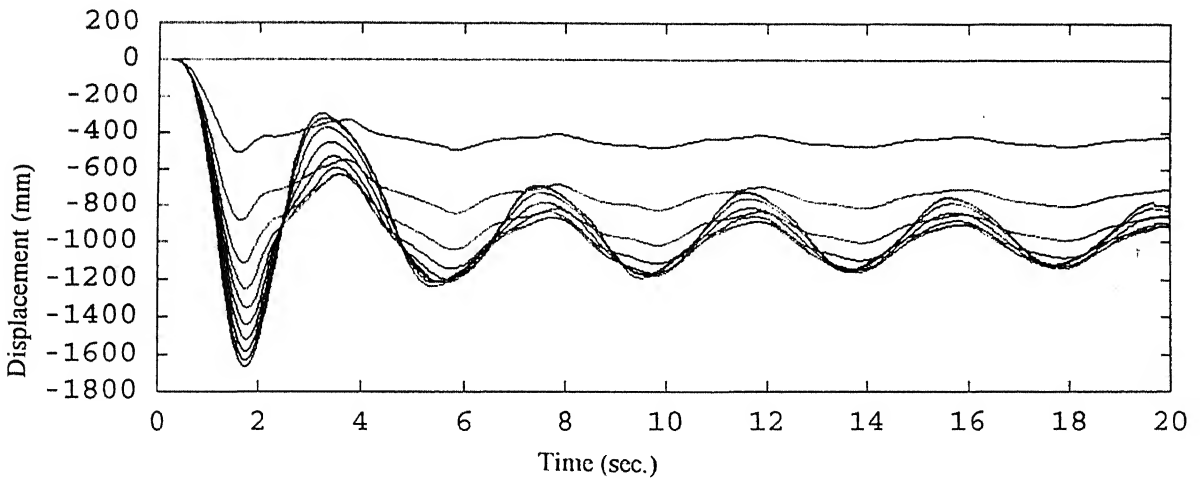
Interior

(b) Design 3

Figure 4.27: Response of Exterior and Interior panel zones of typical storey in a 20-storey MRF.



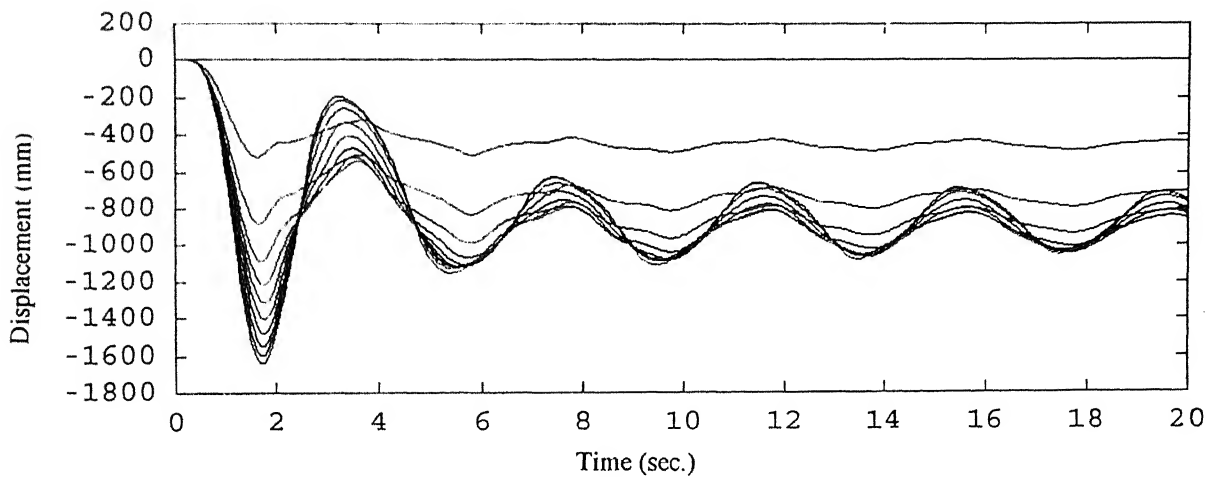
(a)



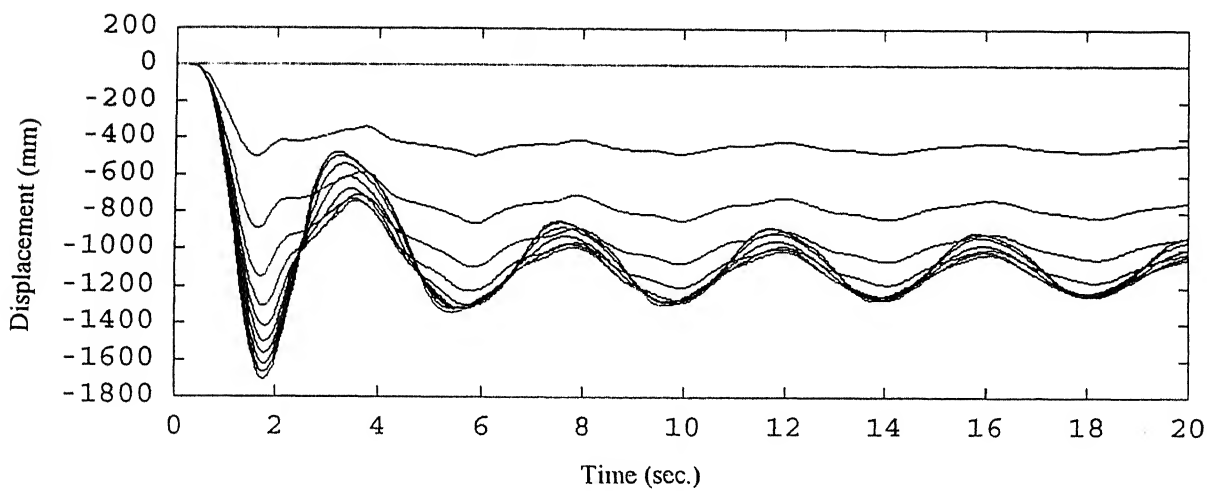
(b)

Figure 4.28: Floor responses of the 20-storey MRF with (a) Design 1, (b) Design 2, (c) Design 3, and (d) Design 4.

contd.....

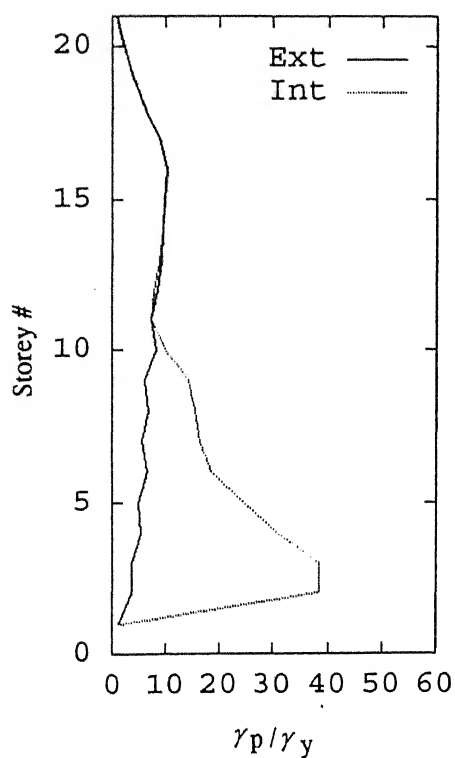


(c)

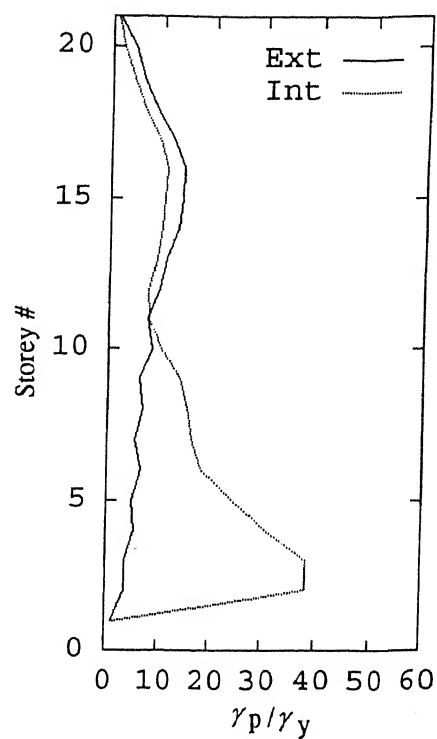


(d)

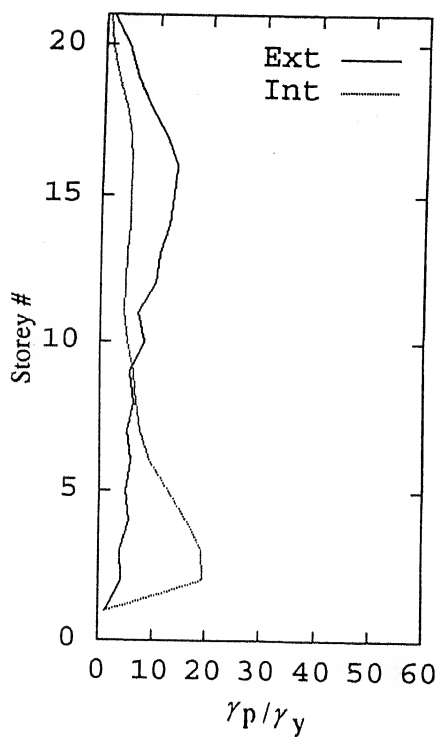
Figure 4.28: Floor responses of the 20-storey MRF with (a) Design 1, (b) Design 2, (c) Design 3, and (d) Design 4.



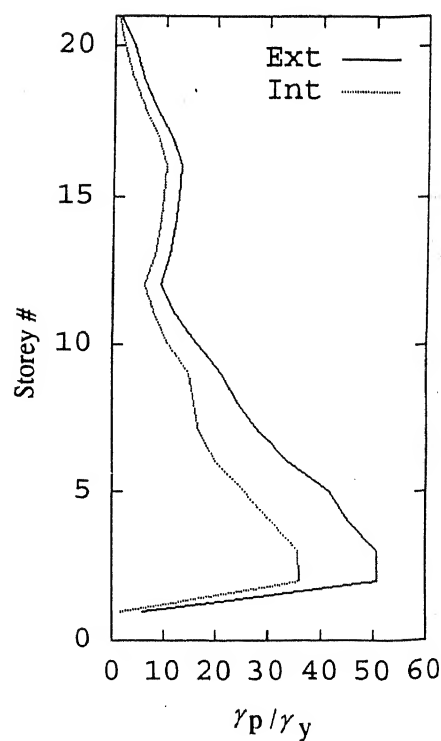
(a)



(b)



(c)



(d)

Figure 4.29 : Ductility factors of Interior and Exterior joint panels of 20-storey MRF with (a) Design 1, (b) Design 2, (c) Design 3, and (d) Design 4.